University of New Hampshire
University of New Hampshire Scholars' Repository

Master's Theses and Capstones | Student Scholarship

Spring 2007

Hydrodynamic modeling of Hampton/Seabrook Harbor, New Hampshire

Kimberly D. Leung
University of New Hampshire, Durham

Follow this and additional works at: https://scholars.unh.edu/thesis

Recommended Citation
Leung, Kimberly D., "Hydrodynamic modeling of Hampton/Seabrook Harbor, New Hampshire" (2007). *Master's Theses and Capstones*. 271.
https://scholars.unh.edu/thesis/271

This Thesis is brought to you for free and open access by the Student Scholarship at University of New Hampshire Scholars' Repository. It has been accepted for inclusion in Master's Theses and Capstones by an authorized administrator of University of New Hampshire Scholars' Repository. For more information, please contact nicole.hentz@unh.edu.

HYDRODYNAMIC MODELING OF HAMPTON/SEABROOK HARBOR, NEW HAMPSHIRE

by

KIMBERLY D. LEUNG

Bachelor of Science, University of California - San Diego, 2004

THESIS

Submitted to the University of New Hampshire
in Partial Fulfillment of
the Requirements for the Degree of

Master of Science
in
Ocean Engineering

May, 2007

Reproduced with permission of the copyright owner. Further reproduction prohibited without permission.

UMI Number: 1443615

INFORMATION TO USERS

The quality of this reproduction is dependent upon the quality of the copy submitted. Broken or indistinct print, colored or poor quality illustrations and photographs, print bleed-through, substandard margins, and improper alignment can adversely affect reproduction.

In the unlikely event that the author did not send a complete manuscript and there are missing pages, these will be noted. Also, if unauthorized copyright material had to be removed, a note will indicate the deletion.

UMI®

UMI Microform 1443615

Copyright 2007 by ProQuest Information and Learning Company.

All rights reserved. This microform edition is protected against unauthorized copying under Title 17, United States Code.

ProQuest Information and Learning Company
300 North Zeeb Road
P.O. Box 1346
Ann Arbor, MI 48106-1346

Reproduced with permission of the copyright owner. Further reproduction prohibited without permission.

This thesis has been examined and approved.

Thesis Director, M. Robinson Swift
Professor of Mechanical Engineering

Kenneth C. Baldwin
Professor of Mechanical Engineering

David W. Fredriksson
Assistant Professor of Ocean Engineering
United States Naval Academy

Igor I. Tsukrov
Associate Professor of Mechanical Engineering

March 27, 2007
Date

Reproduced with permission of the copyright owner. Further reproduction prohibited without permission.

ACKNOWLEDGMENTS

Thank you to my family and friends who have supported me and made this possible.

I would like to thank everyone who has patiently guided me through my education and thesis at UNH: my committee M. Robinson Swift, Kenneth Baldwin, David Fredriksson, and Igor Tsukrov; Jon Scott who was a tireless and invaluable help with modeling and life; and Semme Djikstra, Robert Moynihan, Larry Ward, James Irish, James Case, Andrew McLeod, Andrew Armstrong, Kevin Knuuti, and Anna Burke for help with data and fieldwork.

Thanks to my colleagues at Ocean Engineering for the good times, and for showing me how to survive winter.

Kimberly Leung, March 2007

Reproduced with permission of the copyright owner. Further reproduction prohibited without permission.

TABLE OF CONTENTS

Reproduced with permission of the copyright owner. Further reproduction prohibited without permission.

Reproduced with permission of the copyright owner. Further reproduction prohibited without permission.

LIST OF TABLES

Reproduced with permission of the copyright owner. Further reproduction prohibited without permission.

LIST OF FIGURES

Reproduced with permission of the copyright owner. Further reproduction prohibited without permission.

Reproduced with permission of the copyright owner. Further reproduction prohibited without permission.

ABSTRACT

HYDRODYNAMIC MODELING OF HAMPTON/SEABROOK HARBOR, NEW HAMPSHIRE

by

Kimberly Leung

University of New Hampshire, May 2007

The Hampton/Seabrook estuary is located at the southern end of the New Hampshire Seacoast area. As it is a dynamic system, tidally dominated, and continually changing, two major changes have become issues in recent years: erosion of a sandbar (threatening waterfront homes), and sediment deposition in Seabrook Harbor. Flow between the Blackwater River and the harbor carved a channel between waterfront homes on River Street and the sandbar referred to as "middle ground," and there was concern about further coastal erosion in this area. Additionally, while Seabrook Harbor has previously been dredged yearly to provide temporary relief for boat traffic, the dredging served to increase velocity differences between the River Street breach (high) and the harbor (low), which promoted sediment deposition. During the winter of 2005, as part of the ACOE National Shoreline Erosion Control Development and Demonstration

Program, a channel was dredged through the northern part of middle ground, and the material was deposited in the River Street breach area.

Reproduced with permission of the copyright owner. Further reproduction prohibited without permission.

As part of the post-construction modeling effort, the ACOE-developed finite element hydrodynamic model RMA2 was applied to the post-dredge Hampton/Seabrook Estuary. RMA2 is a two-dimensional, vertically averaged hydrodynamic model capable of calculating water surface elevations and velocities, for both steady-state and dynamic analyses, and generates a solution based on existing physical conditions and boundary conditions.

Field data were organized, including bathymetry from several surveys, tide station data, and acoustic Doppler current profile (ADCP) velocity measurements. Post-dredge bathymetry was used to develop the computer finite element mesh, and ocean forcing boundary conditions were generated using tidal prediction techniques and tidal constituents from nearby stations outside the harbor. Model predictions were compared with both tidal elevation and tidal current observation data in the calibration process.

Observations of model predictions as well as field observations were made, and recommendations for improvement and further work were presented.

Reproduced with permission of the copyright owner. Further reproduction prohibited without permission.

CHAPTER 1

MOTIVATIONS AND DESCRIPTION OF ESTUARY

1.1 Hampton Estuary

The Hampton/Seabrook estuary is located at the southern end of the New Hampshire Seacoast area, and is about 9 km long and 5 km wide (See Figure 1.1). Used for boat mooring and servicing, as well as for recreation, it is a dynamic system, tidally dominated, and continually changing. Two changes that have become issues in recent years are the River Street breach and sediment deposition in Seabrook Harbor. Flow between the Blackwater River and the harbor carved a channel between waterfront homes on River Street and the sandbar referred to as "middle ground," and there was concern about further coastal erosion in this area (Figure 1.2). Additionally, while Seabrook Harbor has previously been dredged yearly to provide temporary relief for boat traffic, the dredging served to increase velocity differences between the River Street breach (high) and the harbor (low), which promoted sediment deposition.

Reproduced with permission of the copyright owner. Further reproduction prohibited without permission.

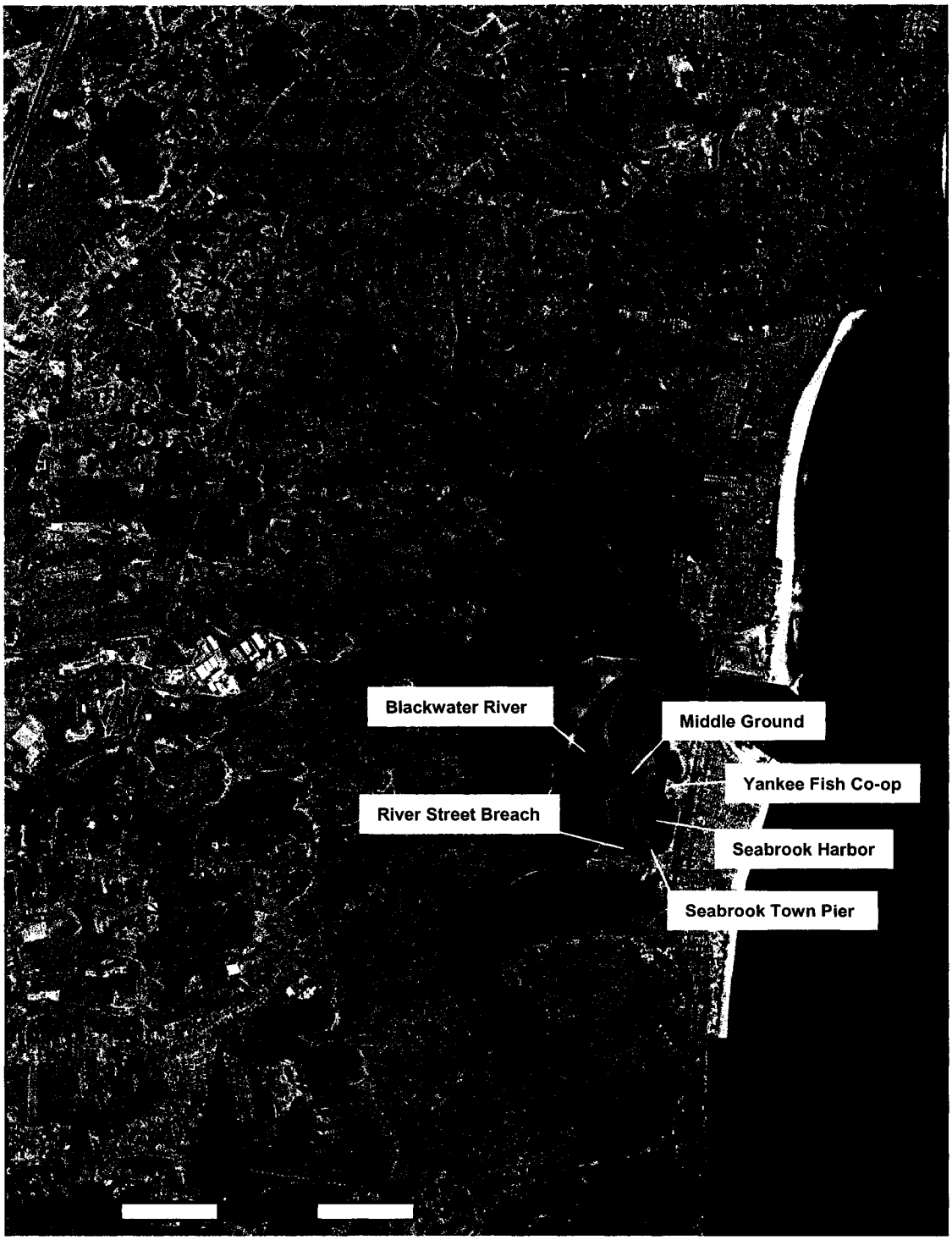

Figure 1.1 Aerial photo of the Hampton/Seabrook estuary (1 September 2000).

Reproduced with permission of the copyright owner. Further reproduction prohibited without permission.

Figure 1.2 Middle Ground area, showing the erosion in the River Street breach (1 September 2000).

Under Congressional dictation (as a Congressional Add in the fiscal year ending September 2002), the U.S. Army Corps of Engineers (ACOE) completed a detailed project design to dredge a channel through middle ground (where water had flowed historically), and fill in the breach with the dredged material (see Figure 1.3) (House Report 107-258, 2001, and pers. communication, K. Knuuti, 2007)). It was hoped that this would draw the flow away from the breach (reducing erosion in front of the waterfront homes near the breach), and ease velocity differences near the harbor (reducing sediment deposition in the channel and harbor area). Figure 1.3 shows the recommended bathymetry, as well as Mahmutoglu's (2001) predictions of the new velocities that would occur in the area. The simulated velocities at Yankee Fish Co-op and the Seabrook Town Pier show a decrease in magnitude, which would generally promote sediment deposition. However, the predictions also show a decreased difference

Reproduced with permission of the copyright owner. Further reproduction prohibited without permission.

between the flow coming through the River Street breach (Seabrook Town Pier) and the flow in the Seabrook Harbor (Yankee Fish Co-op). Much of the pre-construction deposition in the harbor was due to the high flow through the breach, which suspended sediments, and the low flow in the harbor, which allowed the suspended sediment to settle out.

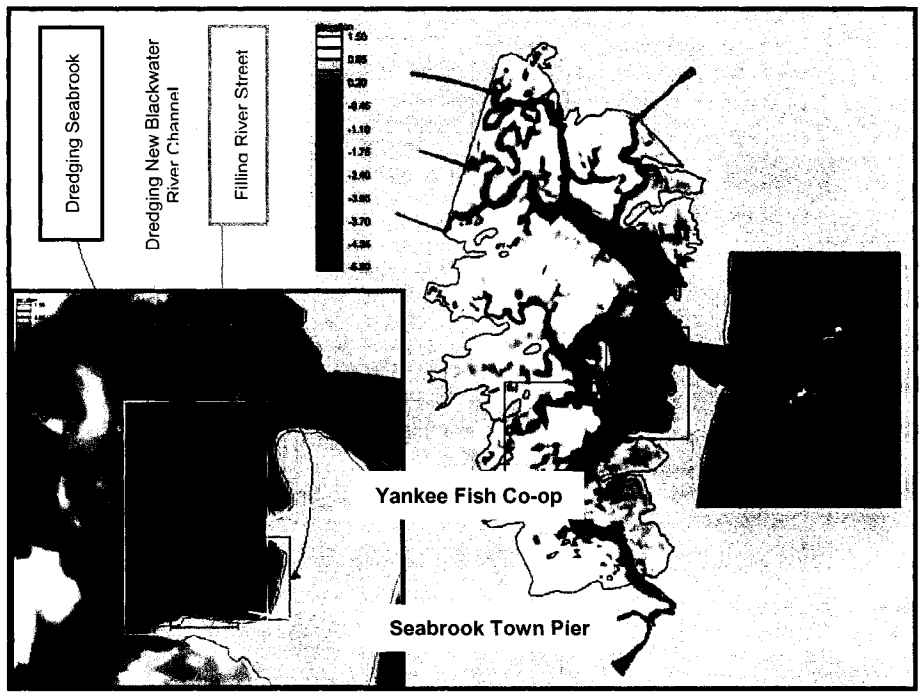

(a)

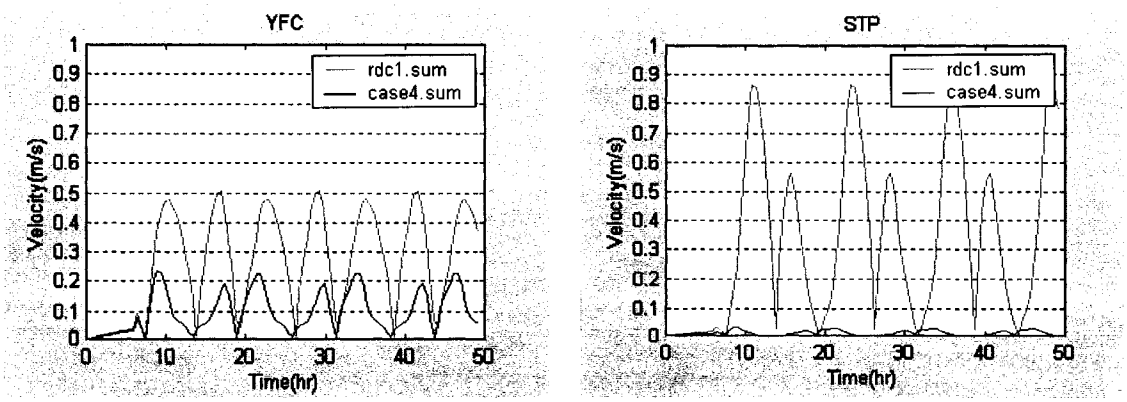

(b)

Figure 1.3 (a) Model bathymetry of recommended changes, and (b) results at Yankee Fish Cooperative and Seabrook Town Pier, where rdc1.sum is the model prediction for pre-dredge conditions, and case4.sum is the prediction for the recommended configuration (Mahmutoglu, 2001).

Reproduced with permission of the copyright owner. Further reproduction prohibited without permission.

During the winter of 2005, these recommendations were executed as part of the ACOE National Shoreline Erosion Control Development and Demonstration Program. Commonly referred to as Section 227 (of the U.S. Water Resources and Development Act of 1996), this coastal shoreline protection program emphasizes innovative and unconventional designs to help prevent or mitigate coastal erosion and to improve shoreline sediment retention. A variety of shore protection devices and methods are being constructed, administered, and evaluated at sites throughout the United States with diverse shoreline morphologies and issues. The program requires at least two sites on the Atlantic coast, two on the Pacific coast, two on the Great Lakes, and one on the Gulf of Mexico. These shore protection structures must have scientific support for projected performance and must not affect the aesthetic appeal of the area (Curtis, 2001).

The recommended channel was dredged through the northern part of middle ground, and the material was deposited in the River Street cut area (Figure 1.4). To keep the fill in place, thermoplastic sheet pile bulkheads were constructed on both sides of the former cut, to an elevation of -0.3 m with respect to the NAVD88 datum, and rock blankets were installed at the base for stabilization (Figure 1.5). Additionally, both the Blackwater River, to the west of middle ground, and Seabrook Harbor, to the east of middle ground, were dredged to maintain enough depth for boats to navigate the area (Figure 1.4).

Reproduced with permission of the copyright owner. Further reproduction prohibited without permission.

Figure 1.4 Post-construction (12 May 2005) aerial photo, showing the River Street breach filled in (red arrow), and dredged areas in the Blackwater River (blue arrows) and Seabrook Harbor (green arrow).

Reproduced with permission of the copyright owner. Further reproduction prohibited without permission.

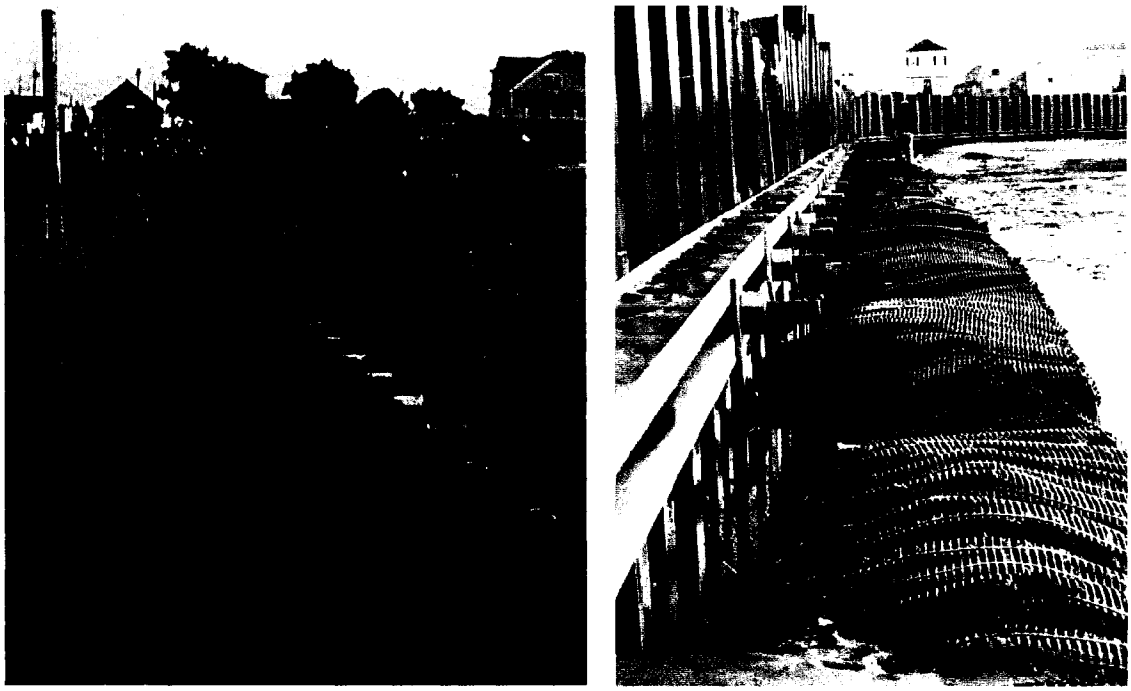

(a) (b)

Figure 1.5 (a) View of thermoplastic sheet pile bulkheads on the Harbor side of Middle Ground, looking south toward River Street, and (b) rock blanket stabilization at the base of the bulkheads.

Post-construction monitoring efforts were carried out by researchers at UNH working with and funded in part by the ACOE. These included collecting sediment samples and bathymetric, tidal elevation, current, and meteorological data, and developing a hydrodynamic model. This thesis describes the process of developing and calibrating this model.

1.2 Objectives

The purpose of this effort was to apply the ACOE-developed finite element hydrodynamic model RMA2 to the post-dredge Hampton/Seabrook Estuary. RMA2 is a two-dimensional, vertically averaged hydrodynamic model capable of calculating water surface elevations and velocities, for both steady-state and dynamic analyses, and generates a solution based on existing physical conditions and boundary conditions.

Reproduced with permission of the copyright owner. Further reproduction prohibited without permission.

Specific objectives include:

- Use post-dredge bathymetry to develop the computer model finite element mesh,
- Use tidal analysis prediction techniques to specify the ocean forcing boundary conditions,
- Compare and calibrate tidal elevation observation data,
- Compare and calibrate with tidal current observation data.

The resulting model will be useful for investigating specific areas of interest not covered by the field program. Velocity distribution at newly developed erosion sites is one important example. New remediation scenarios may also be explored as well as using currents as the basis for applying the companion sediment transport modules (RMA4, SED2D). In addition, comparisons with both surface elevation and current data also contribute to understanding of model capabilities and how best to apply the model.

1.3 Approach

The physics and theoretical basis of the model were examined and input requirements identified as described in Chapter 2. Next, relevant aspects of the field program were organized, including bathymetry from several surveys, tide station data, and acoustic Doppler current profile (ADCP) velocity measurements (Chapter 3). Model application (Chapter 4) began by establishing the mesh and bathymetry. The starting point for this task was based on the previous mesh/bathymetry documented in Mahmutoglu (2001) and an ACOE report, Letter et al. (2005). For the model described here, water depths and other parameters for the dredged region were processed and

Reproduced with permission of the copyright owner. Further reproduction prohibited without permission.

entered to reflect the changes in bathymetry. Bottom friction, turbulence mixing, and marsh porosity parameters were initially specified from first principles and later modified in the calibration phase. The open ocean boundary condition was specified using tidal constituents from nearby stations outside the harbor. Calibration/comparison was carried out using both tidal elevation and current measurements. Results for current distribution over the tidal cycle are provided in Chapter 5.

Reproduced with permission of the copyright owner. Further reproduction prohibited without permission.

CHAPTER 2

MODEL THEORY

2.1 Suitability of RMA2

Modeling is a useful tool for investigating the hydrodynamics of an estuary such as Hampton/Seabrook Harbor. A model can be defined as an approximation of actual conditions, and it can be manipulated to investigate and predict the effects of bathymetric and other physical changes. In the past, physical models were commonly used; a scale model of the study site was built, and using the concept of similitude, factors such as roughness were adjusted to create conditions similar to those of the actual site. It is now more common to use numerical models (also known as computer models) to generate solutions based on geometry and boundary conditions as input.

The hydrodynamics of Hampton/Seabrook Harbor are dominated by tidal circulation driven by the water surface elevation of the Atlantic Ocean to the east. Since there is little freshwater input during most of the year, flow is well-mixed with depth; a 3-D model is unnecessary, and a horizontally 2-D model is appropriate. A 1-D model such as HEC-RAS is insufficient due to the complex nature of the horizontal geometry and, therefore, the flow.

TABS RMA2, a two-dimensional, vertically averaged hydrodynamic model, was chosen for this project for two reasons: suitability and past use. Originally developed by Norton, King and Orlob (1973) for the U.S. Army Corps of Engineers, it is capable of

Reproduced with permission of the copyright owner. Further reproduction prohibited without permission.

calculating water surface elevations and two-dimensional velocities, for both steady-state and dynamic analyses, and generates a solution based on user-specified physical conditions and boundary conditions. RMA2 can also simulate wetting and drying with marsh porosity and is therefore suited to computing hydrodynamics in tidal flats and wetlands (King et al., 2001). Additionally, the Mahmutoglu (2001) model developed for the pre-dredge analysis used RMA2, and using it for this simulation would not only allow direct comparison, but also allowed the post-dredge simulation to make use of parts of the original mesh and bathymetry.

2.2 Finite Element Analysis

The computational power behind RMA2 is based on the method of finite element analysis (FEA). In this method of analysis, a region of complex geometry is subdivided into simple geometric shapes called finite elements; the network of elements is called a mesh (Chandrupatla and Belegundu, 2002). Equations are then developed to approximate the solution for each element. These individual element equations are then assembled into a system of simultaneous equations that ensure the solutions are continuous at the junctions (nodes) of element corners. Boundary conditions are applied at the point(s) of loading, and the system of equations is solved for the unknowns at each node, using techniques from linear algebra (Chapra and Canale, 2002). While FEA is only an approximate method, the accuracy of a solution can be increased by refining the mesh in areas of particular interest.

Reproduced with permission of the copyright owner. Further reproduction prohibited without permission.

2.3 Governing Equations

RMA2 computes a finite element solution to the Reynolds form of the Navier-Stokes equations (differential equations which describe the motion of a constant-density, viscous fluid) for turbulent flows. Friction is calculated with the Manning's or Chezy equation, and eddy viscosity coefficients are used to define turbulence characteristics (King et al., 2001). These governing equations consist of the depth-integrated forms of the equations of motion (conservation of momentum) in two horizontal directions,

$$h\frac{\partial u}{\partial t}+hu\frac{\partial u}{\partial x}+hv\frac{\partial u}{\partial y}-\frac{h}{\rho}\left[E_{xx}\frac{\partial^2 u}{\partial x^2}+E_{xy}\frac{\partial^2 u}{\partial y^2}\right]+gh\left[\frac{\partial a}{\partial x}+\frac{\partial h}{\partial x}\right]+\frac{gun^2}{\left(1.486h^{1/6}\right)^2}\left(u^2+v^2\right)^{1/2}-\zeta V_a^2\cos\psi-2hv\omega\sin\Phi=0 \tag{2.1}$$

$$h\frac{\partial v}{\partial t}+hu\frac{\partial v}{\partial x}+hv\frac{\partial v}{\partial y}-\frac{h}{\rho}\left[E_{yx}\frac{\partial^2 v}{\partial x^2}+E_{yy}\frac{\partial^2 v}{\partial y^2}\right]+gh\left[\frac{\partial a}{\partial y}+\frac{\partial h}{\partial y}\right]+\frac{gvn^2}{\left(1.486h^{1/6}\right)^2}\left(u^2+v^2\right)^{1/2}-\zeta V_a^2\sin\psi-2hu\omega\sin\Phi=0 \tag{2.2}$$

and the continuity equation (conservation of mass).

$$\frac{\partial h}{\partial t}+h\left(\frac{\partial u}{\partial x}+\frac{\partial v}{\partial y}\right)+u\frac{\partial u}{\partial x}+v\frac{\partial h}{\partial y}=0. \tag{2.3}$$

Nomenclature in the above equations is defined below:

h	=	water depth (from bottom to surface)
u,v	=	velocities in Cartesian directions
x,y,t	=	Cartesian coordinates and time
ρ	=	density of fluid
E	=	eddy viscosity coefficients
		for xx = normal direction on x-axis surface
		for yy = normal direction on y-axis surface
		for xy and yx = shear direction on each surface

Reproduced with permission of the copyright owner. Further reproduction prohibited without permission.

g	=	acceleration of gravity
a	=	elevation of bottom
n	=	Manning's roughness n-value
1.486	=	conversion of n from SI (metric) to English units
ζ	=	empirical wind shear coefficient
V_a	=	wind speed
ψ	=	wind direction
ω	=	rate of earth's angular rotation
Φ	=	local latitude

The equations of motion and continuity (Equations 2.1, 2.2, and 2.3) are solved using the Galerkin method of weighted residuals, which converts differential equations approximately into a system of linear equations, which in turn can be solved using approaches from linear algebra. Elements are two-dimensional and the shape functions are quadratic for velocity and linear for depth. Spatial integration is performed by Gaussian integration and time derivatives are solved with a nonlinear finite difference approximation.

The unsteady calculations advance in time stepwise using an implicit solution. The time derivatives are replaced by a nonlinear finite difference approximation in which values are assumed to vary over each time interval in the form:

$$f(t) = f(t_0) + at + bt^c \qquad t_0 \le t < t_0 + \Delta t \qquad \textbf{(2.4)}$$

where

$f(t)$	=	value at end of time step
$f(t_0)$	=	value at start of time step
a	=	partial of f with respect to t_0
b,c	=	coefficients assumed to be constant (within the context of solving for the next time step)

Reproduced with permission of the copyright owner. Further reproduction prohibited without permission.

The coefficients b and c were determined by numerical experiments and are not user-specified input variables. The value of c is 1.5 (Norton and King, 1977). As a result, relatively large time steps are acceptable (Thomas and McAnally, 1985).

The model solution is implicit, and Newton-Raphson nonlinear iteration is used to solve the set of equations by means of a front-type solver, which assembles a section of the matrix and solves it before moving on to the next portion to assemble and solve (King et al., 2001).

2.4 Modeling Process

The general method for hydrodynamic modeling in RMA2 can be seen in Figure 2.1. It involves building the mesh for the study site, setting up the appropriate input files, running the model, and calibrating the model to real data. It is an iterative process; once the model has run and predictions generated, the predictions are compared to field data. Adjustments are made to the input (mesh, material properties, or boundary conditions) and the process begins again. This is repeated as necessary until the predictions are considered accurate.

Reproduced with permission of the copyright owner. Further reproduction prohibited without permission.

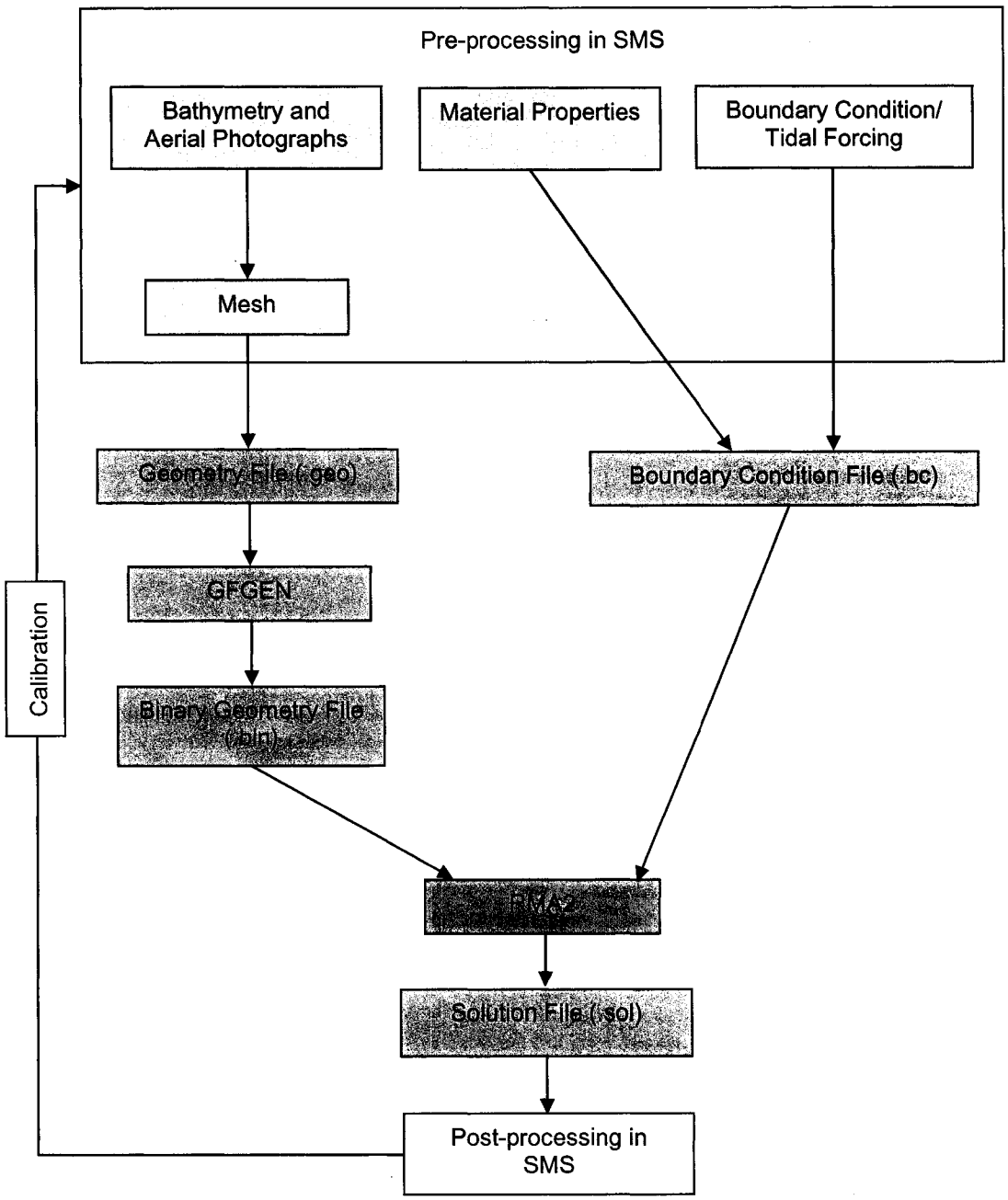

Figure 2.1 Flow diagram of hydrodynamic modeling process

Reproduced with permission of the copyright owner. Further reproduction prohibited without permission.

2.4.1 Bathymetry and Mesh

The first step is to develop a bathymetry input file in the form of an .xyz file, with depths positive upward. Using this bathymetry, the next step is to generate a mesh, the quality of which is one of the largest influences on the success of the model, so care must be taken with this process. Element size, shape, and orientation must be considered when creating the mesh. Smaller elements - thus a finer mesh - increase the accuracy of the solution, but the larger the number of elements, the greater the computational time. Therefore, the key to optimizing the model is to balance accuracy and computation time. One way to do this is to refine the mesh only in the areas of interest, leaving the rest of the mesh relatively coarse where accuracy is less crucial. Good element shape properties include maintaining a length to width ratio of less than 10:1, and avoiding highly distorted triangles and rectangles (King et al., 2001). To help facilitate the wetting/drying function in RMA2, element orientation should be set so that element edges parallel bathymetric contours. This allows a smoother transition between wet and dry elements.

2.4.2 Material Properties

Once the mesh is generated, "material properties" must be assigned to each element in the mesh. "Material properties" is RMA2's term for parameters that pertain to bottom roughness, turbulence, and marsh porosity.

2.4.2.1 Bottom Roughness

Changing bottom roughness, or bed friction, is accomplished by specifying the Manning's number n occurring in the bottom stress terms in Eqns 2.1 and 2.2. Varying n

Reproduced with permission of the copyright owner. Further reproduction prohibited without permission.

allows some control over the fluid velocity magnitude and direction, through the calculation of bottom shear stress. The equation for bottom shear stress in a steady state, open channel river flow situation is given by

$$\tau = \rho g R S , \tag{2.6}$$

where ρ is the density of water, g is the acceleration of gravity, R is the hydraulic mean channel radius, and S is the bed slope.

Manning's equation for uniform, steady channel flow in rivers is

$$V = 1.49 \frac{R^{2/3} S^{1/2}}{n}, \tag{2.7}$$

where V is velocity and n is Manning's n.

Solving Eqn. 2.7 for S and substituting into Eqn. 2.6 produces an equation for the bottom shear stress in terms of Manning's n, the velocity, and the geometric properties of the channel so that

$$\tau = \rho g \left(\frac{n}{1.49} \right)^2 \frac{V^2}{R^{1/3}}. \tag{2.8}$$

It is assumed that the same approach applies to reversing tidal flows. Letting R equal the depth (appropriate approximation for wide channels), the x- and y-components of bottom shear stress in terms of Manning's n are

$$\tau_x = \rho g \left(\frac{n}{1.49} \right)^2 \frac{u\sqrt{u^2 + v^2}}{h^{1/3}} \tag{2.9}$$

Reproduced with permission of the copyright owner. Further reproduction prohibited without permission.

and

$$\tau_y = \rho g \left(\frac{n}{1.49} \right)^2 \frac{v\sqrt{u^2 + v^2}}{h^{1/3}}, \tag{2.10}$$

where h is channel depth (distance from bottom to surface).

Roughness parameter n may be assigned manually or automatically. Manual assignment can be made for either individual elements or by groups of elements. Automatic assignment involves assignment according to depth at each iteration; given user-specified parameters, a curve is generated for n as a function of depth.

2.4.2.2 Eddy Viscosity

Turbulence may be defined as temporal fluctuations in velocity that promote mixing (see, for example, Fox and MacDonald, 1998). Lateral mixing of momentum between faster and slower areas effectively acts as horizontal friction or damping. The Galerkin method used by RMA2 requires a certain amount of artificial damping in the form of added horizontal turbulence mixing in order to achieve stability. This turbulence is specified in RMA2 in terms of eddy viscosity (E_{xx}, E_{xy}, and E_{yy} in the horizontal Reynold's stress terms in the equations of motion, Equations 2.1 and 2.2). Although the eddy viscosity, as defined in RMA2, includes both the molecular viscosity and the effects of turbulence from the Reynold's stress terms, it is the Reynold's stress turbulence that dominates. It is difficult to estimate the value of E, but analogy with physical conditions implies that turbulence exchanges depend on the momentum of the fluid and the distance over which that momentum is applied. Therefore, as the element size decreases, or the velocity decreases, E should decrease. The eddy viscosity equation is

Reproduced with permission of the copyright owner. Further reproduction prohibited without permission.

$$E_{xy}\frac{\partial^2 u}{\partial y^2} = \mu\frac{\partial^2 u}{\partial y^2} - \rho\frac{\partial \overline{u'v'}}{\partial y} \tag{2.11}$$

where

E_{xy} = eddy viscosity
ρ = density of water
μ = molecular viscosity
u', v' = turbulent deviations of the instantaneous velocity from the average velocities u,v
$\overline{u'v'}$ = time average of fluctuations (horizontal Reynolds stress/-ρ).

Note that the first term on the right hand side of Equation 2.11 (molecular viscosity term) is much less than the second term (Reynolds stress term).

RMA2 provides three methods to specify turbulence in the form of E, the turbulent exchange coefficient: direct assignment, automatic assignment by Peclet number, and automatic assignment Smagorinsky coefficient.

Direct assignment involves assigning an E to each element, or group of elements, based on a representative element length and maximum streamwise velocity. Automatic assignment by Peclet number allows E to be adjusted for each iteration, based on element size and the *calculated* velocity. The Peclet number and minimum velocity are specified, where Peclet number is given by

$$P = \frac{\rho u dx}{E} \tag{2.12}$$

and P is Peclet number, ρ is the density of water, u is velocity, dx is the characteristic element size, and E is eddy viscosity. It is recommended that P be between 15 and 40. It should be remembered that as area and velocity increase, eddy viscosity increases, so the Peclet number should be specified at a lower value.

Reproduced with permission of the copyright owner. Further reproduction prohibited without permission.

Automatic assignment by Smagorinsky coefficient allows real-time adjustment of eddy viscosity based on the calculated velocity. This method considers the velocity gradients in calculating the appropriate eddy viscosity, and is especially relevant for highly turbulent areas such as near structures. Eddy viscosity is given in terms of Smagorinski coefficient by

$$E = TBFACT * A\left[\left(\frac{\partial u}{\partial x}\right)^2 + \left(\frac{\partial v}{\partial y}\right)^2 + 2\left(\frac{\partial u}{\partial x} + \frac{\partial v}{\partial y}\right)\right] \tag{2.13}$$

where:

$TBFACT$ = Smagorinsky coefficient
A = the area of the element
$\frac{\partial u}{\partial x}$ and $\frac{\partial v}{\partial y}$ = average elemental change in the velocity component
E = eddy viscosity.

TBFACT has a recommended value range of 0.094 and 0.2 (King et al., 2001).

2.4.2.3 Marsh Porosity

The marsh porosity tool in RMA2 is useful for tidal models because it allows elements to transition gradually between wet and dry states. Having an element suddenly go dry and turn off causes large instabilities in the model, so marsh porosity essentially gradually lowers the ability of an element to hold water, keeping at least a thin "film" of water (the residual water volume) in an element that is drying out until all associated nodes are dry. The opposite occurs as water levels rise: the element rejoins the mesh as soon as one of its nodes becomes wet again.

Reproduced with permission of the copyright owner. Further reproduction prohibited without permission.

A wetted area curve shown in (Figure 2.2) defines the surface area of standing water as a function of water surface elevation. Figure 2.2(a) shows a realistic curve that would be possible to use if detailed bathymetric contours were available; since this data is not usually available, an approximate curve is used to describe the wetted area for each node (Figure 2.2(b)). It can be described with four parameters: AC1, AC2, AC3, and AC4. AC1 is the vertical distance between average regional bed elevation (A0) and the minimum regional bed elevation, AC2 is the transition range of the regional nodal distribution, AC3 is the minimum wetted surface area factor (the point at which the node goes dry), and AC4 (not specified by user) is the minimum regional bed elevation. "Regional" refers to the area in the immediate vicinity of a node. AC3 should be small (on the order of 0.01) but always greater than zero (King et al., 2001).

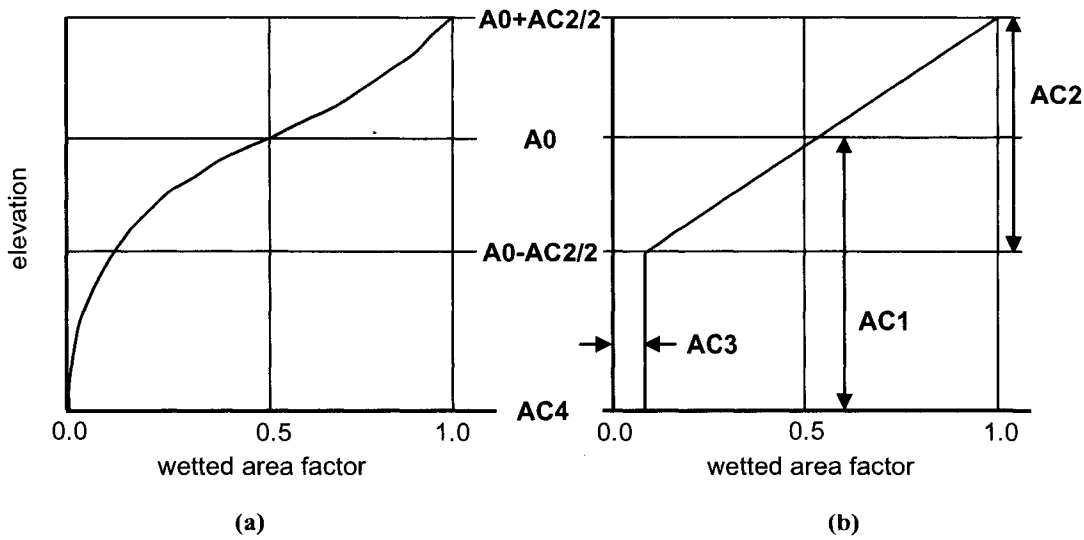

Figure 2.2 Wetted nodal region area definition by marsh porosity (King et al., 2001). (a) Nodal wetted area curve obtained from field data, and (b) schematized nodal wetted area curve obtained by approximation.

Reproduced with permission of the copyright owner. Further reproduction prohibited without permission.

2.4.3 Boundary and Initial Conditions

The final inputs to the model are the boundary conditions and the initial conditions. Boundary conditions must be applied to nodes or nodestrings to drive the model. A boundary condition may be in the form of a flow rate, water surface elevation (WSE), reflecting boundary, rating curve, velocity, or no-slip condition (parallel/slip flow at all boundary nodes is default). In the case of tidal forcing with complicated geometry, water surface elevation (pressure head) is the best option for open boundaries. The boundary condition location should be sufficiently far from the area of interest, so that the boundary condition forcing will not directly affect the results there.

For a transient water surface elevation boundary condition, it is also necessary to specify initial conditions. In RMA2, initial conditions can be in the form of a coldstart or a hotstart. To coldstart the model run, each node is assigned the same initial water surface elevation, and the two-dimensional velocities are assumed to be zero. This method is simple to use, as it involves only assigning the initial water level (making sure it corresponds to the first water level of the boundary condition time series). It does, however, require that this water level be high enough to ensure that all nodes in the mesh are wet (covered) at the beginning of the model run. This usually means that the boundary condition time series must be amended to allow a gradual, artificial ramping down of the water level from the initial water level to a point in the time series (also known as spin-up). It must be gradual for the model to stably converge to a solution. Another disadvantage to this method is that time must be allowed for the model to stabilize and for the influence of the artificially high initial condition to diminish. The initial condition spin-up may take approximately 10 simulated hours, but it may take as

Reproduced with permission of the copyright owner. Further reproduction prohibited without permission.

many as 45 simulated hours for the simulation to stabilize. Figure 2.3 shows an example of an initial condition ramping down to the boundary condition time series.

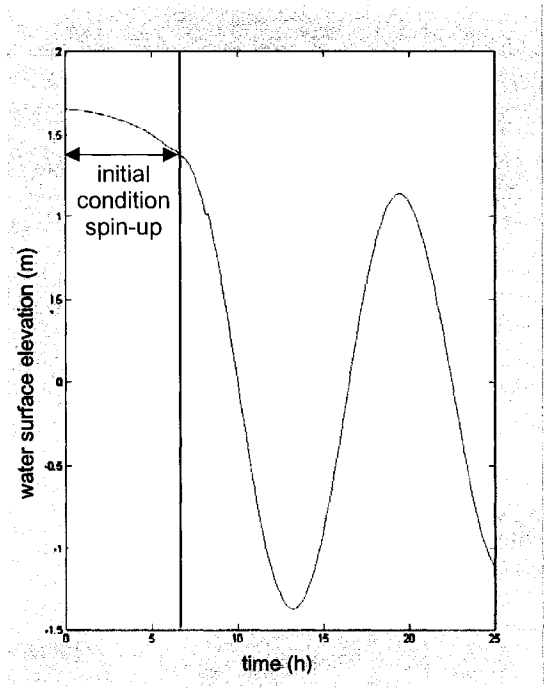

Figure 2.3 Example of initial condition transitioning to boundary condition.

Hotstarting involves the initial conditions being read from the results of a previous model run. It eliminates the time coldstarting takes to spin up, but requires more pre-processing time to make sure that the initial condition in the hotstart record matches the right iteration and time step in the boundary condition file. When running a simulation, there is an option to write output to a hotstart file. If this is turned on, the model writes calculation results to this file either at the end of every time step, or at the end of the entire run. Then, this file can be used to hotstart another model run. This method, however, restricts the use of the hotstart file to models with exactly the same

Reproduced with permission of the copyright owner. Further reproduction prohibited without permission.

geometry, so a particular hotstart file cannot be used once the geometry has been modified.

2.4.4 Running and Calibrating the Model

To run the model, a binary geometry file must first be generated, and for this an executable called GFGEN (Geometry File GENerator) is used. Finally, the RMA2 executable is run.

Modeling is an iterative process and calibration is the procedure used to adjust the model parameters so that model accuracy is optimized. RMA2, in conjunction with SMS, can produce a time series of water levels or velocities at any given point, so it is simple to compare to a relevant series of data collected in the field. The model parameters can then be adjusted (changes must be made logically and with the underlying physics in mind) until a reasonable match is achieved. It can then be assumed that the model is capable of making reasonably accurate predictions.

Reproduced with permission of the copyright owner. Further reproduction prohibited without permission.

CHAPTER 3

MEASUREMENT PROGRAM

3.1 Data Requirements

Physical data are essential for hydrodynamic modeling. It is first necessary to provide an accurate representation of the bathymetry as the basis of the model. Once the model is ready to run simulations, calibration data are needed for comparison with model predictions. For this model, both tidal water surface elevation data and current velocity data were used for calibration. Field data were acquired in the post-dredge field program described by Knuuti et al. (2007).

3.2 Bathymetry Data

Since a comprehensive field program was not carried out to collect a complete data set, bathymetry data came from five different sources and needed to be integrated successively. The data sets are described below and will be referred to as follows: ACOE, State, ERDC, CCOM, and Middle Ground.

3.2.1 ACOE

ACOE bathymetry data (Figure 3.1) was actually obtained before dredging and was used here for the extensive areas not affected by channel changes. It was extracted from the previous model of Hampton Harbor completed by UNH graduate student Serkan

Reproduced with permission of the copyright owner. Further reproduction prohibited without permission.

Mahmutoglu (Mahmutoglu, 2001) and developed further by Joseph Letter of the U.S. Army Corp of Engineers (Letter et al., 2005). This data set was originally assembled using a combination of nautical charts, aerial photography, sounding surveys, and topographic data. Data referenced the New Hampshire State Plane (NHSP) NAD83 horizontal datum and the NAVD88 vertical datum, in meters. (NAVD88 is the North American Vertical Datum of 1988, established in 1991 by a minimum-constraint adjustment of Canadian-Mexican-U.S. leveling observations was performed holding fixed the height of the primary tidal benchmark, referenced to the new International Great Lakes Datum of 1985 (IGLD 85) local mean sea level height value, at Father Point/Rimouski, Quebec, Canada (Zilkoski et al., 1992).) Although it was not up-to-date in the vicinity of the study site, it was the most complete data set, covering the entire area that needed to be modeled for this project. By opening the model geometry file in SMS (RMA2 user interface), it was possible to use the **Mesh → Scatterpoint** tool to create a scatter set from the previous mesh. A scatter set consists of xyz data point, where x and y refer to horizontal coordinates, and the z to elevation. Elevation is measured positive upwards from the datum, as opposed to depth, which is measured positive down from the datum. Since this data set was the most comprehensive, it was used as the base data set, with other, newer sets replacing the areas they covered.

Reproduced with permission of the copyright owner. Further reproduction prohibited without permission.

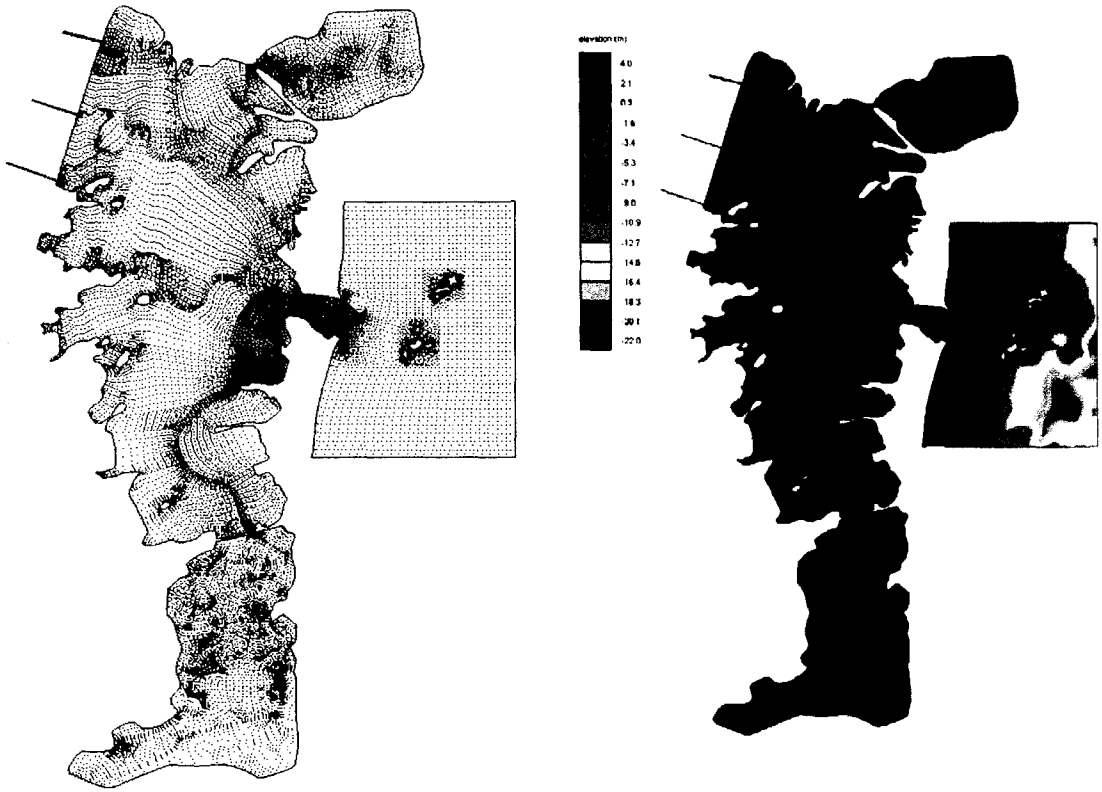

(a) (b)

Figure 3.1 ACOE bathymetry data. (a) Scatter set and (b) contours.

3.2.2 State

The State data set (Figure 3.2) was collected during the winter of 2005 (post-dredge) by Southwind Construction Company of Evansville, Indiana, which was hired to dredge Seabrook Harbor. Their data set was received in the form of an AutoCAD drawing (.dwg) file and was extracted into a tabular format by James Case of UNH's Center for Coastal Ocean Mapping. The area covered was from the southernmost end of Seabrook Harbor to partway up the Hampton River to the northwest, and was referenced to NHSP NAD83 (horizontal), in feet, and NAVD88 (vertical), in tenths of feet. The U.S. Army Corps's conversion program, Corpscon, was used to convert horizontal coordinates and elevations to meters.

Reproduced with permission of the copyright owner. Further reproduction prohibited without permission.

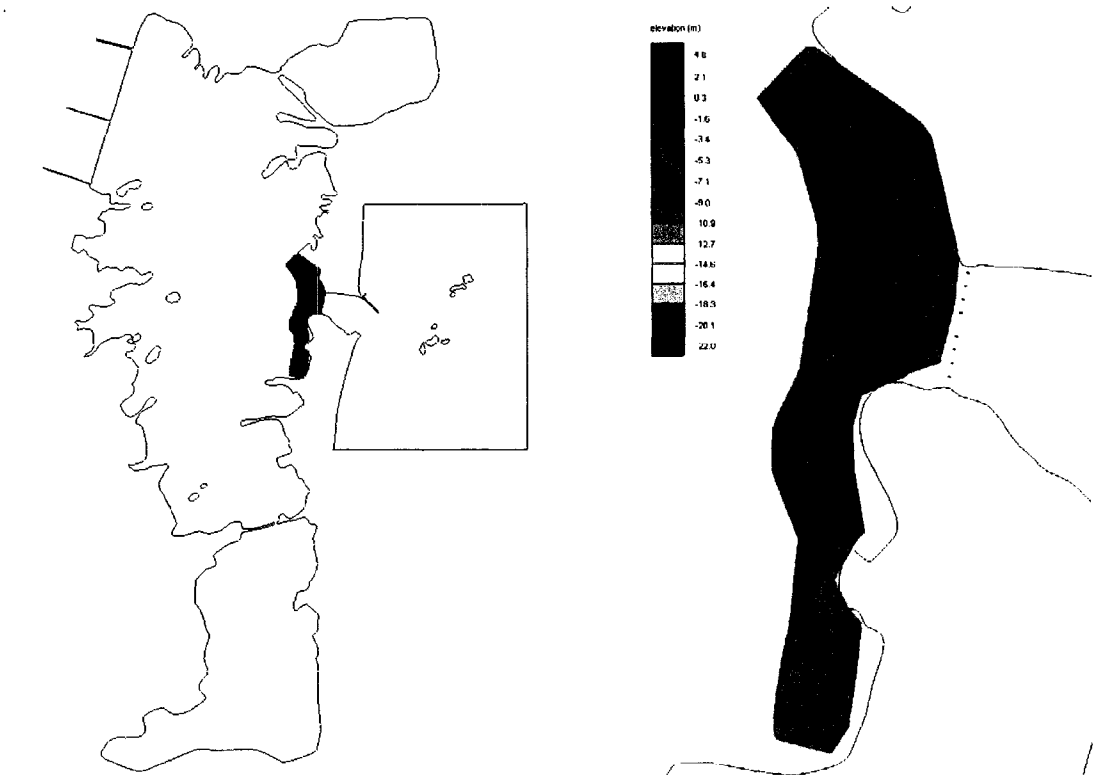

(a) (b)

Figure 3.2 State bathymetry data. (a) Scatter set and (b) contours.

3.2.3 ERDC

Engineer Research and Development Center (ERDC) bathymetric surveys were carried out by the U.S. ACOE for post-dredge conditions (Figure 3.3). The original data set was referenced to NHSP NAD27 (horizontal) and mean low water (MLW) for the tidal epoch of 1941-1960 (vertical), in feet. Kevin Knuuti of the U.S. ACOE Coastal and Hydraulics Laboratory calculated the correction factor for the vertical conversion to NAVD88 [MLW elevation (1941-1959 epoch) – 4.55 ft = NAVD88 elevation], and Corpscon was used to convert from feet to meters, and from NAD27 to NAD83.

Reproduced with permission of the copyright owner. Further reproduction prohibited without permission.

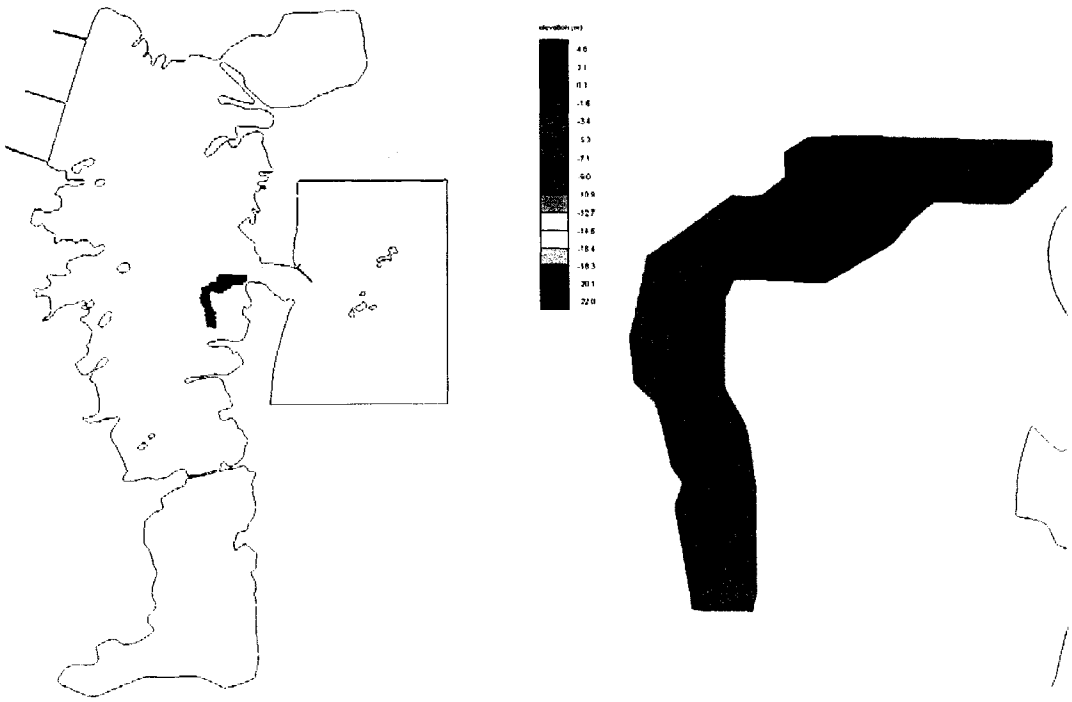

(a) (b)

Figure 3.3 ERDC bathymetry data. (a) Scatter set and (b) contours.

3.2.4 CCOM

The Center for Coastal Ocean Mapping (CCOM) at UNH conducted bathymetric surveys in the summer of 2005 using a custom built pontoon boat, with the sounding equipment listed in Table 3.1 The surveys (Figure 3.4) covered the Blackwater River, the new cut through the northern part of the middle ground sandbar, north of the sandbar, and east to the bridge. There was one line of data collected in Seabrook Harbor, but it was excluded since one line would not produce accurate bathymetry contours. Water level data were collected concurrently in the area to provide tidal depth corrections. These data referenced WGS84, which is reasonably equivalent to NHSP NAD83, and NAVD88, in meters (Pers. communication, Jon Scott).

Reproduced with permission of the copyright owner. Further reproduction prohibited without permission.

Table 3.1 Sounding equipment specifications for CCOM bathymetry survey.

CCOM Bathymetry Survey Sounding Equipment
2 Ashtec Z XII phase differential GPS receivers used in PPK mode
1 TSS 335B inertial motion sensor
1 Klein 3000 sidescan sonar
1 Knudsen 320 BP narrow beam dual frequency sounder (50 & 200 KHz)
Hypack software for line planning and survey control

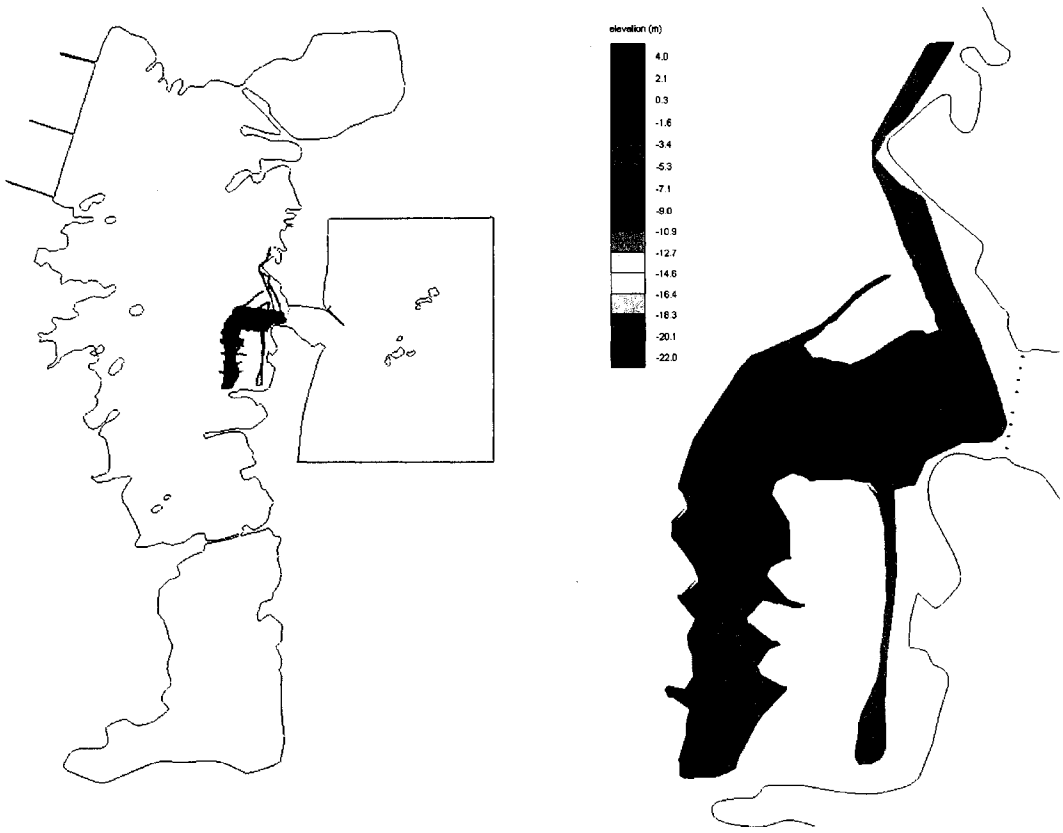

(a) (b)

Figure 3.4 CCOM bathymetry data. (a) Scatter set and (b) contours.

3.2.5 Middle Ground

No post-dredge data points were available for the middle ground area, but it was essential to obtain them, since it was the location of major changes. Using a Nikon AE7 surveying level and a recreational-grade differential GPS unit, six points and elevations were surveyed by the author and Kevin Knuuti of the U.S. Army Corps of Engineers at low tide across the former River Street cut, in addition to two points at the top edge of the

Reproduced with permission of the copyright owner. Further reproduction prohibited without permission.

bulkhead. Surveying took place on 17 October 2005. Accuracy of the elevation was expected to be less than 0.01 meters, and that of the horizontal coordinates was +/- 10 meters (Pers. communication, Kevin Knuuti). Time constraints restricted the survey to these eight points, so each elevation was extrapolated across the sand bar, and the bulkhead elevation was extrapolated along both sides, using a geo-referenced aerial photograph for guidance (Figure 3.5). The original data set (pre-dredge ACOE) for the rest of middle ground was referenced to NHSP NAD83 and NAVD88, in meters, and did not need to be converted.

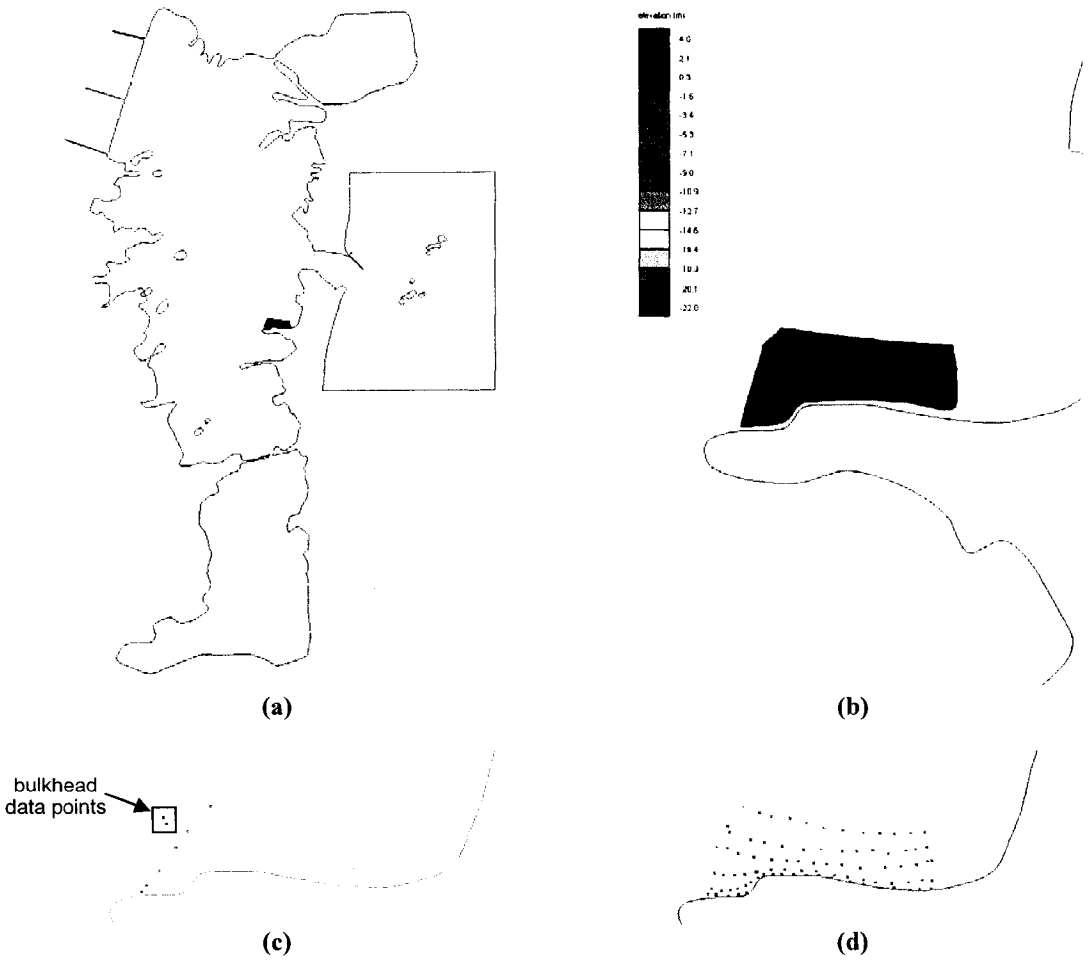

Figure 3.5 Middle ground (a) scatter set, (b) contours, (c) collected data points, and (d) magnified view of final scatter set.

Reproduced with permission of the copyright owner. Further reproduction prohibited without permission.

Additionally, field observations provided estimates of elevations immediately outside of the bulkheads, since bathymetric surveys did not get close enough to provide data in that area.

3.2.6 Integration of Data Sets

To integrate the data sets into one comprehensive bathymetry data set, a hierarchy needed to be established to determine which data set would take precedence over which. As mentioned above, the pre-dredge ACOE data set was the most comprehensive, albeit not the most recent. The CCOM data set was next imported into SMS, and the ACOE scatter points that were covered by the CCOM data were deleted. The two data sets were merged using the **Merge Scatter Set** tool.

The ERDC data set was covered by the more recent (more than six months later) extensive CCOM survey, and therefore was not used. When compared, ERDC elevations were generally less than 0.3 meters lower than CCOM elevations, which can possibly be explained by sediment filling in the dredged channel in the six months between surveys.

Although the CCOM data set was more recent and believed to be more accurate than the State data, it did not sufficiently cover the Seabrook Harbor area, one of the main areas of interest. The CCOM data were retained in the bridge area, but the State data set was used north and south of that (Figure 3.6). When the State data set was merged with the ACOE/CCOM data set, there appeared to be a discrepancy between the two sets in the bridge area and along the east edge of the middle ground shoal (Figure 3.7(a)). To test whether this was due to the actual bathymetry or whether there was a datum issue involved, lines were drawn along the edges where ACOE/CCOM and State data

Reproduced with permission of the copyright owner. Further reproduction prohibited without permission.

overlapped (Figure 3.7(b)). Adjacent elevations from each data set were noted along each line (one data set on either side of the line), and it was found that the State set consistently had higher elevations in the same areas, and that the average difference was about 0.8 meters (APPENDIX A). This was considered to be reasonable evidence that there was a datum error in one of the sets. Since the Center for Coastal Ocean Mapping provided more information on equipment specifications and methodology than the dredging company, there was more confidence in the accuracy of the CCOM data set. Consequently, each elevation in the State data set was decreased by 0.8 meters, and this appeared to fix the discrepancy (Figure 3.7(c)). Finally, the collected and extrapolated data for middle ground was merged with the ACOE/CCOM/State scatter set, resulting in the final bathymetry (Figure 3.8).

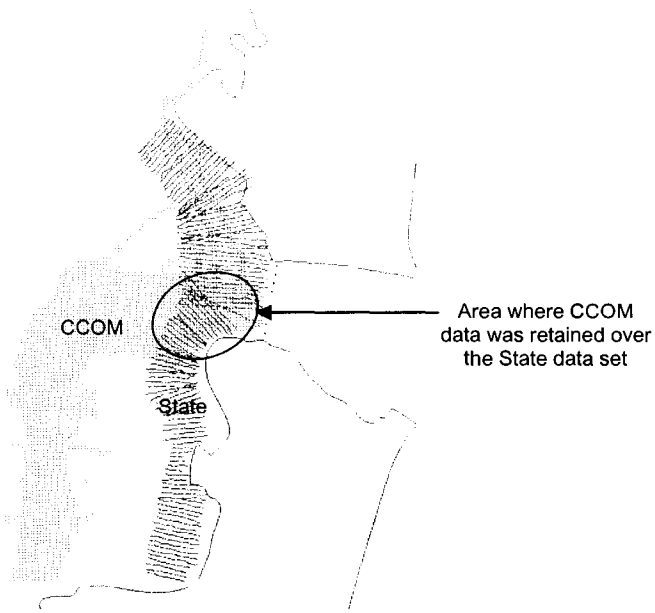

Figure 3.6 Overlap of CCOM and State bathymetry data sets.

Reproduced with permission of the copyright owner. Further reproduction prohibited without permission.

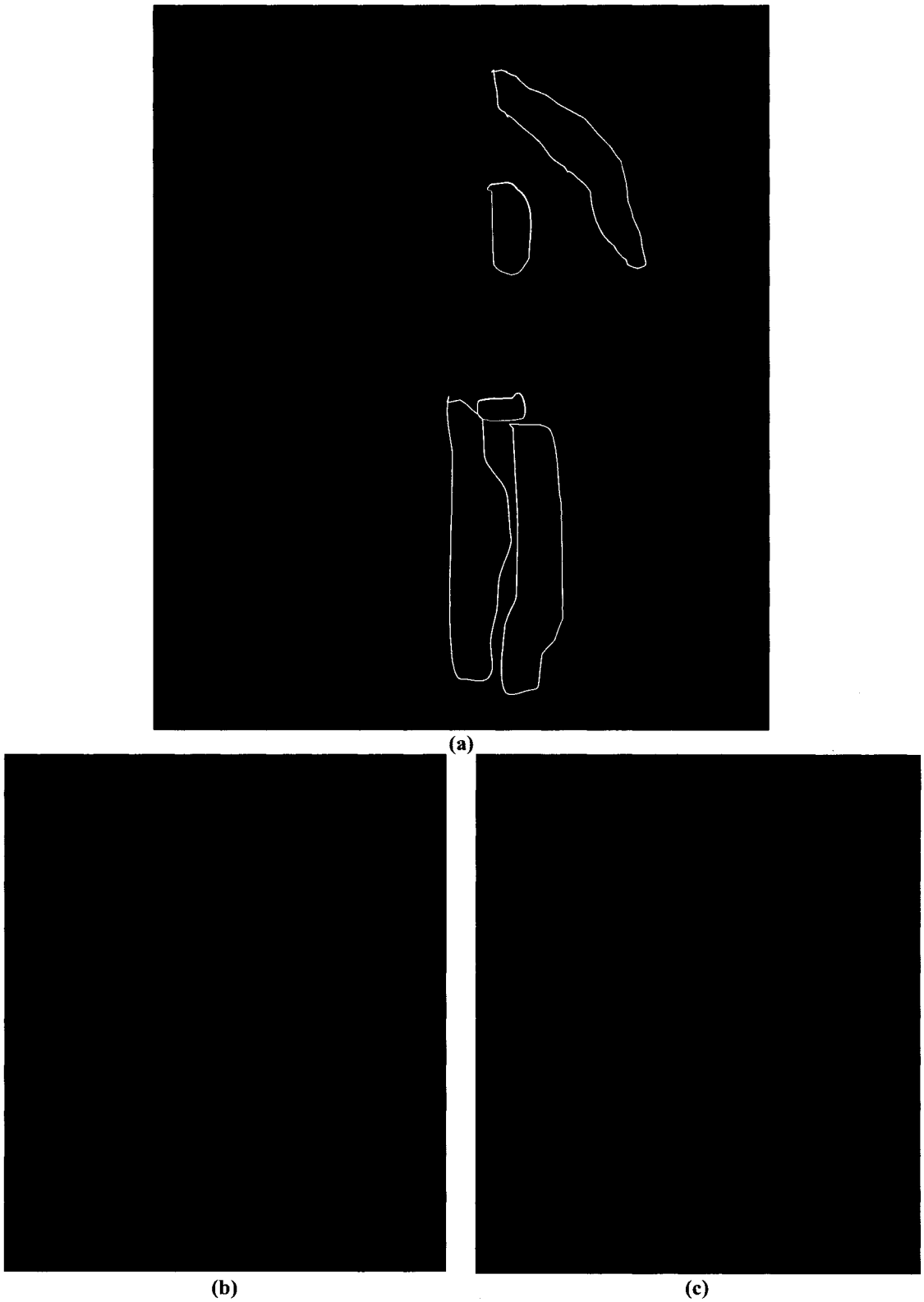

Figure 3.7 (a) Contours showing discrepancies between ACOE/CCOM and State sets, (b) lines showing edges of overlap, and (c) corrected contours.

Reproduced with permission of the copyright owner. Further reproduction prohibited without permission.

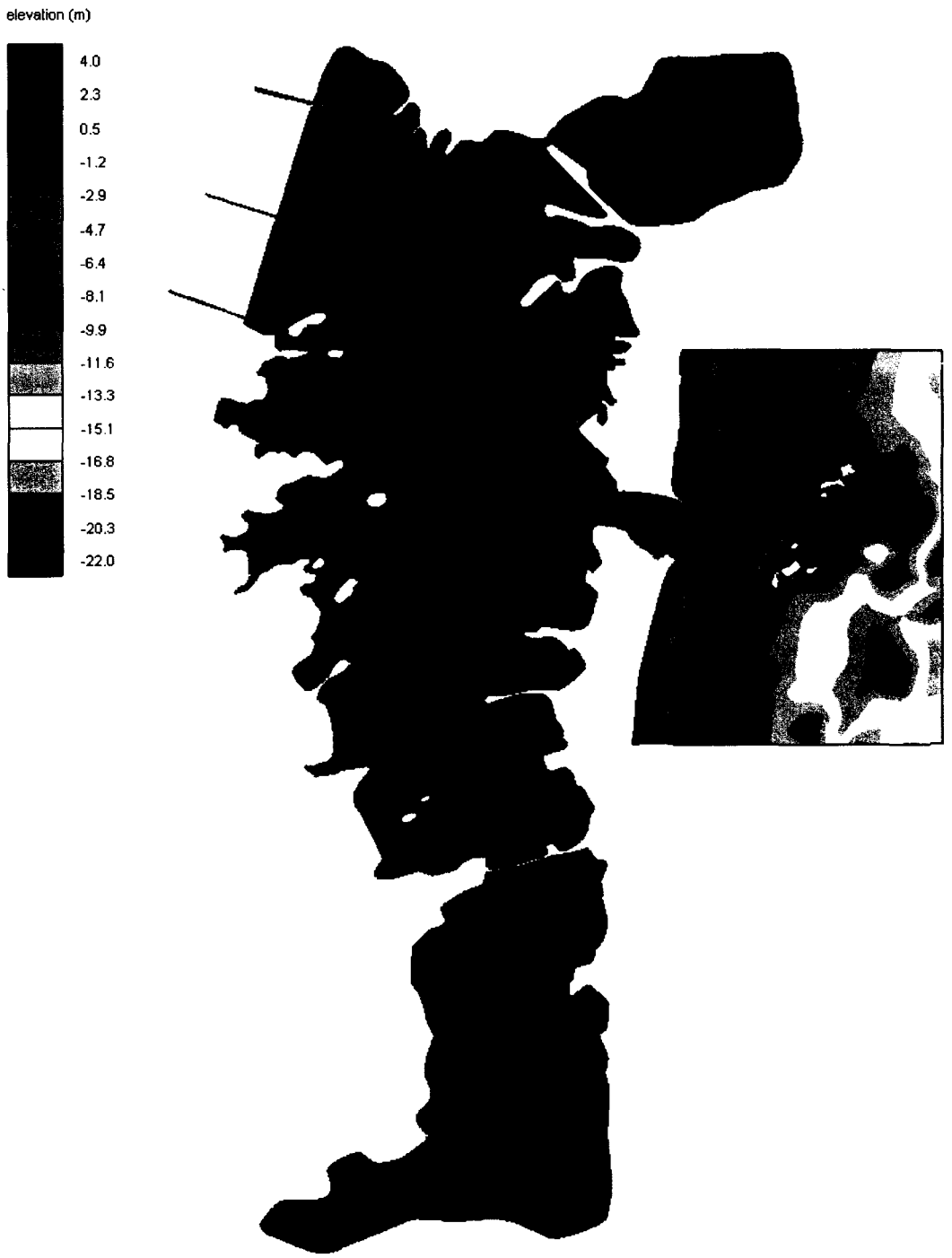

Figure 3.8 Final bathymetry contours.

Reproduced with permission of the copyright owner. Further reproduction prohibited without permission.

3.3 Tidal Water Level Data

During the summer of 2005, tidal water level data were collected as part of the comprehensive post-dredge field monitoring program. Five tide gauges were installed throughout the harbor, and were surveyed relative to local benchmarks to provide a common datum. Figure 3.9 shows the locations of the tide gauges: Normandeau Associates Pier (NAI), Beckmann's Point Jetty (BPJ), Yankee Fish Co-op (YFC), Seabrook Town Pier (STP), and Chouinard Private Pier (CPP). Locations, coordinates, and periods of record are listed in Table 3.2.

Figure 3.9 Locations of tide gauges.

Reproduced with permission of the copyright owner. Further reproduction prohibited without permission.

Table 3.2 Locations and periods of record of tide gauges in the harbor area.

Station	Latitude	Longitude	Description of Location	Periods of Record (2005)
NAI	42° 54.043'	-70° 49.144'	End of the pier belonging to Normandeau Associates, northwest of the inlet in Hampton Harbor	6/24-7/6 7/8-7/13 7/19-10/6
BPJ	42° 53.585'	-70° 48.620	Entrance to Hampton/Seabrook Harbor, at the southeast corner of the channel	7/1-9/1 10/14-10/16
YFC	42° 53.485'	-70° 49.183'	Wooden pile approximately halfway between the Co-op building and the northern end of the Co-op bulkhead	6/2-6/8 6/14-6/22 6/23-8/4
STP	42° 53.278'`	-70° 49.264'	End of the Seabrook Town Pier near the eastern entrance to what used to be the River Street Cut in Seabrook Harbor	6/2-6/8 6/10-6/22 6/23-9/1 9/5-10/6
CPP	42° 53.255'	-70° 49.546'	End of a private pier at the western-most end of River Street, near what used to be the western entrance to the River Street Cut	6/2-6/8 6/14-9/1 10/6-11/3

Each tide gauge station consisted of an Aanderaa Instruments pressure and temperature sensor (Model 3796A) and data logger (Model 3634). With the exception of the BPJ tide gauge, each station also included a permanent tide staff for visual documentation during calibration and downloading. BPJ had only a temporary tide staff during calibration (Ward et al., 2006).

Prior to being installed in the field, the tide gauges were tested in the deep tank at the UNH Chase Ocean Engineering Laboratory. Any pressure sensors or data loggers that displayed errors, drift, or other such problems were replaced (Ward et al., 2006).

Once installed, the tide gauges needed to be leveled (determining absolute elevation of tide staffs in NAVD88) and calibrated. Using standard surveying

Reproduced with permission of the copyright owner. Further reproduction prohibited without permission.

techniques, leveling was conducted on 3 June 2005 for CPP, YFC, and STP, and on 17 August 2005 for NAI and a reference point for BPJ (since the BPJ tide staff could not be permanently installed). The actual BPJ tide staff elevation was leveled on 24 August 2005. NAI was re-leveled on 22 August 2005 due to instrument concerns and a final survey was conducted for CPP, STP and NAI on 22 February 2006 for verification. Each tide station was corrected to the NAVD88 datum by leveling between a New Hampshire Department of Transportation benchmark and a specified mark on the tide staff. All repeat surveys agreed with the originals to within the estimated error of 3 cm (Ward et al., 2006).

The tide gauges were then calibrated in the field by simultaneously taking water level measurements from the pressure sensors and visually observing the water level with the tide staffs every 10 minutes for approximately 3 hours. The calibration data were analyzed using regression analyses and a least squares fit between the sensor and visual readings. The offsets resulting from the analyses were used to correct the data collected by the pressure sensors (Ward et al., 2006).

Accuracy was determined to be approximately 15 cm due to discrepancies between the mean water levels of NAI and BPJ, which showed good agreement with each other, and those of CPP, STP, and YFC, which also showed good agreement with each other. It was expected that that the means for each station would be similar when averaged over several months, but since they were not, the accuracy cannot be any better than the differences between the stations. At present, these discrepancies have not been resolved (Ward et al., 2006).

Reproduced with permission of the copyright owner. Further reproduction prohibited without permission.

The data sets covered a period between 2 June 2005 and 9 November 2005, although not all gauges were functional at all times. The raw data were also subjected to tidal analysis to obtain tidal constituents. Using the tidal constituents to predict surface elevation has the effect of removing the influence of meteorological events (essentially a prediction of the tides due to only astronomical forcing). Periods of record for each tide station are listed in Table 3.2, and plots of water level for each station can be found in APPENDIX B. The data loggers were programmed to average over 2-minute or 5-minute intervals; the 2-minute intervals were used during the CCOM bathymetric survey, and the 5-minute intervals otherwise. The data was subsequently averaged to 10-minute intervals for presentation and other uses, and referenced coordinated universal time (UTC). Table 3.3 lists the tidal constituents resulting from the tidal analysis.

Reproduced with permission of the copyright owner. Further reproduction prohibited without permission.

Reproduced with permission of the copyright owner. Further reproduction prohibited without permission.

Table 3.3 Analyses of tidal constituents for the five stations located in Hampton-Seabrook Harbor (Ward et al., 2006).

	Beckman Point Jetty		Normandeau Pier		Yankee Fish Coop		Seabrook Town Pier		Chouinard's Private Pier	
	amplitude (m)	phase (° Greenwich)	amplitude (m)	phase (° Greenwich)	amplitude (m)	phase (° Greenwich)	amplitude (m)	phase (° Greenwich)	amplitude (m)	phase (° Greenwich)
O1	0.107±0.006	186.4±3.4	0.112±0.007	192.7±3.4	0.116±0.006	193.5±2.9	0.109±0.009	193.3±4.1	0.116±0.007	197.4±3.3
K1	0.149±0.006	216.1±2.4	0.134±0.007	219.3±3.0	0.168±0.007	213.0±2.2	0.138±0.008	211.2±4.0	0.157±0.008	219.6±2.7
N2	0.322±0.017	079.4±2.8	0.313±0.020	081.5±3.5	0.310±0.017	089.7±3.1	0.292±0.022	083.5±4.5	0.308±0.016	092.2±2.9
M2	1.269±0.018	107.6±0.9	1.305 ±0.020	113.1±0.9	1.322±0.017	110.4±0.7	1.312±0.020	112.0±1.0	1.319±0.018	113.9±0.6
S2	0.167±0.018	161.3±6.3	0.200±0.018	161.4±5.4	0.124±0.017	162.0±8.7	0.188±0.019	151.8±6.5	0.143±0.015	166.8±5.7
M4	0.021±0.003	310.5±9.1	0.0300±0.005	000.3±10	0.041±0.004	342.1±6.3	0.038±0.004	345.0±6.4	0.012±0.003	047.2±14
M6	0.004±0.002	266.6±27	0.018±0.002	284.8±9.1	0.014±0.004	265.2±15	0.015±0.002	260.1±7.7	0.012±0.006	295.3±23
M8	0.001±0.001	143.9±41	0.004±0.001	221.7±14	0.002± 001	221.4±50	0.001±0.001	203.3±55	0.006±0.002	246.2±14
	99.4% variance		99.0% variance		99.2% variance		97.9% variance		99.0% variance	

3.4 Tidal Current Data

Tidal current data were also collected as part of the field monitoring program. Current velocity profiles were collected at cross-channel transects using an RD Instruments Broadband 1200Hz Acoustic Doppler Current Meter installed and mounted on a shallow draft UNH research boat. A Leica 412B Differential GPS was used for accurate positioning (Ward et al., 2006)

Figure 3.10 shows the approximate locations of the current transects: Third Piling (HS3P), Blackwater River New Channel (HSBWNC), Blackwater River Old Channel (HSBWOC), and Yankee Fish Co-op (HSYFC). The set of current cross-sections was repeated sequentially as many times as possible, collected over half a tidal period each sampling day, and each transect consisted of two runs across the channel (back and forth) (Ward et al., 2006). Table 3.4 lists the transects, their times, and during which part of the tidal cycle they were acquired.

Reproduced with permission of the copyright owner. Further reproduction prohibited without permission.

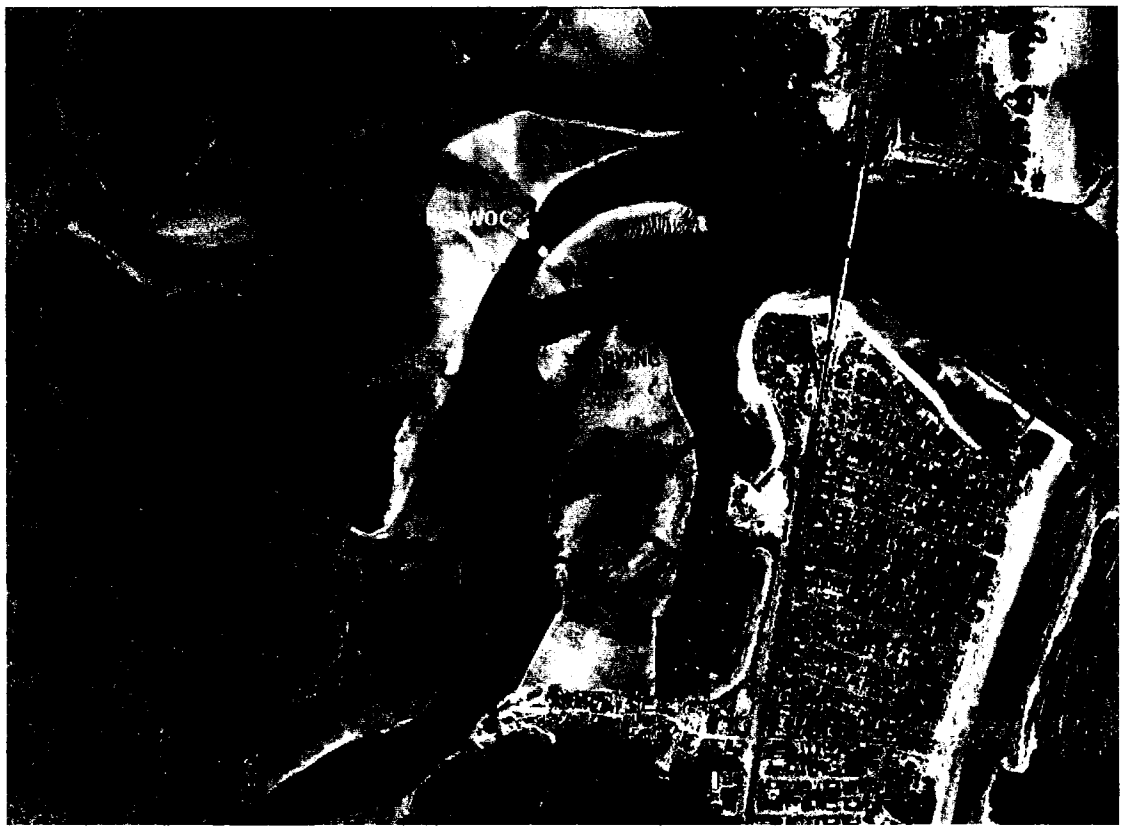

Figure 3.10 Approximate locations of current cross-section transects.

Table 3.4 Times of ADCP current cross-sections.

Transect	Date	Time (UTC)	Tide
HS3P1	23 June 2005	18:17:37	mid flood
HS3P2	23 June 2005	18:21:19	mid flood
HS3P3	23 June 2005	19:39:10	late flood
HS3P4	23 June 2005	19:41:43	late flood
HS3P5	23 June 2005	21:48:12	high water/early ebb
HS3P6	23 June 2005	21:49:24	high water/early ebb
HS3P7	24 June 2005	13:43:34	mid ebb
HS3P8	24 June 2005	13:44:57	mid ebb
HS3P9	24 June 2005	15:24:50	late ebb/low water
HS3P10	24 June 2005	15:27:20	late ebb/low water
HS3P11	24 June 2005	16:36:59	early flood
HS3P12	24 June 2005	16:41:01	early flood
HS3P13	24 June 2005	17:47:34	early flood
HS3P14	24 June 2005	17:52:58	early flood
HSBWNC1	23 June 2005	18:39:13	mid flood
HSBWNC2	23 June 2005	18:41:04	mid flood
HSBWNC3	23 June 2005	21:06:28	high water
HSBWNC4	23 June 2005	21:57:47	early ebb
HSBWNC5	23 June 2005	21:58:44	early ebb

Reproduced with permission of the copyright owner. Further reproduction prohibited without permission.

HSBWNC6	24 June 2005	14:07:13	late ebb
HSBWNC7	24 June 2005	14:08:52	late ebb
HSBWNC8	24 June 2005	14:11:36	late ebb
HSBWNC9	24 June 2005	14:13:38	late ebb
HSBWNC10	24 June 2005	15:44:46	low water
HSBWNC11	24 June 2005	15:46:31	low water
HSBWNC12	24 June 2005	16:54:59	early flood
HSBWNC13	24 June 2005	16:57:04	early flood
HSBWNC14	24 June 2005	18:09:19	mid flood
HSBWNC15	24 June 2005	18:11:47	mid flood
HSBWOC1	23 June 2005	18:33:56	mid flood
HSBWOC2	23 June 2005	18:35:27	mid flood
HSBWOC3	24 June 2005	13:57:18	late ebb
HSBWOC4	24 June 2005	13:59:20	late ebb
HSBWOC5	24 June 2005	14:00:42	late ebb
HSBWOC6	24 June 2005	15:37:46	low water
HSBWOC7	24 June 2005	15:39:34	low water
HSBWOC8	24 June 2005	16:49:03	early flood
HSBWOC9	24 June 2005	16:50:25	early flood
HSBWOC10	24 June 2005	18:04:03	mid flood
HSBWOC11	24 June 2005	18:06:08	mid flood
HSYFC1	23 June 2005	18:48:35	mid flood
HSYFC2	23 June 2005	18:50:24	mid flood
HSYFC3	23 June 2005	21:12:48	high water
HSYFC4	23 June 2005	21:14:12	high water
HSYFC6	24 June 2005	14:26:23	late ebb
HSYFC7	24 June 2005	14:28:49	late ebb
HSYFC8	24 June 2005	15:55:03	early flood
HSYFC9	24 June 2005	15:57:05	early flood
HSYFC10	24 June 2005	17:05:50	early flood
HSYFC11	24 June 2005	18:19:41	mid flood
HSYFC12	24 June 2005	18:23:08	mid flood

The vertical distribution of the velocity was obtained by sampling velocity in 0.25-meter bins, except for the top ~0.7 meters and bottom ~0.5 meters, where the ADCP is unable to determine velocity. Raw data were processed using RD Instruments' Winriver software. The processed files organized the data into ensembles that included the velocity magnitude and direction for each bin, along with related data such as measured total depth, position, date and time (Eastern Daylight), and water temperature.

Reproduced with permission of the copyright owner. Further reproduction prohibited without permission.

An ensemble was created every 1-2 seconds as the ADCP moved along the transect, but every 10 ensembles were averaged during processing to create a single velocity profile approximately every 13 seconds. Graphical presentation of the data can be found in APPENDIX C.

Reproduced with permission of the copyright owner. Further reproduction prohibited without permission.

CHAPTER 4

MODEL APPLICATION

4.1 Programs Used

For this model, RMA2 was used in conjunction with SMS 8.1 on a workstation at the University of New Hampshire's Chase Ocean Engineering Laboratory. SMS, a graphical user interface developed by the Environmental Modeling Research Laboratory at Brigham Young University, can be used to edit the mesh, material properties, and boundary conditions, and to generate graphical results.

4.2 Conceptual Modeling in SMS

RMA2 allows individual elements to have different material properties within a single mesh ("Material properties" is RMA2's term for friction and intertidal zone parameters.). In SMS, elements can be grouped according to common sets of material properties. The simplest way to accomplish this is to draw polygons within the boundary, so that the elements in the area enclosed by each polygon possess the same material properties (Figure 4.1). An aerial photo can be used as a guide to distinguish between different ground cover types, and bathymetry data can be used to make sure the polygons, and therefore elements, follow the bathymetric contours. Once the polygons are drawn, each can be meshed individually (Figure 4.2).

Reproduced with permission of the copyright owner. Further reproduction prohibited without permission.

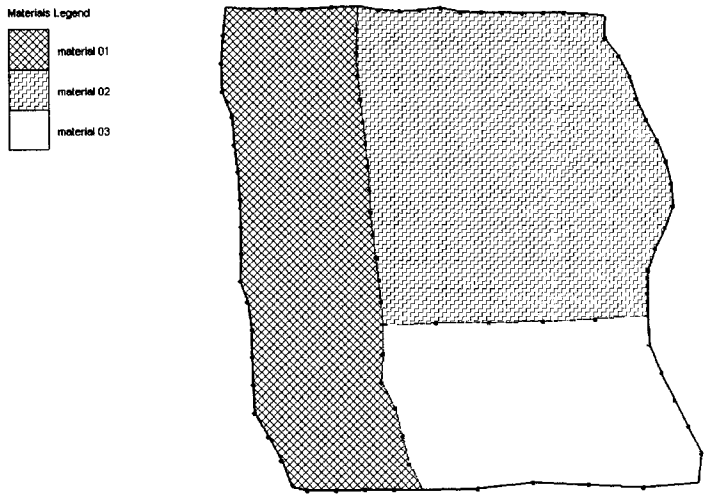

Figure 4.1 Polygons of different material types.

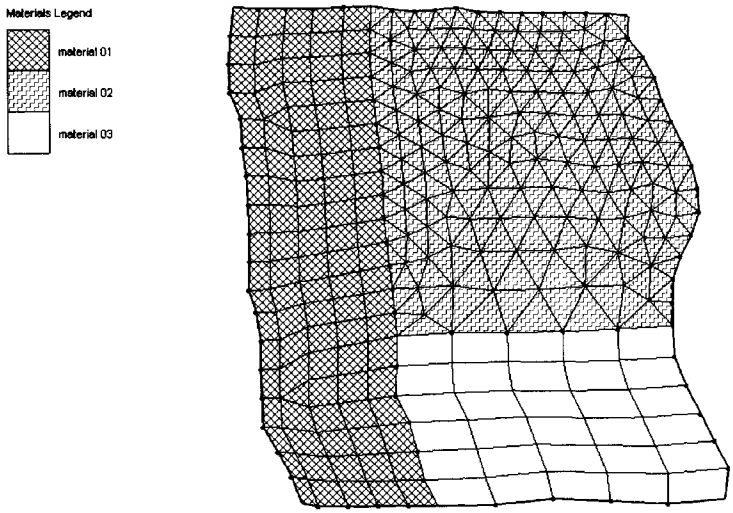

Figure 4.2 Each polygon meshed individually.

4.3 Mesh Generation

There are several methods of meshing in SMS: patching, adaptive tessellation, paving, adaptive density, and scalar paving density. In the case of Hampton/Seabrook Harbor, an existing mesh (ACOE) was available, so it was possible to use this one as a

Reproduced with permission of the copyright owner. Further reproduction prohibited without permission.

starting point, and simply edit to reflect the bathymetric changes. The ACOE mesh was adapted from the UNH mesh, and the process used to generate the UNH mesh is documented in Mahmutoglu (2001).

The ACOE mesh was opened in SMS, along with the new integrated bathymetry data set, and the bathymetry was interpolated to the mesh, replacing any old bathymetry data that were associated with the mesh. Since some of the mesh elements no longer followed the contours of the bathymetry (Figure 4.3), the mesh was edited to reflect the changes in the Middle Ground area, using both the contours and the geo-referenced aerial photograph for guidance (Figure 4.4).

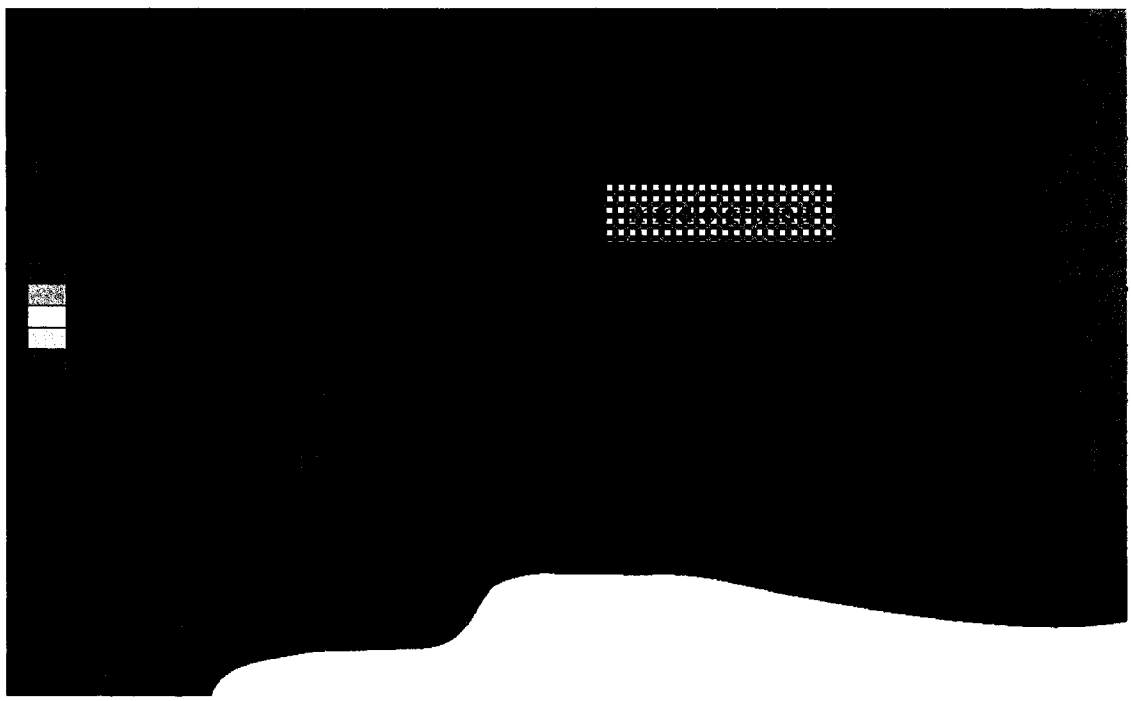

Figure 4.3 Old mesh with new bathymetry. Box indicates where changes in the mesh are needed.

Reproduced with permission of the copyright owner. Further reproduction prohibited without permission.

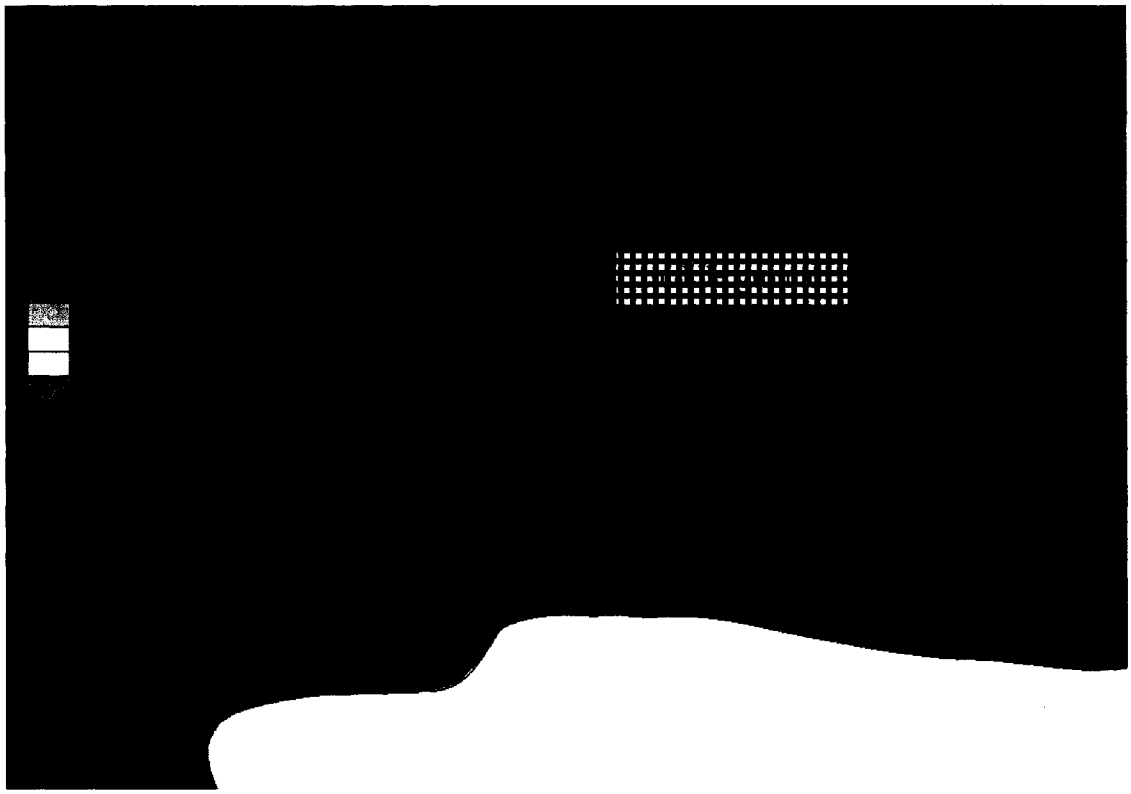

Figure 4.4 Mesh updated to reflect new harbor bathymetry.

To check the condition of the new elements, the "mesh quality" option in the display menu was turned on. This checks for minimum interior angle, ambiguous gradient (saddle-shaped element), concave quadrilaterals, maximum slope, element area change (between two elements), number of elements connected (maximum of eight), and maximum interior angle, and flags problem elements so that they can be fixed. Once these issues were resolved, the bathymetry was re-interpolated to this new version of the mesh. This reassigned elevations to each node in the mesh, since editing involved moving nodes.

The final mesh is shown in Figure 4.5. It contained 14,434 elements with a typical length of approximately 25 meters in the areas of interest, and 100 meters in the other areas.

Reproduced with permission of the copyright owner. Further reproduction prohibited without permission.

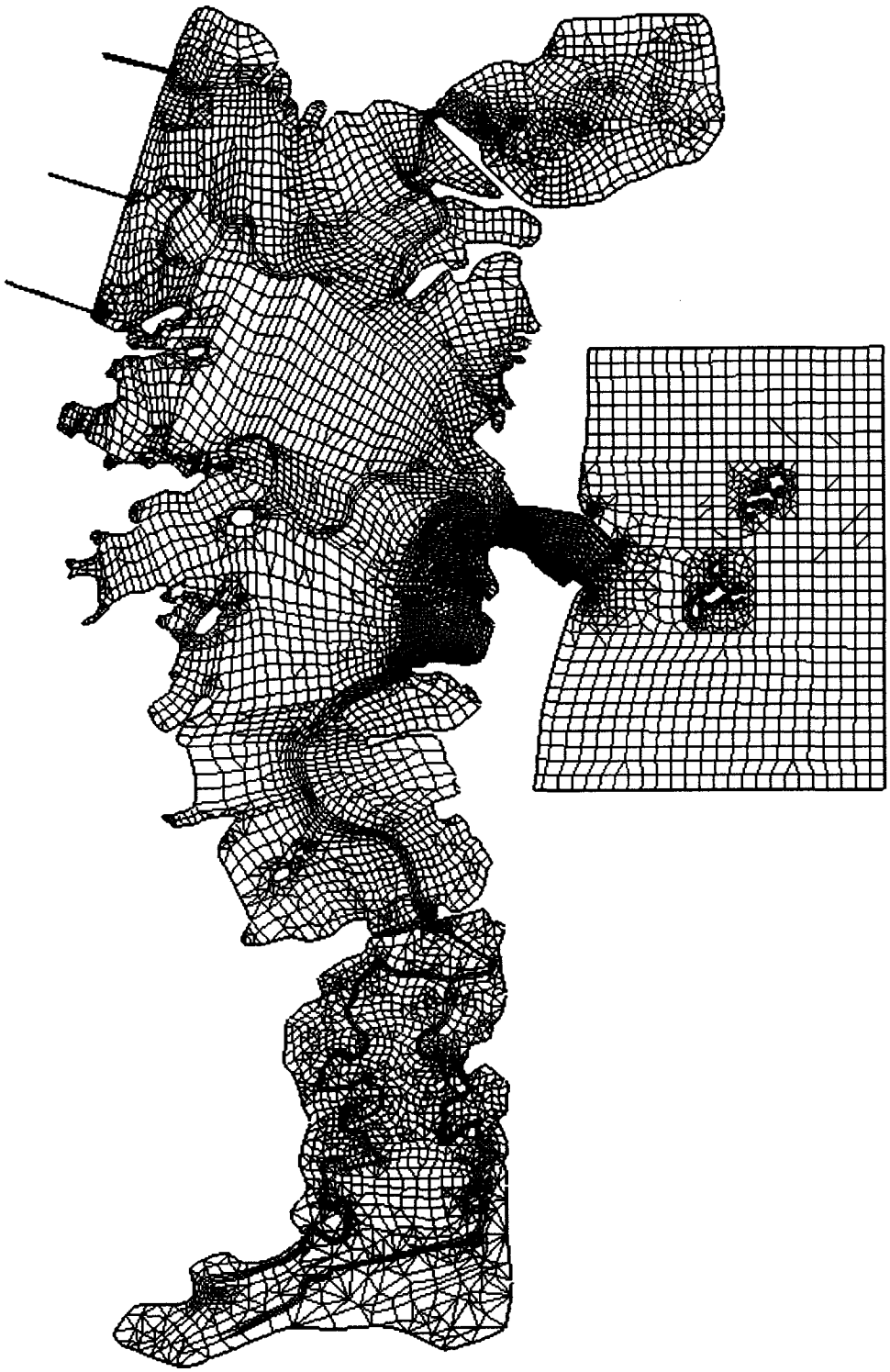

Figure 4.5 Final mesh.

Reproduced with permission of the copyright owner. Further reproduction prohibited without permission.

4.4 Material Properties

Although material properties were previously assigned in the ACOE mesh, it was unclear how they were generated, so they were deleted and materials were reassigned from scratch so that if adjustments needed to be made during calibration, they could be done so with logic and an understanding of the underlying physics. Material groups were defined based on the bathymetry and aerial photo. Figure 4.6 shows the distribution. Groups were differentiated by both ground cover/bottom type and significant differences in depth (e.g. river versus sandbar, although both have a sand cover). Numerical values for material properties (such as Manning number, Peclet number, and marsh porosity parameters) were next assigned on a group-by-group basis. An initial assignment was made based on recommendations in the program documentation to get the model running. Values were subsequently revised as necessary in the calibration process to improve comparisons between predictions and field observations.

Reproduced with permission of the copyright owner. Further reproduction prohibited without permission.

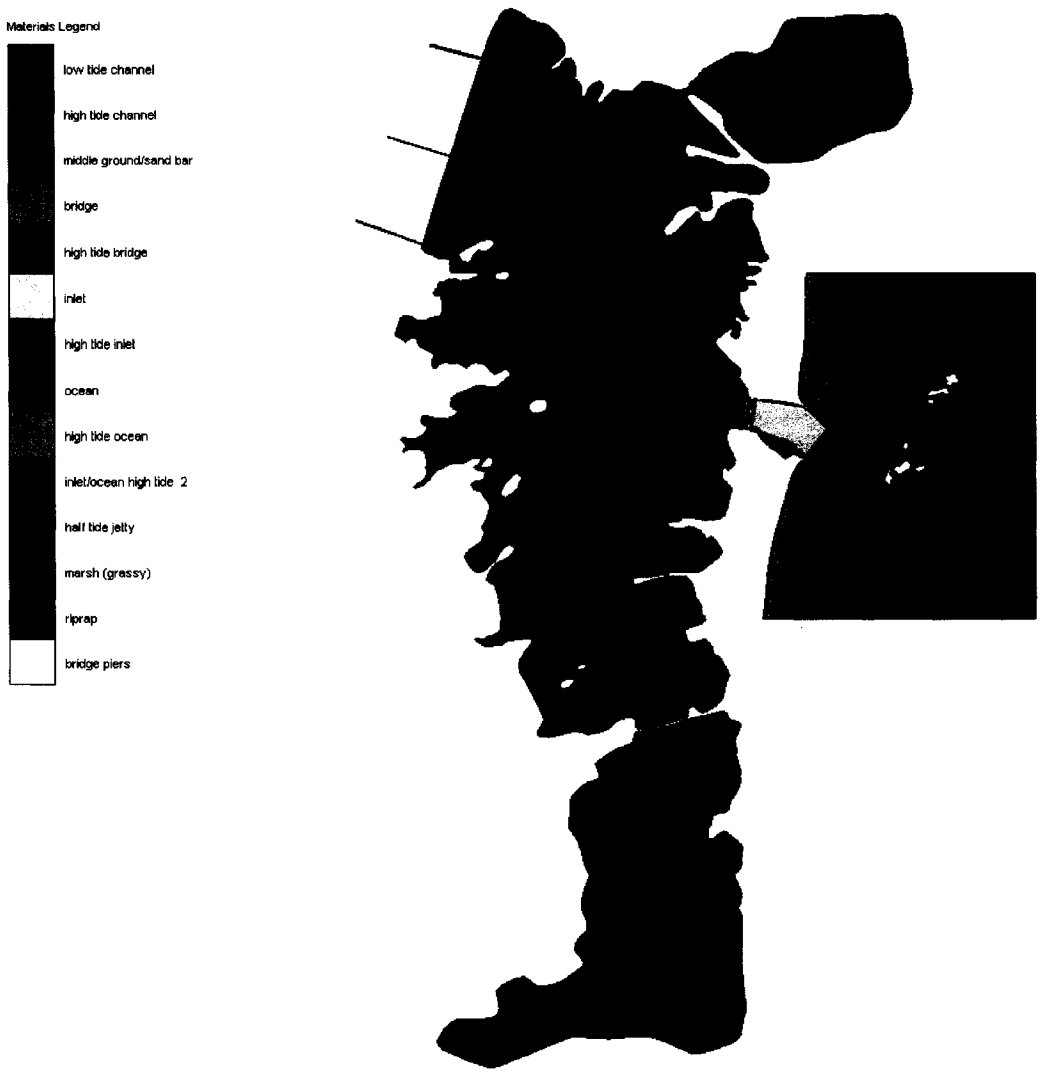

Figure 4.6 Material type distribution.

4.4.1 Bottom Roughness

Manning's roughness, n, was specified with the automatic roughness-by-depth tool, which uses an exponential curve defined by user-specified coefficients to re-calculate n for every element after each iteration. The equation used for generating this curve is (Capps, 1989):

Reproduced with permission of the copyright owner. Further reproduction prohibited without permission.

$$n = \frac{rdnv}{avgd^{rdc}} + \left(rdv \times e^{\left(-\frac{avgd}{vegd} \right)} \right) \tag{4.1}$$

where

n	=	roughness coefficient
$rdnv$	=	maximum Manning's n for non-vegetated water
$avgd$	=	calculated depth
rdv	=	Manning's n for vegetated water
rdc	=	roughness-by-depth coefficient
$vegd$	=	depth at which vegetation affects roughness.

For this model, the Mississippi River Delta default values were specified, depicted in Figure 4.7. As seen in the figure, the Manning's n curve was defined with n = 0.026 for vegetated water, and n = 0.2 for non-vegetated water. Depth for vegetation effects was 2.0 m, and the roughness curve coefficient was 0.08. This curve was assigned to all material groups.

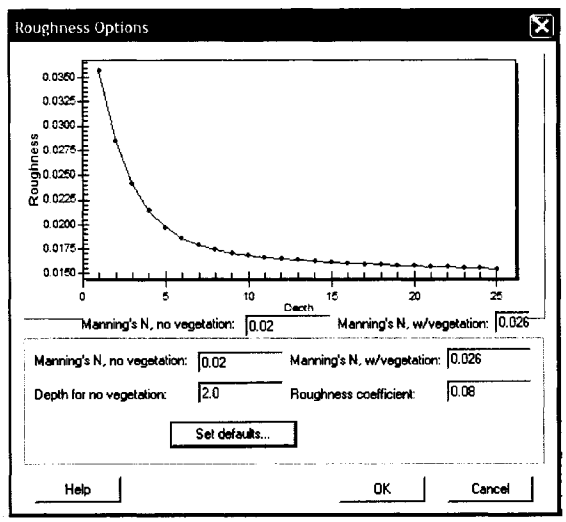

Figure 4.7 Mississippi River Delta default values for the roughness-by-depth option.

Reproduced with permission of the copyright owner. Further reproduction prohibited without permission.

4.4.2 Eddy Viscosity

Eddy viscosity and marsh porosity required more careful consideration when choosing values for each material group. As described in Chapter 2, it is recommended that P have a value between 15 and 40, and it should be remembered that as area and velocity increase, eddy viscosity increases, so the user-specified Peclet number should decrease (see Equation 2.12). Material groups were assigned a P value between 15 and 40, and a minimum velocity between 0.5 and 1.5 m/s. Generally, groups with mostly smaller elements were assigned a higher P, as were those where the velocity was expected to be low (e.g. vegetated marsh areas).

As mentioned above, elements with greater area and higher velocities generally have higher eddy viscosity values. A larger Smagorinsky coefficient (*TBFACT*) will result in a higher eddy viscosity. A value of 0.05 was chosen for TBFACT since it is the default value listed in the RMA2 User's Guide (King et al., 2001). Final eddy viscosity parameters are provided below (after calibration in Table 4.3).

4.4.3 Marsh Porosity

Marsh porosity values were chosen by examining the elevations of the nodes in each material group. The average elevation above minimum elevation in each group was approximated for AC1, and AC2 was approximated as the range of elevations for each group. AC3 was assigned a value of 0.02 for all elements. Final values for AC1-3 are provided in Table 4.3 (after calibration).

Reproduced with permission of the copyright owner. Further reproduction prohibited without permission.

4.5 Preliminary Boundary Conditions

The boundary condition used for this model was a time series of water surface elevation (pressure head) applied at the open ocean boundary. Initially, the boundary condition time series used in the ACOE simulation was applied, and only at the eastern boundary, to start the model running. Figure 4.8 shows the nodestring (a series of consecutive nodes) that was created for this boundary condition. Subsequent boundary conditions are discussed later in this chapter.

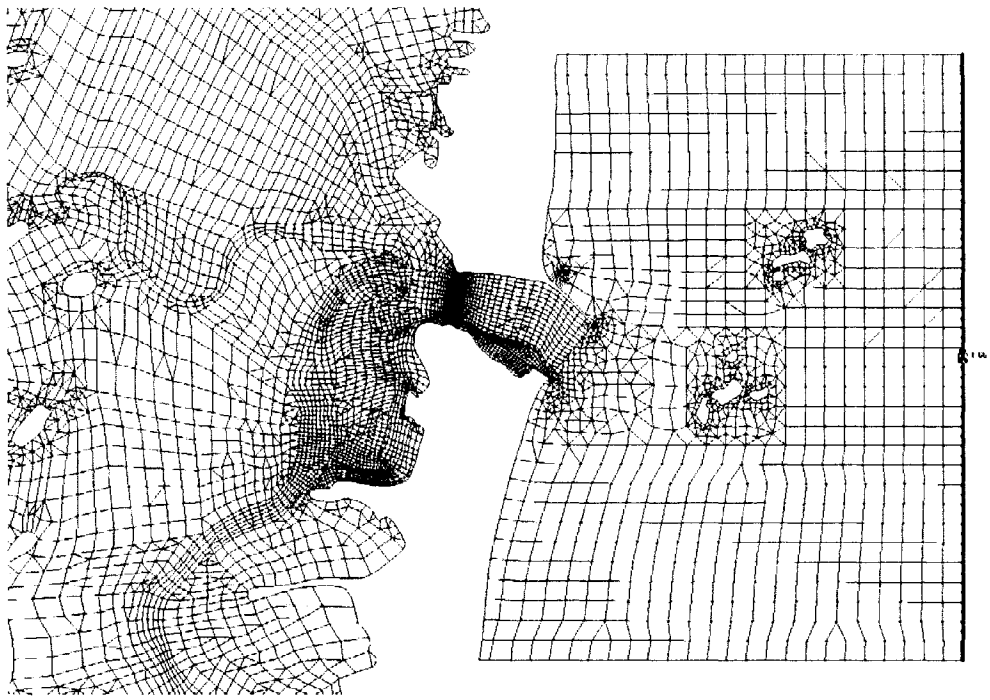

Figure 4.8 Boundary condition nodestring at only eastern boundary.

In addition to boundary conditions, it is also necessary to apply initial conditions. The initial condition for this model was specified as a natural high tide of 1.66 m, which occurred on 31 October 2000 at 18:52 (Greenwich Time) (Mahmutoglu, 2001).

Reproduced with permission of the copyright owner. Further reproduction prohibited without permission.

4.6 Running the Model

Running the model requires first generating the binary geometry file using GFGEN, and then running the RMA2 executable. For this model, GFGEN Version 4.5 and RMA2 Version 4.56 were used. Although RMA2 4.56 is the most recent version, it has a maximum front width (maximum number of nodes for which equations can be solved simultaneously (Heimann, 2001) of 1000, smaller than earlier versions, and this model had a front width of 1231. However, it was not possible to use an earlier version with a larger front width; the capability of using the Smagorinsky method to assign eddy viscosity is a new feature in the version 4.56, and needed to be used in this model. Consequently, a .dat file named r2memsize was used to re-dimension the RMA2 executable. R2memsize allows parameters such as the maximum front width and maximum number of elements to be changed. Figure 4.9 shows an example.

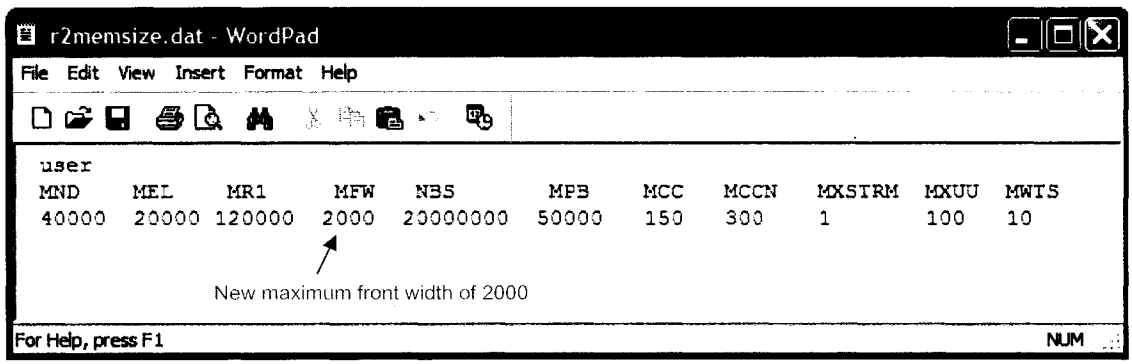

Figure 4.9 Example of the r2memsize.dat file used to customize model parameters.

Reproduced with permission of the copyright owner. Further reproduction prohibited without permission.

4.7 Boundary Conditions

Once the model was debugged and running, more appropriate boundary conditions were developed and applied. Figure 4.10 shows the nodestring created for the new boundary conditions. Water surface elevations were applied to the north and south boundaries, as well as the east. Again, the initial condition for this model was specified as a natural high tide of 1.66 m, which occurred on 31 October 2000 at 18:52 (Greenwich Time) (Mahmutoglu, 2001).

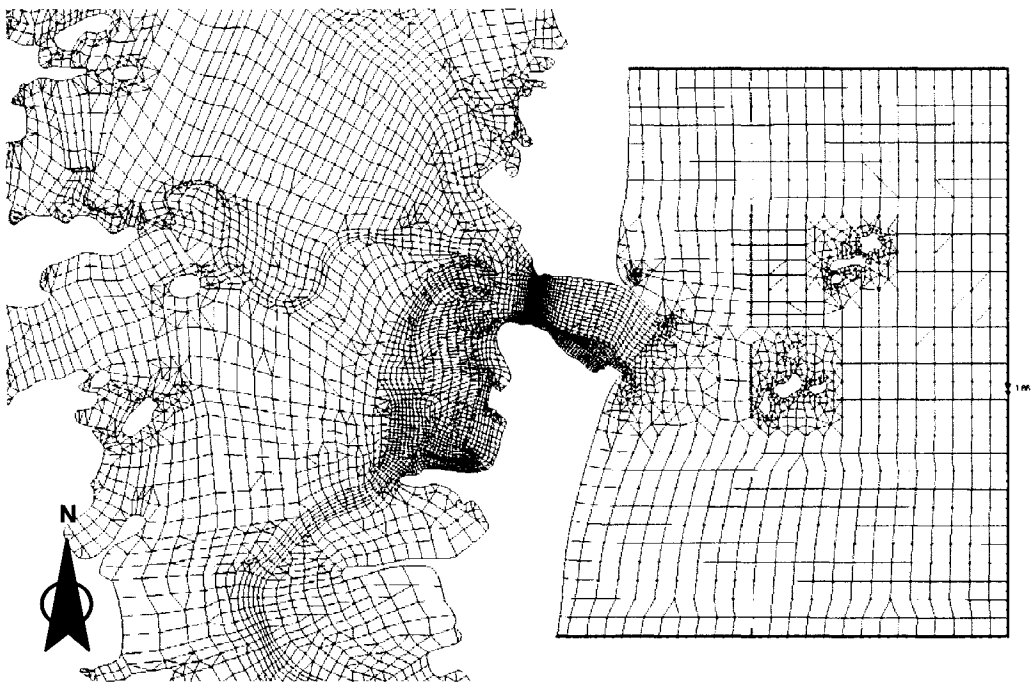

Figure 4.10 Full boundary condition nodestring, at north, east, and south boundaries.

4.7.1 BCGEN

In the previous UNH model, the Mahmutoglu (2001) interpolated tidal constituents from five regional tide stations to each individual node of the boundary

Reproduced with permission of the copyright owner. Further reproduction prohibited without permission.

nodestring, to account for minor differences in phase and amplitude over the boundary. The interpolation of five major amplitude and phase constituents was done using a program was written in Matlab called BCGEN for Boundary Condition GENerator. The program then calculated a time series for each node by superimposing five constituents of the form:

$$\eta((x,y),t) = a_{(x,y)} \sin\left(\omega t + \theta_{(x,y)} \frac{\pi}{180} \right) \tag{4.2}$$

where

$\eta((x,y),t)$	=	water surface elevation for given (x,y) coordinates and time
ω	=	wave period
(x,y)	=	position with respect to NHSPC NAD83 (meters)
$a_{(x,y)}$	=	amplitude of wave, given (x,y) coordinates
t	=	time in h
$\theta_{(x,y)}$	=	phase of wave, given (x,y) coordinates.

This produced an output file in the form of the RMA2 boundary condition file (.bc), and contained a time series of water surface elevations for each node (See Appendix D for code). However, it was never tested to see if these small differences in amplitude and phase along the boundary had a significant effect on the water surface elevations inside the estuary. Furthermore, this approach generates only a representative time series, not one for a specific time interval which was needed for comparisons with field measurement data.

4.7.2 Sensitivity Analysis

A sensitivity analysis was done, to see if the boundary conditions could be simplified without affecting the model results. The model was run twice, once with

Reproduced with permission of the copyright owner. Further reproduction prohibited without permission.

boundary conditions generated from BCGEN. The second version interpolated to a single node in the middle of the nodestring, and the time series for this node was applied to the entire nodestring. Water surface elevations were compared at five locations throughout the harbor; the results are shown in Figure 4.11. It can be concluded that, inside the harbor, there is no significant difference between the results using the different cases of boundary conditions, and it is therefore sufficient to apply a single time series of elevations to the boundary.

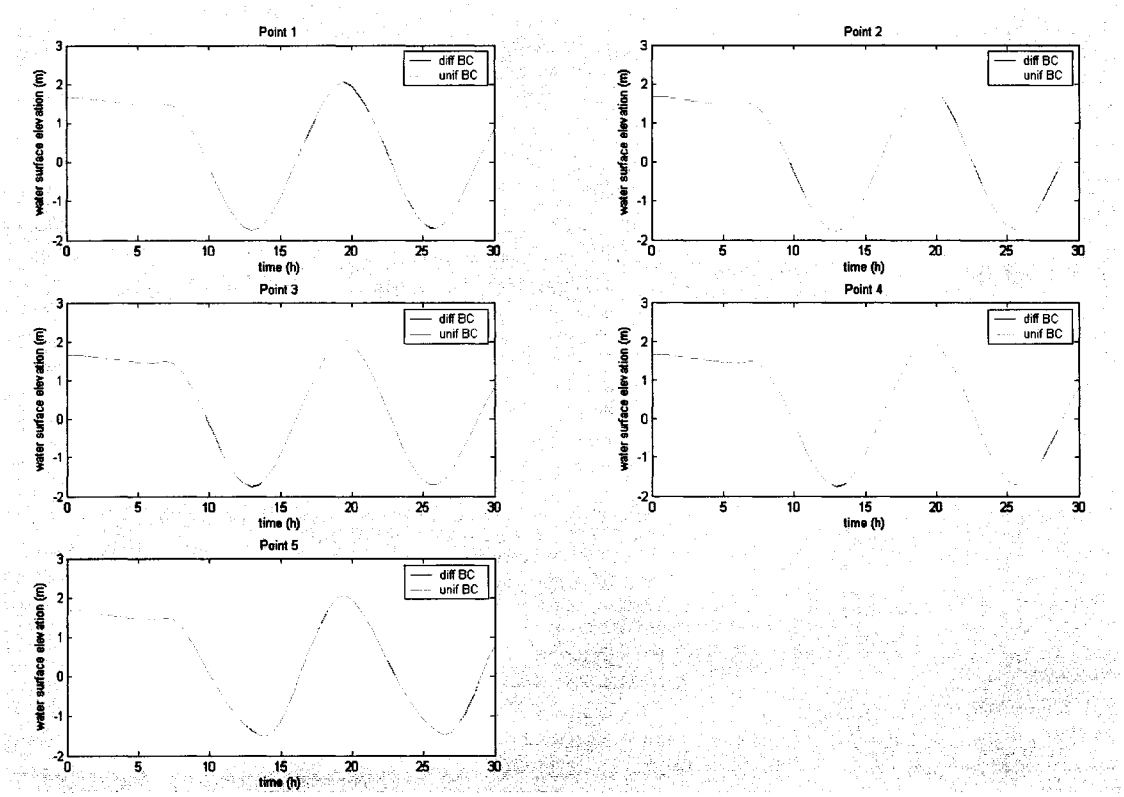

Figure 4.11 Water level comparisons throughout the harbor for the boundary conditions sensitivity analysis. It can be seen that the comparisons are nearly identical, showing that it is unnecessary to have a different boundary condition at each node.

Reproduced with permission of the copyright owner. Further reproduction prohibited without permission.

4.7.3 T_TIDE

To predict surface elevation at specific dates/times, the tidal analysis program T_TIDE was used. T_TIDE is another set of programs written in Matlab, and described in Pawlowicz et al. (2002). T_TIDE is capable of performing tidal analysis of measured data, where the tidal signal is modeled as the sum of a set of sinusoids at specific frequencies related to astronomical forcing. The signal is resolved into a set of these tidal constituents, and constituent amplitude and phase is calculated, along with relevant confidence intervals. In addition, T_TIDE can take any number of these constituents, or constituents from an external source, and calculate a predicted time series of water surface elevations. This capability was used to compute model boundary condition surface elevation time series using tidal constituents interpolated spatially from nearby tide stations.

An additional Matlab program was written around T_TIDE to produce the boundary conditions for this model. TCON_INT (code can be found in Appendix D) uses the same five stations (see Figure 4.12) as BCGEN, and interpolates the phase and amplitude from each tidal constituent to a node in the middle of the boundary nodestring (Figure 4.13). The resulting constituents and their respective confidence intervals are supplied as input to T_PREDIC, one of T_TIDE's subprograms (T_PREDIC is used here as a subprogram within TCON_INT). Table 4.1 shows the information and data for each station used, and Table 4.2 shows the input parameters supplied to TCON_INT/T_PREDIC. Figure 4.14 shows a series produced by T_PREDIC, which was applied to the entire nodestring, and used to calibrate the model.

Reproduced with permission of the copyright owner. Further reproduction prohibited without permission.

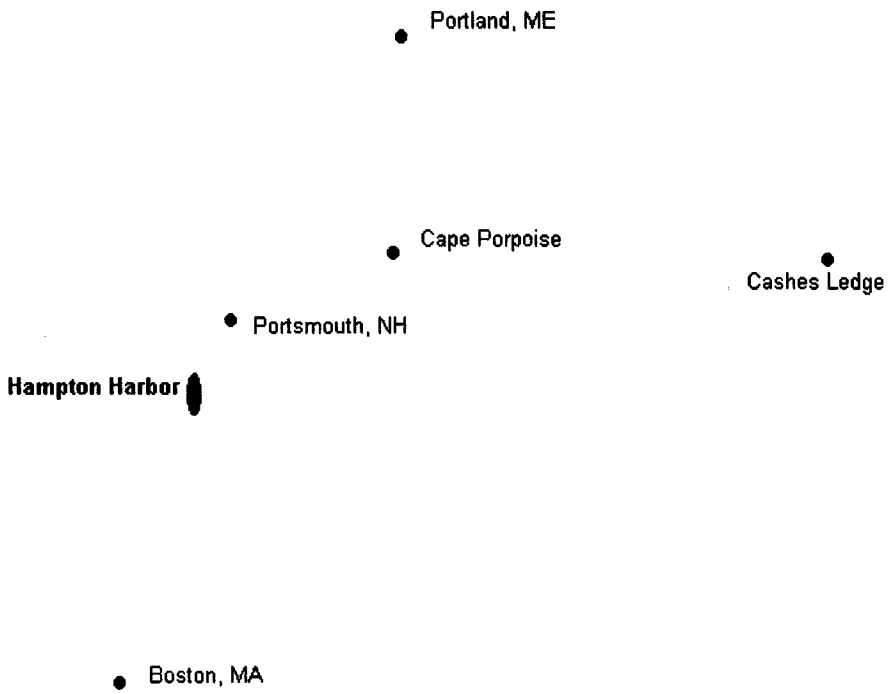

Figure 4.12 Locations of buoys that provided tidal data for the generation of the boundary condition time series.

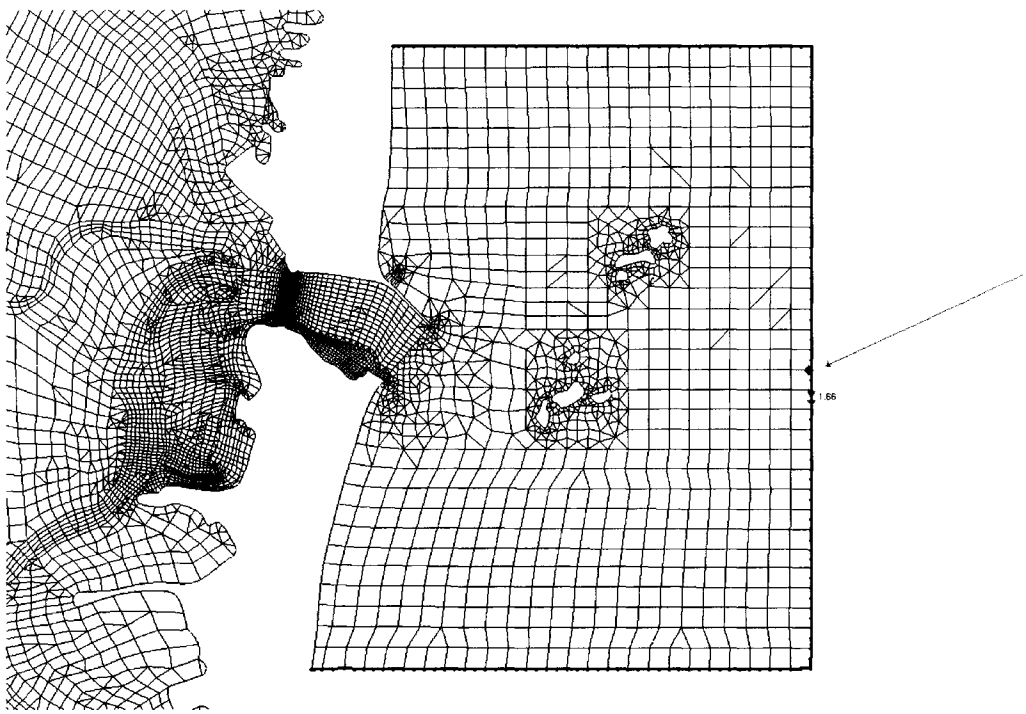

Figure 4.13 Location of node used for interpolation in tcon_int.m for the boundary condition.

Reproduced with permission of the copyright owner. Further reproduction prohibited without permission.

Table 4.1 Tidal data for each station used in boundary condition, and interpolated constituents for Hampton outer boundary (Moody et al., 1984).

	Portsmouth	[redacted]	C. Porpoise	Boston	Cape Ann
Latitude	43° 05' N	43° 39' N	43° 13' N	42° 21' N	43° 11' N
Longitude	70° 44' W	70° 15' W	70° 17' W	71° 03' W	69° 05' W
M2 amplitude	1.303	1.330	1.272	1.345	1.200
N2 amplitude	0.278	0.296	0.299	0.301	0.282
S2 amplitude	0.203	0.217	0.203	0.219	0.195
K1 amplitude	0.141	0.139	0.129	0.140	0.125
O1 amplitude	0.112	0.111	0.106	0.111	0.101
M2 phase	107	103	103	111	98
N2 phase	76	73	71	82	66
S2 phase	143	138	134	146	126
K1 phase	204	202	204	207	198
O1 phase	185	183	185	189	186

Amplitude is in m, phase is in degrees Greenwich

Table 4.2 Input parameters for tcon_int.m.

Parameter	Input into TCON.m
x	List of x-coordinates of stations in NHSP (easting)
y	List of y-coordinates of stations in NHSP (northing)
z(constituent)a	List of constituent amplitudes for stations
z(constituent)p	List of constituent phases for stations
Parameter	**Input into T-PREDIC.m**
tidecon	Matrix containing [fmaj emaj ph eph]
fmaj	List of interpolated constituent amplitudes
emaj	95% confidence intervals for fmaj
ph	List of interpolated constituent phases
eph	95% confidence intervals for ph
names	List of names of tidal constituents
time	Specified times for which output is desired
freq	Frequency of tidal constituents (cycles/hr)
latitude	Latitude in decimal degrees north

Reproduced with permission of the copyright owner. Further reproduction prohibited without permission.

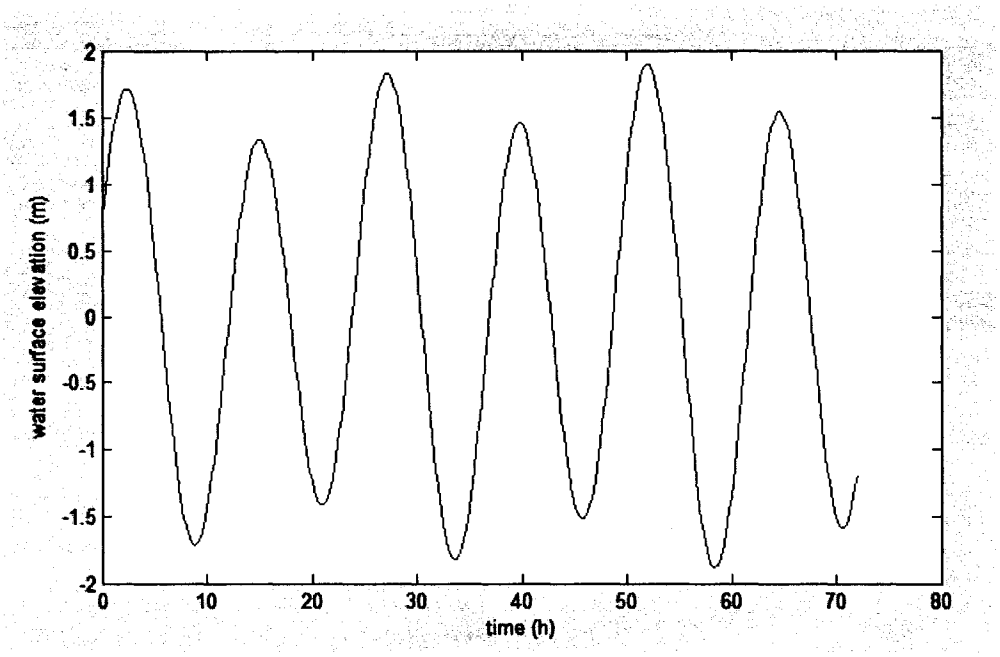

Figure 4.14 Boundary condition water level time series generated by tcon_int.m and t_tide.m. Start date and time was 2 July 2005 0020.

4.8 Calibrating the Model – Water Surface Elevation

To calibrate the model with water level data, an "observation coverage" was created in the SMS interface. This consisted of a set of discrete points at which a time series of model-predicted water level data could be extracted from the results (also used in the sensitivity analysis mentioned above). These points were located using the horizontal coordinates listed in Table 3.2 so that the model results and field data could be compared directly. Figure 4.15 shows the observation coverage on top of the model domain.

After numerous iterations, the best possible combination of material properties was found, resulting in the comparison found in Figure 4.16. In this set, predicted tidal elevation is compared with directly recorded surface elevation (which may include non-tidal processes). The material property values are found in Table 4.3.

Reproduced with permission of the copyright owner. Further reproduction prohibited without permission.

To further verify the accuracy of the results, the field data without the residual (i.e. wind, storms, etc) were compared with the model predictions. To isolate the tidal signal, tidal constituents obtained from tidal analysis of the field data were used to calculate surface elevation for the comparison period. Figure 4.17 shows the results, with very good agreement. This improvement in agreement over the raw data comparison is to be expected, since the boundary conditions were generated from only the phase and amplitude of the tidal constituents, not from actual surface elevation records.

Although there was good agreement between the model and field data for four of the calibration points, the model predictions for Chouinard's Private Pier (CPP) again over-predicted water levels at the lower tides, in addition to showing a phase shift. Several changes were tested in an attempt to determine the reason for the discrepancy.

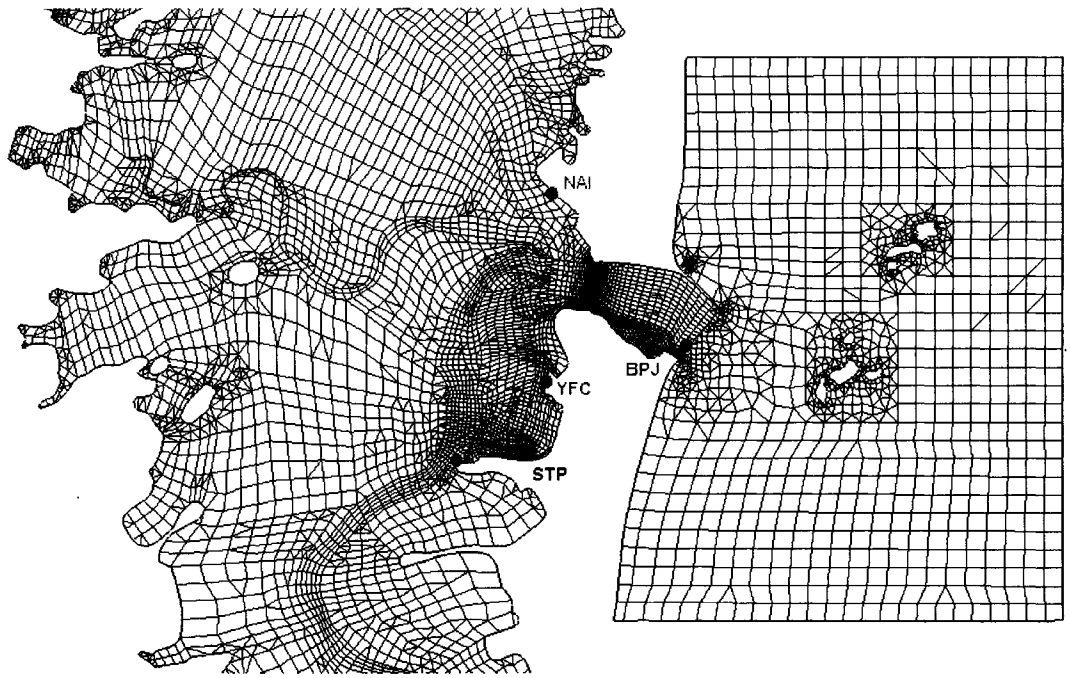

Figure 4.15 Observation points at locations of tide gauges, where field and model data were compared.

Reproduced with permission of the copyright owner. Further reproduction prohibited without permission.

Table 4.3 Material groups and parameters.

Material No.	Material Group	Peclet Number	Manning's n Value	ALT	ATR	CD
1	low tide channel	15	1.5	6	4	0.02
2	high tide channel	10	0.5	4.5	3	0.02
3	middle ground/sand bar	10	0.5	5.5	4	0.02
4	bridge	20	1.5	3	2	0.02
5	high tide bridge	20	1	5	3.2	0.02
6	inlet	20	1	4	2.667	0.02
7	high tide inlet	20	0.75	5	3	0.02
8	ocean	15	1.5	3	2	0.02
9	high tide ocean	15	1.5	4	2.667	0.02
10	inlet/ocean high tide 2	40	0.5	5	3.2	0.02
11	half tide jetty	20	0.5	4	2.667	0.02
12	marsh (grassy)	Smag (TBFACT = 0.05)		4.5	3	0.02
13	riprap	10	1.5	5	3.3	0.02
14	bridge piers	Smag (TBFACT = 0.05)		4	2.667	0.02

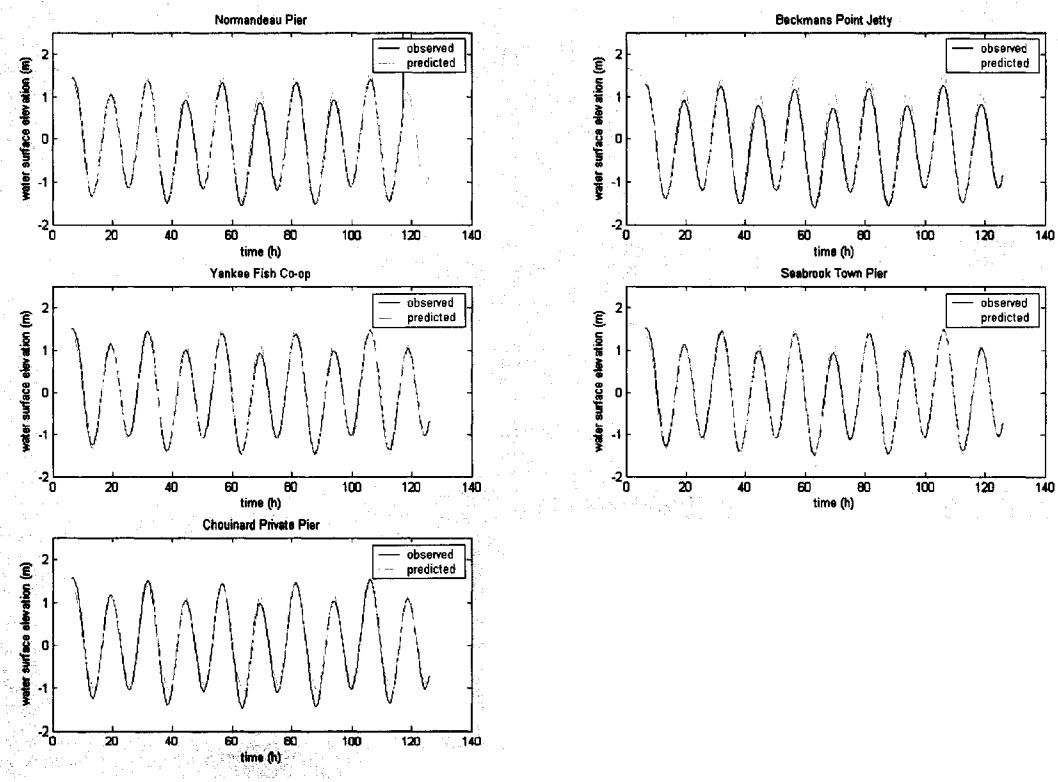

4.16 Comparison of predicted (model generated) and directly observed water levels (Start date and time was 1 July 2005 1740).

Reproduced with permission of the copyright owner. Further reproduction prohibited without permission.

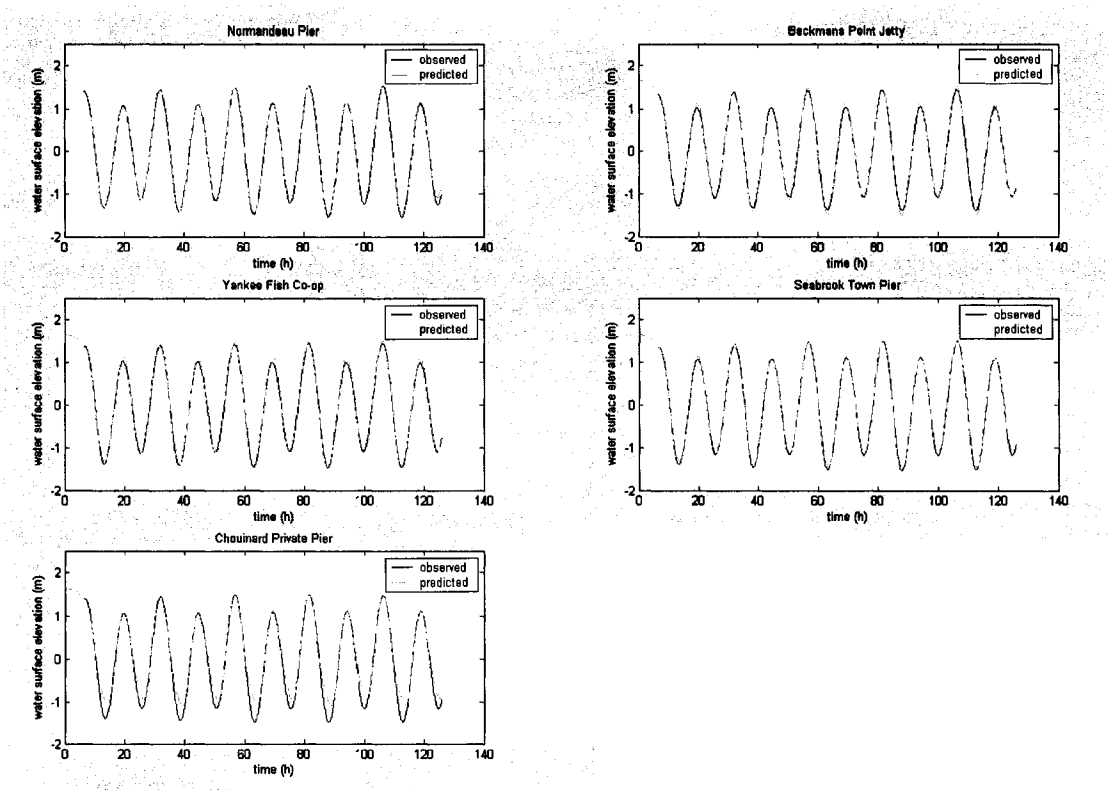

Figure 4.17 Comparison of predicted (model generated) and observed water levels without residual (Start date and time was 1 July 2005 1740).

Upon examination of the bathymetry data in the vicinity of the CPP tide station, it was noted that there seemed to be a berm across the Blackwater River south of Chouinard's pier, while in the actual river no such berm is visible. The node elevations in that area were adjusted to "remove" the berm and determine if this was causing the discrepancy. Figure 4.18 shows the area of interest; the model results did not show much improvement.

Reproduced with permission of the copyright owner. Further reproduction prohibited without permission.

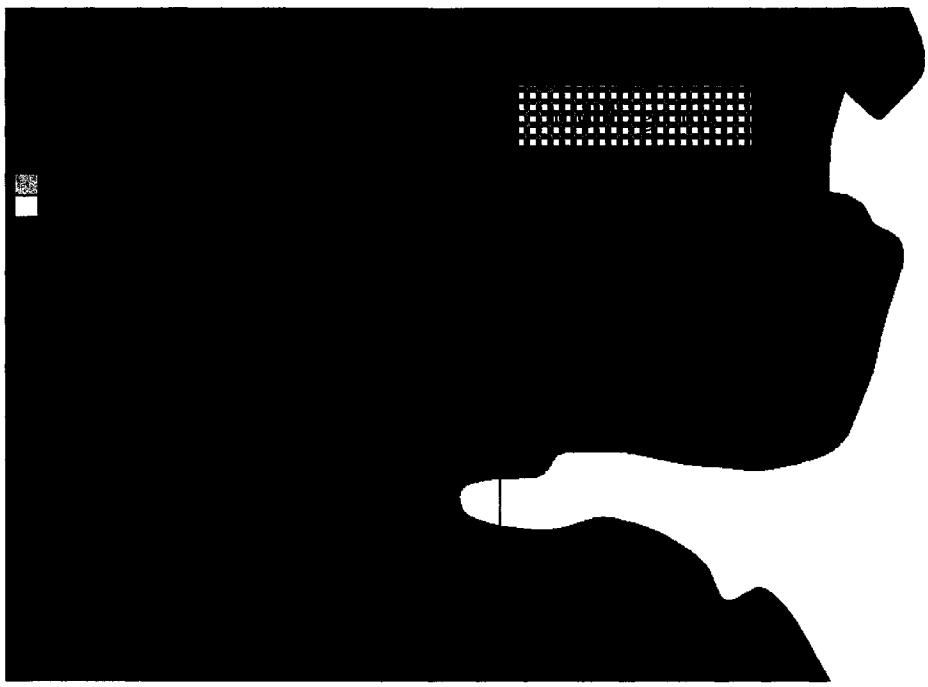

Figure 4.18 Area of model with possibly inaccurate bathymetry where there appears to be a berm in the Blackwater River.

Noting that the channel elevations south of the 286 bridge were exactly uniform throughout the entire channel, it was thought that maybe the tidal prism in that area was too large, and that the depth of the channel was causing the discrepancy. To test this, the depths were decreased along the entire channel, changing the node elevations from -2.0 m to -1.5 m. Figure 4.19 shows the area where changes were made. Again, there was no significant improvement in the model results.

Reproduced with permission of the copyright owner. Further reproduction prohibited without permission.

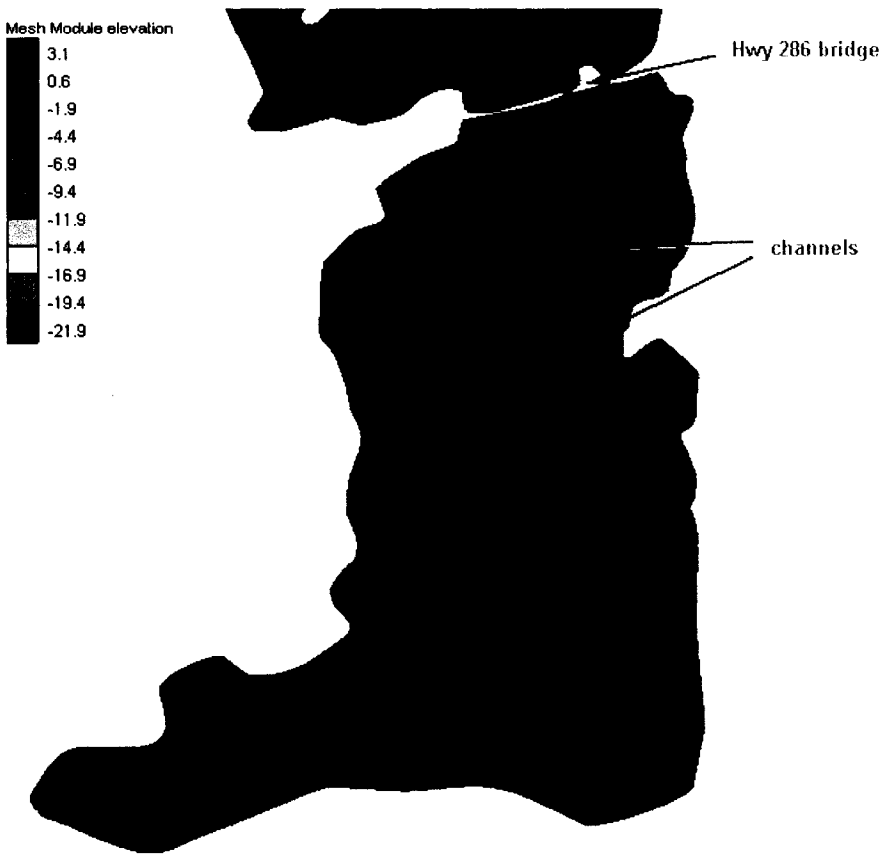

Figure 4.19 Channels south of Hwy 286 bridge where elevation was changed to decrease prism.

Finally, since the previous model (Mahmutoglu, 2001) did not include the area south of the 286 bridge, but still produced sufficient hydrodynamic results in the harbor, the abovementioned part of the model mesh was removed. It was also thought that the unrealistic channel bathymetry provided further justification for excluding the area. The remaining volume south of the bridge was comparable to that of the previous model. This seemed to have the best results for CPP observed surface elevation, shown in Figure 4.20 along with the new model domain. It should be noted, however, that such a drastic truncation of the mesh may not be the "best" solution overall. Reducing model tidal prism will obviously affect velocity in the Blackwater River just north of the 286 bridge – an effect investigated in the next section.

Reproduced with permission of the copyright owner. Further reproduction prohibited without permission.

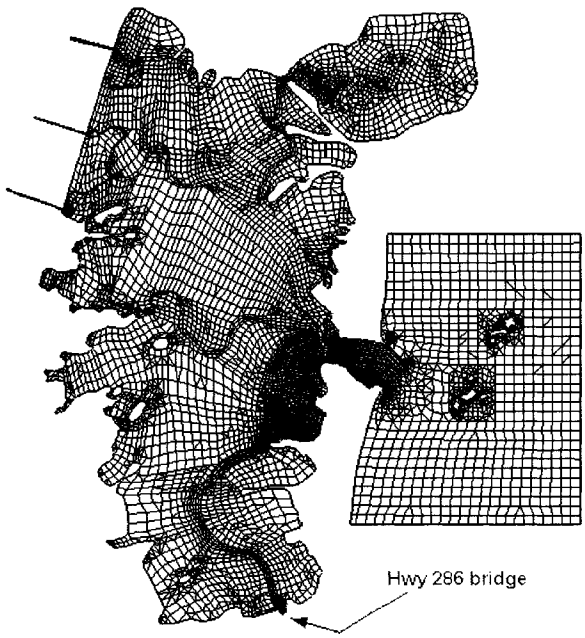

(a)

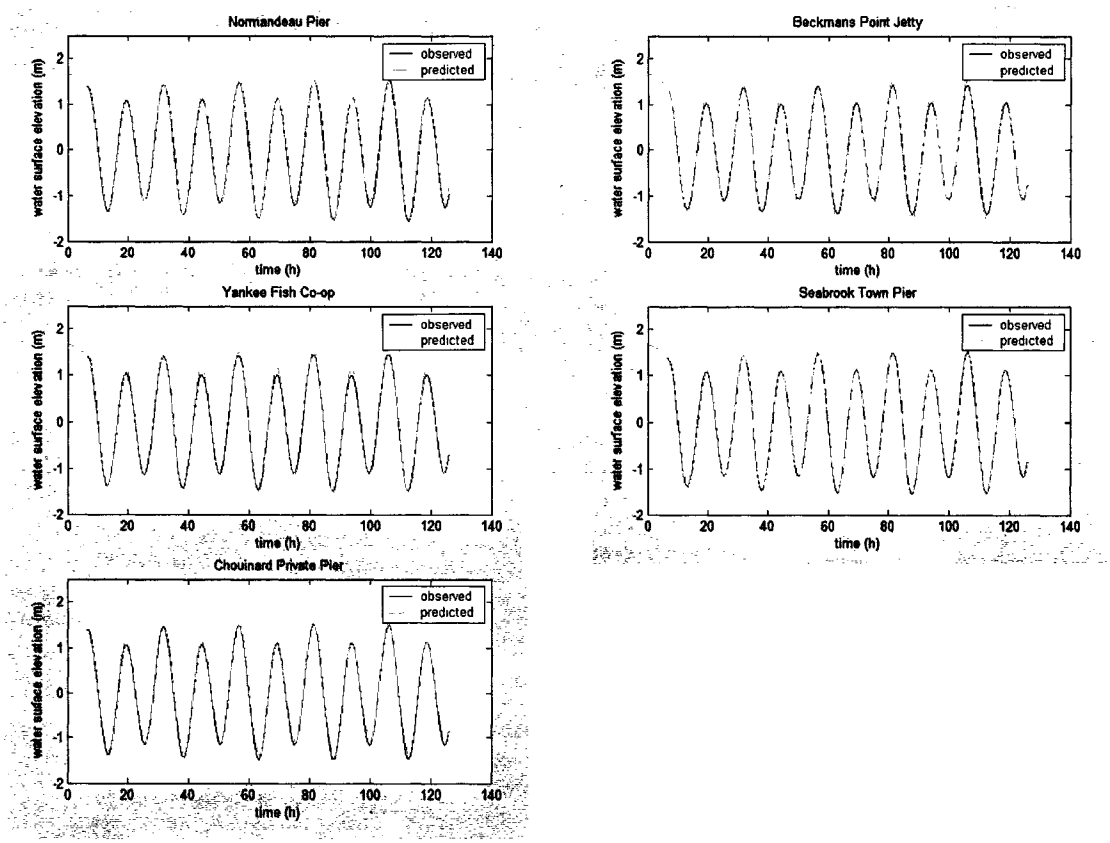

(b)

Figure 4.20 (a) Model domain with area south of 286 bridge deleted, and (b) improved CPP comparison results from this simulation.

Reproduced with permission of the copyright owner. Further reproduction prohibited without permission.

4.9 Calibrating the Model – Current Velocities

Since spatial variability is inevitable in turbulent flow, it is standard to make velocity comparisons with cross-section averaged currents. Point measurements, the alternative, can be subject to processes such as small-scale fronts, horizontal shear, and flow alteration due to local topography not represented by the model (Erturk et al., 2002). For this calibration with current data, velocities were compared over time for cross-channel averages of velocity in the along-channel direction (ebb considered positive, flood negative).

Field data were available in the form of cross-sectional profiles, as mentioned in Chapter 3. Each file included data for one transect (cross-section), and was organized in velocity depth profiles along that transect. Each profile of velocity magnitude and direction was depth-averaged, and these resulting averages were cross-section averaged to produce a single magnitude and direction for each transect.

Similarly, model predictions were extracted at 1-hour time steps along a similar transect, and the already-depth-averaged velocities were averaged along that transect. Since the transects taken in the field were of different lengths (due to tidal conditions) and locations, an approximation of the average position was used to extract the model predictions (Figure 4.21)

For both data sets, the along-channel velocity magnitude (ebb positive) was calculated using

$$ACV = v\cos(\theta - d) \tag{4.3}$$

where

Reproduced with permission of the copyright owner. Further reproduction prohibited without permission.

ACV = along-channel velocity in ebb direction
v = velocity magnitude
θ = velocity direction
d = direction of along-channel ebb flow.

Figure 4.21 "Average" cross-sections used to compare model data and field observations.

The along channel ebb direction was estimated from measured current direction during mid-flood and mid-ebb. These directions were adjusted (slightly) so that ebb differed from flood by 180°. To confirm that the ebb direction result was reasonable, it was compared with channel direction and vector plots that can be seen in Chapter 5.

The field data were first compared to the model results from the simulation that excluded the area south of the 286 bridge, since that version had the best water level calibration. However, it was suspected that the area south of the 286 bridge might contribute positively to the simulation of currents in the southern part of the harbor, so

Reproduced with permission of the copyright owner. Further reproduction prohibited without permission.

the field data were next compared to the simulation which included the full model domain. Figure 4.22 shows these two comparisons at HS3P (in the Blackwater River north of the 286 bridge, see Figure 3.10). It can be seen that the latter version better predicts currents at the HS3P cross-section.

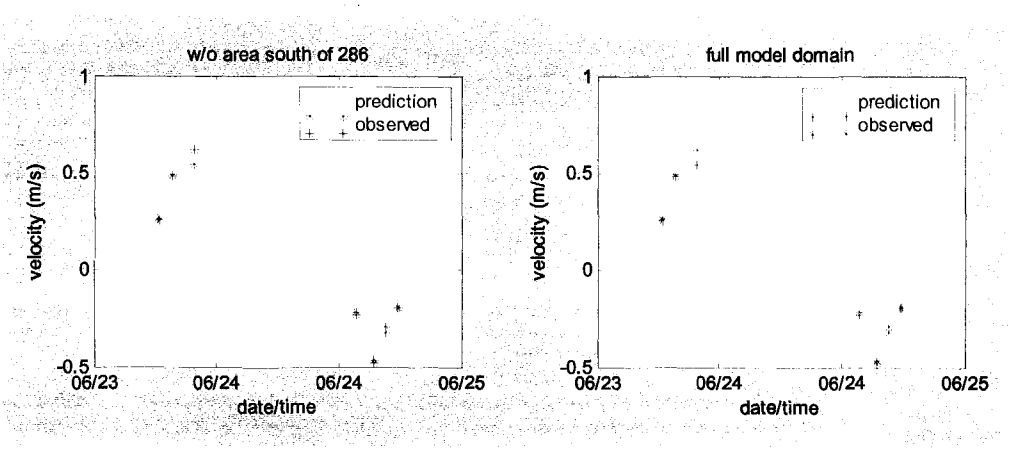

Figure 4.22 Comparison of model-predicted and observed along-channel velocities, for simulations with and without the area south of the Hwy 286 bridge.

Reproduced with permission of the copyright owner. Further reproduction prohibited without permission.

CHAPTER 5

RESULTS

With water level and current calibrations, improvement of one may result in deterioration of the other. Therefore, to develop a model that can predict both water level and current flow to the best of its abilities, it is necessary to find a balance between the two. In finding this balance, it was decided that the model which included the area south of the 286 bridge yielded the best all-around results. While the water level predictions at the CPP station were less accurate, the predictions at the remaining stations were quite good, and the improvement to the current predictions was considerable. Current predictions are also important because they directly relate to sediment transport – the principal motivation for completing this study. Final water level and current comparisons are summarized in Figure 5.1. Error statistics can be found in Table 5.1.

The model predicts a tidal range of approximately 3 meters for all stations except CPP, which displays a tidal range of about 2.5 meters. Maximum elevations were slightly over 1.5 meters at each station, and appeared to predict uniform maximum elevations within the harbor. Maximum elevation at BPJ was slightly lower.

Along-channel velocities were highest in the Blackwater River at HS3P, reaching over 0.7 m/s in the ebb direction. Velocities were higher in the newly dredged channel through Middle Ground (HSBWNC) than in the old channel (HSBWOC), which supports

Reproduced with permission of the copyright owner. Further reproduction prohibited without permission.

the construction design - one goal of the project was the decrease velocity in the Blackwater River by diverting the flow through the new channel. Velocities were lowest near HSYFC, which is also to be expected since the closure of the River Street breach prevents through flow in Seabrook Harbor. Vector plots of the velocity distribution are shown in Figures 5.3-5.9.

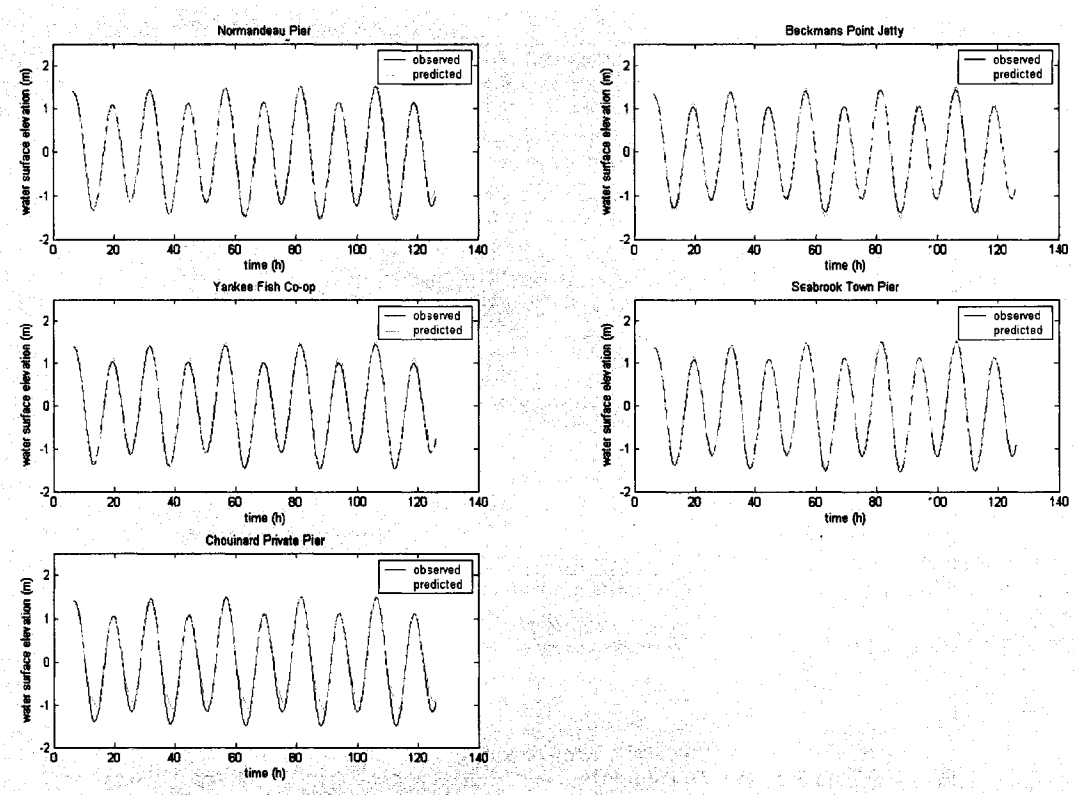

Figure 5.1 Final water level comparisons (started on 1 July 2005 1740).

Reproduced with permission of the copyright owner. Further reproduction prohibited without permission.

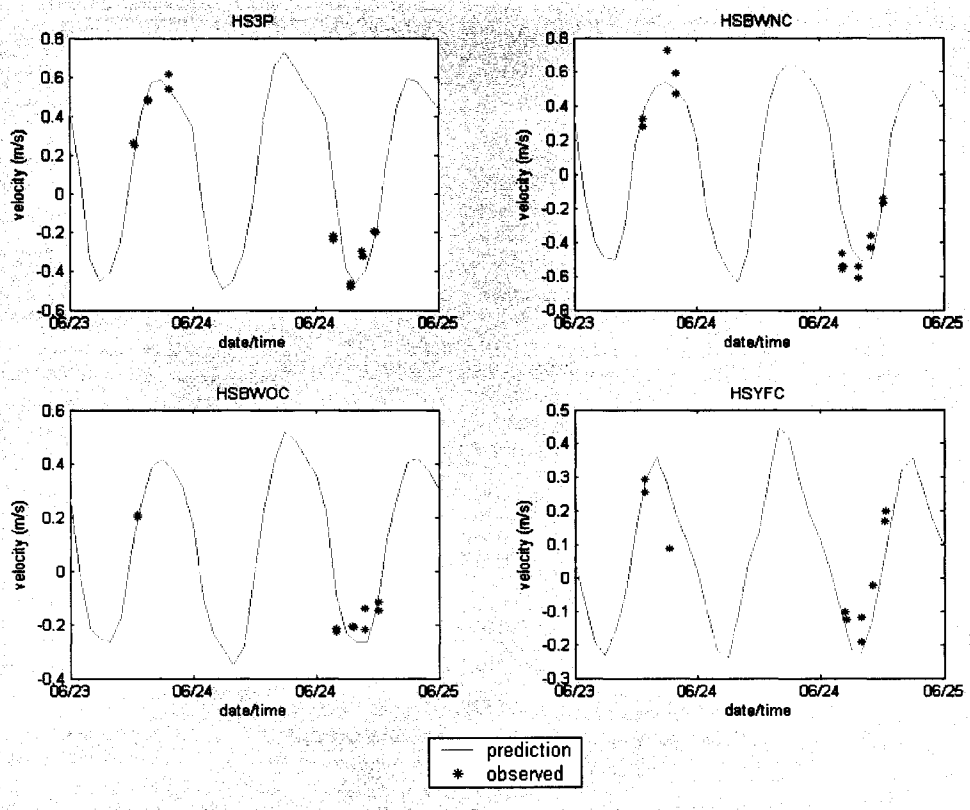

Figure 5.2 Final along-channel current velocity comparisons.

Table 5.1 Summary of Error Statistics.

Station	E_+	E_-	RMS	nRMS	S
NAI	0.144	-0.171	0.065	0.069	0.995
BPJ	0.126	-0.111	0.062	0.072	0.995
YFC	0.132	-0.167	0.075	0.084	0.993
STP	0.082	-0.112	0.048	0.051	0.997
CPP	0.095	-0.546	0.187	0.201	0.960
Transect	**E_+**	**E_-**	**RMS**	**nRMS**	**S**
HSBW3P	0.133	-0.232	0.024	0.262	0.931
HSBWNC	0.191	-0.362	0.048	0.398	0.841
HSBWOC	0.126	-0.143	0.019	0.446	0.801
HSYFC	0.108	-0.196	0.022	0.620	0.616

E_+ is the maximum positive error, E_- is the maximum negative error, RMS is the root mean square error between model predictions and field observations, nRMS is the RMS error normalized by the RMS of the observed values, and S is the skill, defined by $S = 1-(nRMS)^2$. E_+, E_-, and RMS are in meters; nRMS and S are dimensionless (Erturk et al., 2002).

Reproduced with permission of the copyright owner. Further reproduction prohibited without permission.

Figure 5.3 Early flood vector plot (4 July 2005 1110).

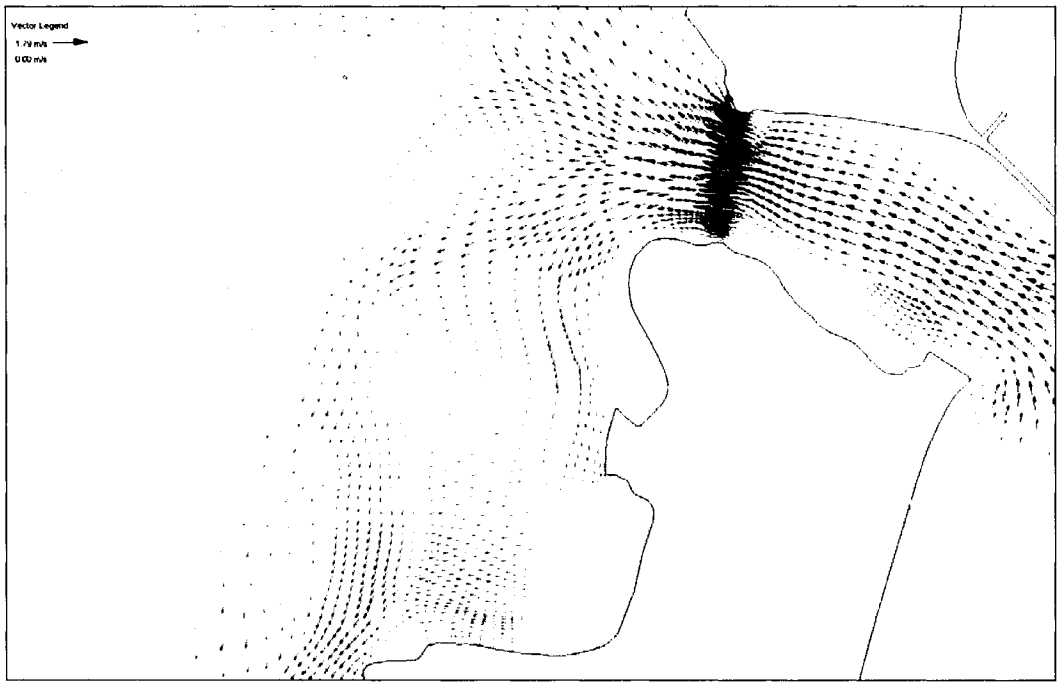

Figure 5.4 Mid flood vector plot (4 July 2005 1310).

Reproduced with permission of the copyright owner. Further reproduction prohibited without permission.

Figure 5.5 Late flood vector plot (5 July 2005 0310).

Figure 5.6 Early ebb vector plot (5 July 2005 0410).

Reproduced with permission of the copyright owner. Further reproduction prohibited without permission.

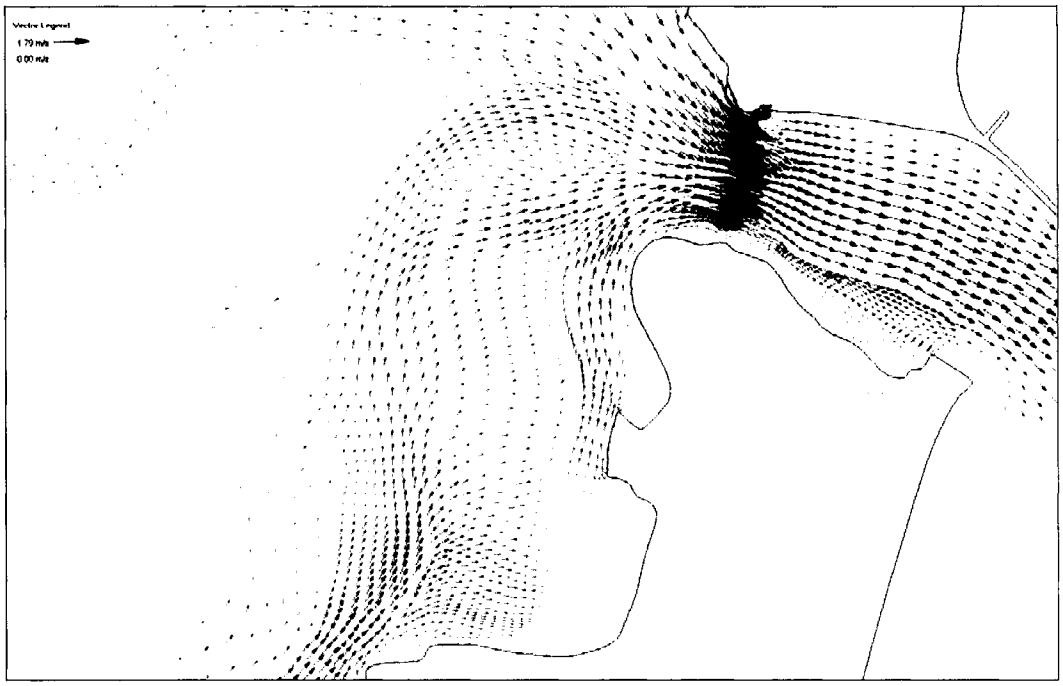

Figure 5.7 Mid ebb vector plot (5 July 2005 0610).

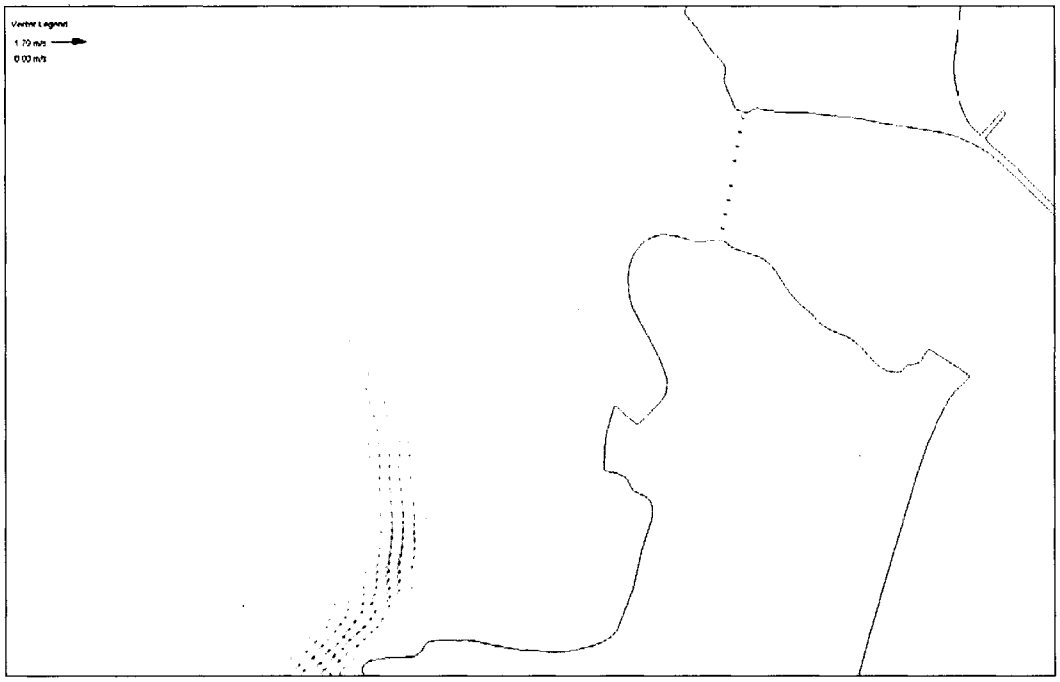

Figure 5.8 Late ebb vector plot (5 July 2005 1110).

Reproduced with permission of the copyright owner. Further reproduction prohibited without permission.

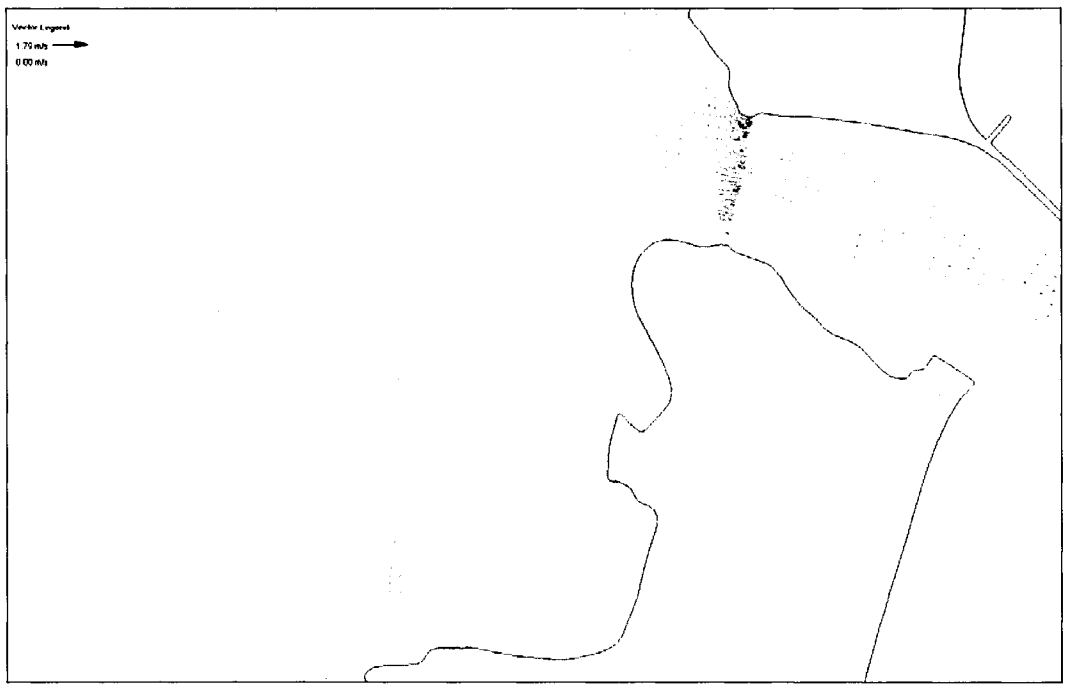

Figure 5.9 Low water vector plot (4 July 2005 1040). The flow is in both directions here, ebbing in the southern part of the harbor and flooding at the inlet.

Reproduced with permission of the copyright owner. Further reproduction prohibited without permission.

CHAPTER 6

DISCUSSION AND CONCLUSIONS

6.1 Evaluation of Comparisons

Final water level comparisons showed good agreement, excluding CPP, but there were still slight discrepancies, on the order of less than 2% of the tidal range. It is unclear what exactly causes the discrepancy at CPP, but it is obvious that the area south of the 286 bridge has a significant effect on the predictions. It should be kept in mind, however, that measurement error could be as large as 15 cm.

The along-channel current comparisons also showed very good agreement. Velocity comparisons are rarely perfect, due to reasons mentioned in Chapter 4, but this comparison demonstrated that the model predictions are fundamentally sound. Discrepancies could be due to temporal variability of field data collection, local non-tidal conditions not captured by the model, or meteorological conditions. There seemed to be no consistent pattern of disagreement; therefore it was concluded that the model predictions would not be improved significantly by further refinement of material properties.

Reproduced with permission of the copyright owner. Further reproduction prohibited without permission.

6.2 Recommendations

While this model was found to adequately predict both water levels and current velocities, several things could be done to further improve its accuracy and usefulness. Further investigation into the water level discrepancy at CPP would be important; perhaps a more accurate set of bathymetry data south of the 286 bridge would improve results.

Additionally, since Hampton Harbor is so dynamic and always changing, updated bathymetry data would be necessary if the model were to be applied to more recent conditions. Continued monitoring of new erosion, both at the edges of Middle Ground and in the dredged channels, would provide insight into the sediment transport that occurs in the harbor. Furthermore, using the results of this model to apply a sediment transport model (such as RMA4) to the system would provide a numerical analysis of the sediment transport processes.

Reproduced with permission of the copyright owner. Further reproduction prohibited without permission.

LIST OF REFERENCES

Reproduced with permission of the copyright owner. Further reproduction prohibited without permission.

Barnes, H. 1967. Roughness Characteristics of Natural Channels. Washington: United States Government Printing Office.

Capps, S.A. 2003. Modeling a Mississippi River Diversion Into a Louisiana Wetland. MS Thesis, Louisiana State University.

Chandrupatla, T.R. and A.D. Belegundu. 2002. Introdution to Finite Elements in Engineering. Upper Saddle River: Prentice Hall.

Chapra, S.C. and R.P. Canale. 2002. Numerical Models for Engineers. New York: McGraw-Hill.

Curtis, W.R. 2001. Overview of the National Shoreline Erosion Control Program. Coastal and Hydraulics News, v. CHL-01-1, US Army Engineer Research and Development Center, Vicksburg, MS. General

Ertürk, Ş.N., A. Bilgili, M.R. Swift, W.S. Brown, B. Çelikkol, J.T.C. Ip, and D.R. Lynch. 2002. "Simulation of the Great Bay Estuarine System: Tides with tidal flats wetting and drying," *J. Geophys. Res.*, 107(C5), 3038

Fox, R.W. and A.T. McDonald. 1998. Introduction to Fluid Mechanics. Boston: John Wiley & Sons.

Heimann, D.C. 2001. "Numerical simulation of streamflow distribution, sediment transport, and sediment deposition along Long Branch Creek in northeast Missouri," U.S. Geological Survey Water-Resources Investigations Report 01–4269, 61 p.

House Report 107-258, 107th Congress, 1st Session. 2001. Making Appropriations for Energy and Water Development for the Fiscal Year Ending September 30, 2002, and for Other Purposes.

King, I.P., B.P. Donell, J.V. Letter, W.H. McAnally Jr., and W.A. Thomas. 2001. "Users Guide to RMA2 WES Version 4.5," U.S. Army Corps of Engineers, Engineer Research and Development Center, Waterways Experiment Station, Coastal Hydraulics Laboratory, Vicksburg, MS.

Knuuti, Kevin, P.E., CEERD-HN-C, Principal Investigator/ERDC Project Manager. 2005.

Larry G. Ward, James D. Irish, Thomas C. Shevenell, Jon P. Scott, and Semme Dijkstra. 2006. Field Investigation to Support Hydrodynamic and Sediment Transport Models of the Channel Cut Fill Project in Hampton-Seabrook Harbor, NH: Tasks, Deployments and Methods, and Database (A 227 Program Study Report). Draft. U.S. Army Corps of Engineers, Waterways Experiment Station, Vicksburg, MS.

Reproduced with permission of the copyright owner. Further reproduction prohibited without permission.

Letter, J.V., W.L. Boyt, and S.B. Hetzel. 2005. TABS-MD Hydrodynamic and Sediment Investigation of Hampton/Seabrook Harbor, New Hampshire (A 227 Program Study Report). ERDC/CHL TR-05-XX. Vicksburg, MS: U.S. Army Engineer Research and Development Center.

Mahmutoglu, S. 2001. Hydrodynamic Modeling of the Tidal Flow in Hampton/Seabrook Harbor, NH. MS Thesis, University of New Hampshire, Durham, New Hampshire.

Moody, J., B. Butman, R.C. Beardsley, W.S. Brown, W. Boicourt, P. Daifuku, J.D. Irish, D.A. Mayer, H.E. Mofjeld, B. Petrie, S. Ramp, D. Smith and W.R. Wright. 1984. "Atlas of Tidal Elevation and Current Observations on the Northeast American Continental Shelf and Slope," U.S. Geological Survey Bulletin No. 1611, U.S. Government Printing Office.

Norton, W.R. and I.P. King. 1977. "Operating Instructions for the Computer Program RMA2-2V," Resource Management Associates, Lafayette, CA.

Norton, W.R, I.P. King, and G.T. Orlob. 1973. "A Finite Element Model for Lower Granite Reservoir," prepared for US Army Engineer District, Walla Walla, WA, Water Resources Engineers, Walnut Creek, CA.

Pawlowicz, R., B. Beardsley, and S. Lentz. 2002. "Classical tidal harmonic analysis including error estimates in MATLAB using T_TIDE," *Computers and Geosciences* 28 (2002), 929-937.

Scott, Jon P., Computer Modeling Group, Ocean Engineering, University of New Hampshire, Durham, NH. 2006.

Sturm, Terry W. 2001. Open Channel Hydraulics. Boston: McGraw-Hill.

Thomas, W.A. and W.H. McAnally Jr. 1985. "User's Manual for the Generalized Computer Program System: Open-Channel Flow and Sedimentation, TABS-2," Instruction Report HL-85-1, Hydraulics Laboratory, Dept. of the Army, Waterways Experiment Station, Corps of Engineers.

Zilkoski, D.B., J.H. Richards, and G.M. Young. 1992. "Results of the General Adjustment of the North American Datum of 1988," *Surveying and Land Information Systems*, Vol. 52, No. 3, pp. 133-149

Reproduced with permission of the copyright owner. Further reproduction prohibited without permission.

APPENDICES

Reproduced with permission of the copyright owner. Further reproduction prohibited without permission.

APPENDIX A

State Bathymetry Datum Study

Objective: to determine whether the discrepancy was due to a datum issue, i.e. if the differences are uniform.

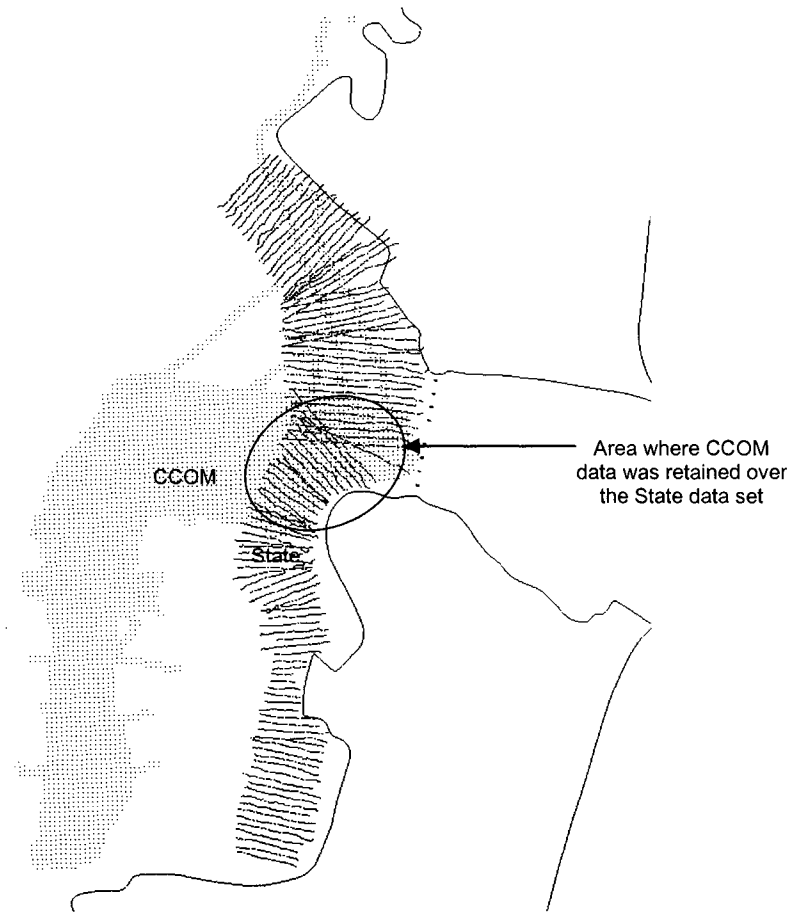

Reproduced with permission of the copyright owner. Further reproduction prohibited without permission.

Lines drawn at edge of dataset overlap. Elevation was noted at adjacent points on either side of the lines, and listed in the table below.

Elevations (m)				
CCOM	**State**		**difference**	
-3.28	-2.32		-0.96	
-4.68	-3.57		-1.11	
-5.9	-5.21		-0.69	
-5.59	-5.24		-0.35	
-4.32	-3.32		-1	
-2.7	-2.37		-0.33	
-2.62	-1.43		-1.19	
-1.99	-1.24		-0.75	
-1.93	-0.94		-0.99	
-2.14	-1.39		-0.75	
			-0.812	**avg line 1**

Reproduced with permission of the copyright owner. Further reproduction prohibited without permission.

-3.28	-2.06		-1.22	
-4.35	-3.48		-0.87	
-4.82	-4.08		-0.74	
-4.95	-4.33		-0.62	
-4.54	-3.69		-0.85	
-3.83	-2.71		-1.12	
-3.27	-2.34		-0.93	
-2.98	-2.43		-0.55	
-3.03	-2.45		-0.58	
-2.93	-2.12		-0.81	
-2.96	-2.21		-0.75	
			-0.82182	**avg line 2**
-2.68	-1.96		-0.72	
-3.19	-2.36		-0.83	
-3.32	-2.35		-0.97	
-3.64	-2.75		-0.89	
-3.12	-2.57		-0.55	
-1.64	-0.86		-0.78	
-3.15	-2.29		-0.86	
-3.25	-2.41		-0.84	
-3.61	-2.79		-0.82	
-4.87	-4.18		-0.69	
-4.8	-4.17		-0.63	
-4.08	-3.25		-0.83	
-3.9	-3.17		-0.73	
-3.91	-3.21		-0.7	
-3.81	-2.74		-1.07	
-3.22	-2.37		-0.85	
-2.56	-1.92		-0.64	
-2.58	-2		-0.58	
-2.54	-2.12		-0.42	
-2.57	-2.03		-0.54	
-2.49	-1.97		-0.52	
-2.93	-2.03		-0.9	
			-0.74364	**avg line 3**

Reproduced with permission of the copyright owner. Further reproduction prohibited without permission.

APPENDIX B

Water Level Records (Knuuti et al., 2007)

Water levels are in meters, and reference the NAVD88 datum.

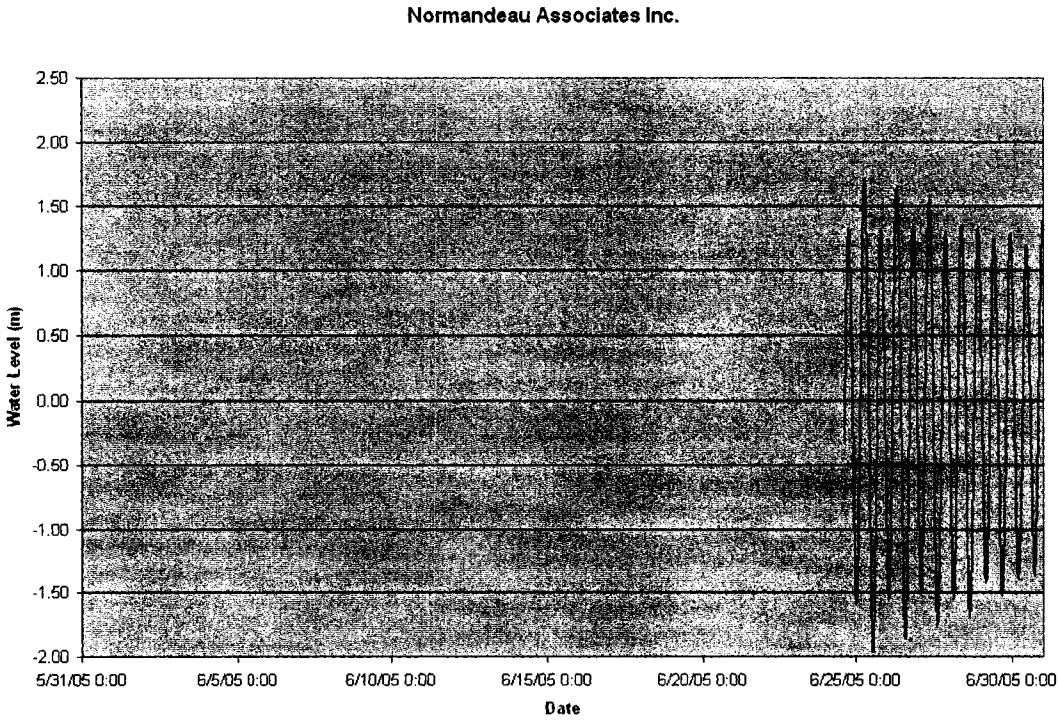

Reproduced with permission of the copyright owner. Further reproduction prohibited without permission.

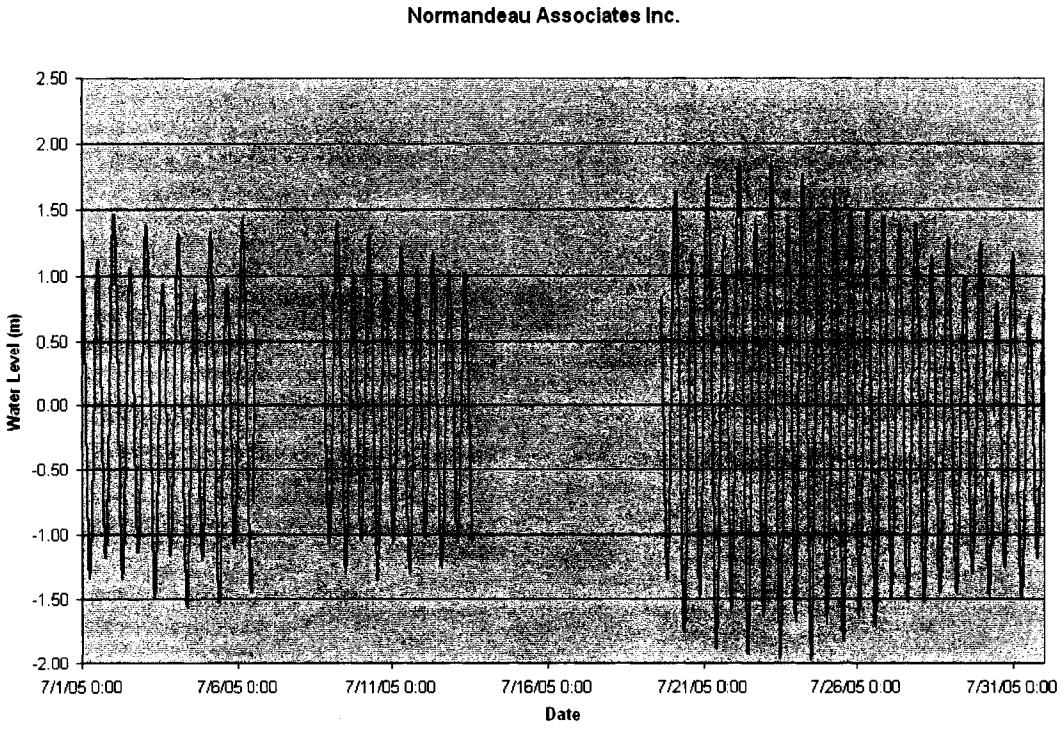

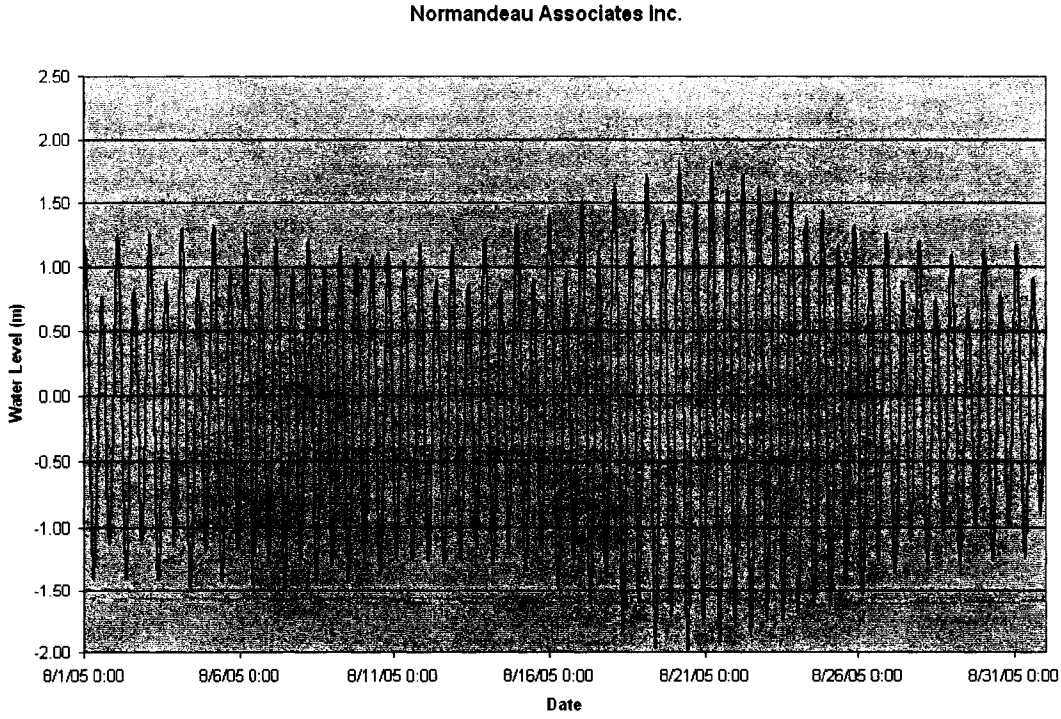

Reproduced with permission of the copyright owner. Further reproduction prohibited without permission.

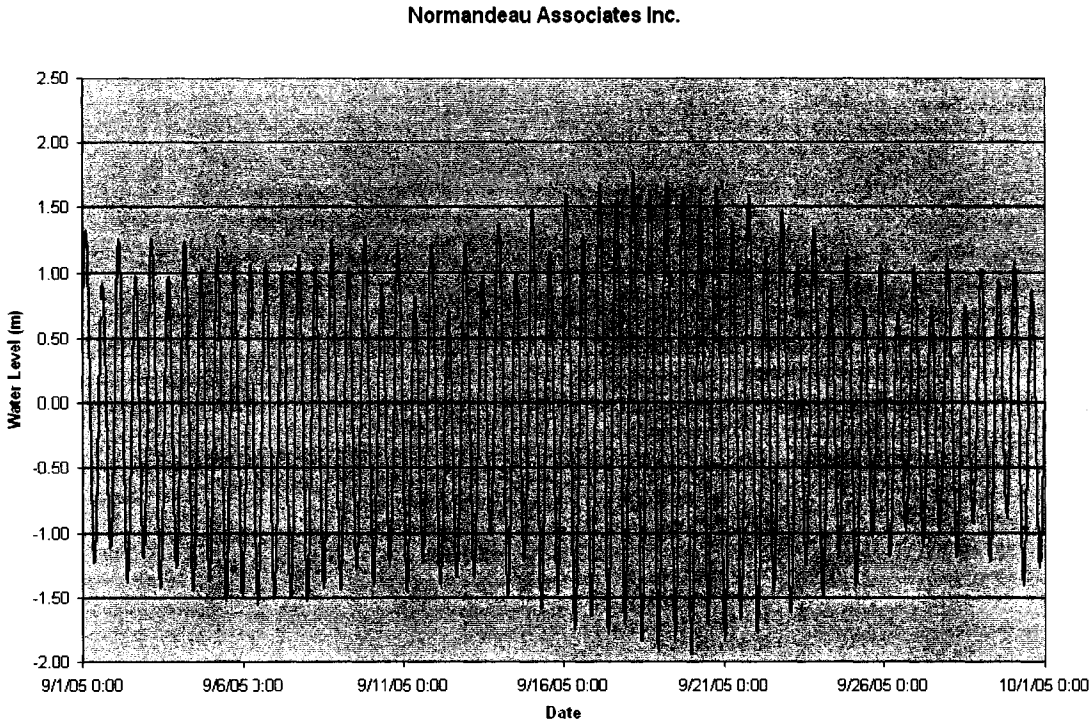

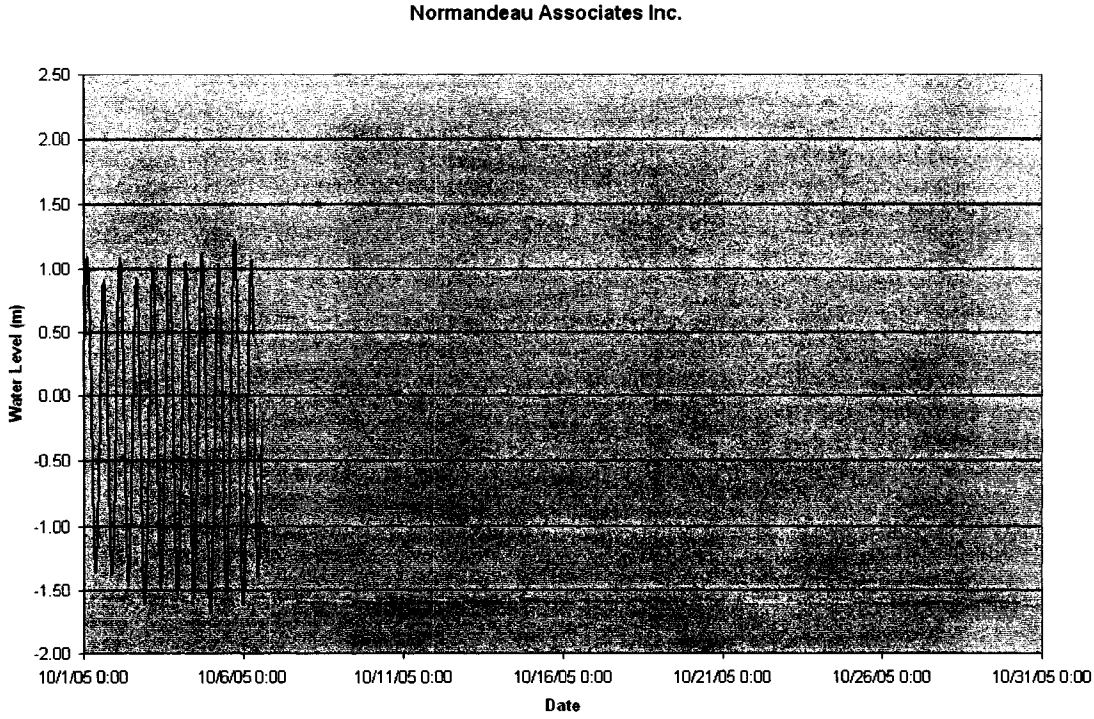

Reproduced with permission of the copyright owner. Further reproduction prohibited without permission.

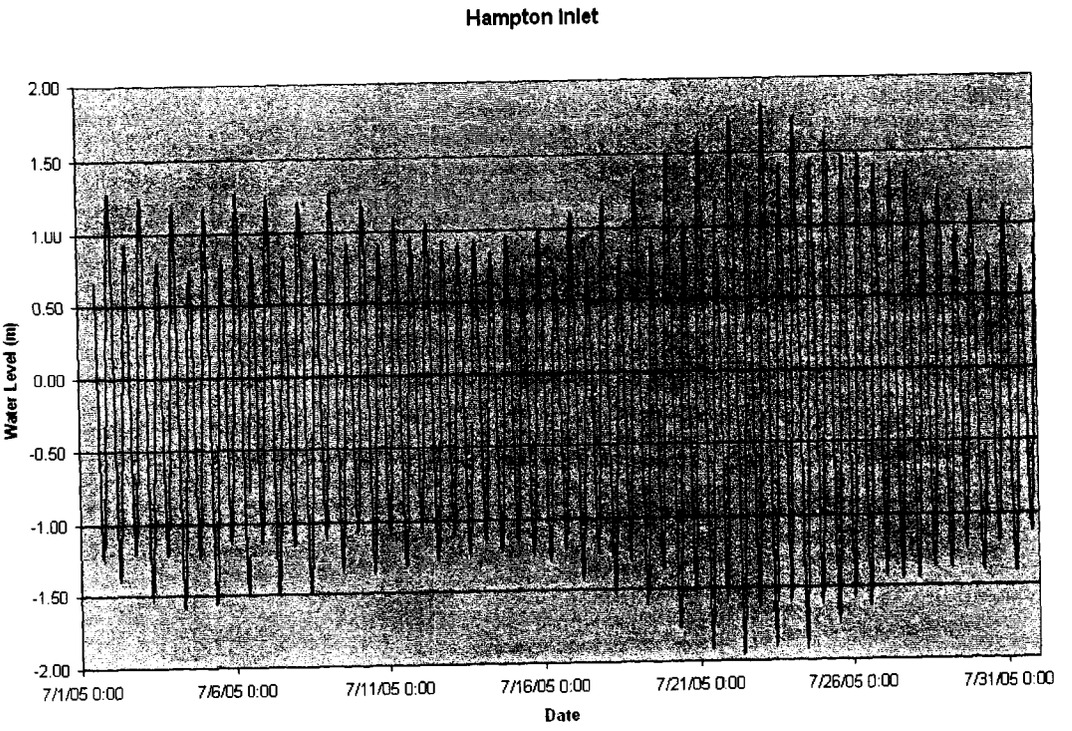

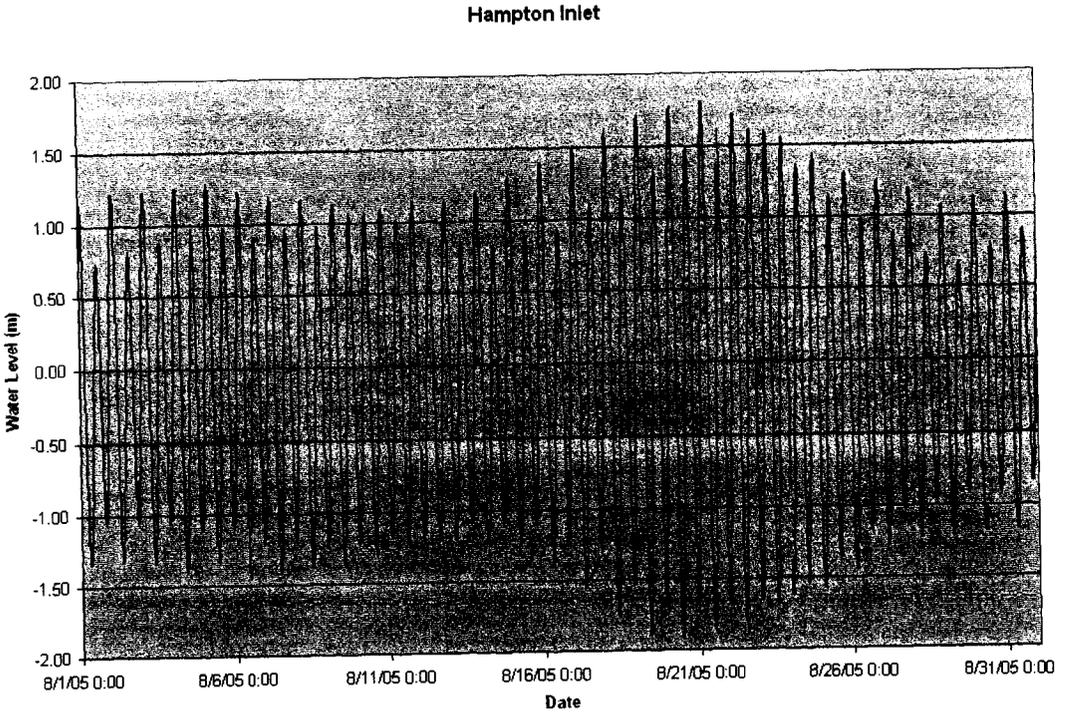

Reproduced with permission of the copyright owner. Further reproduction prohibited without permission.

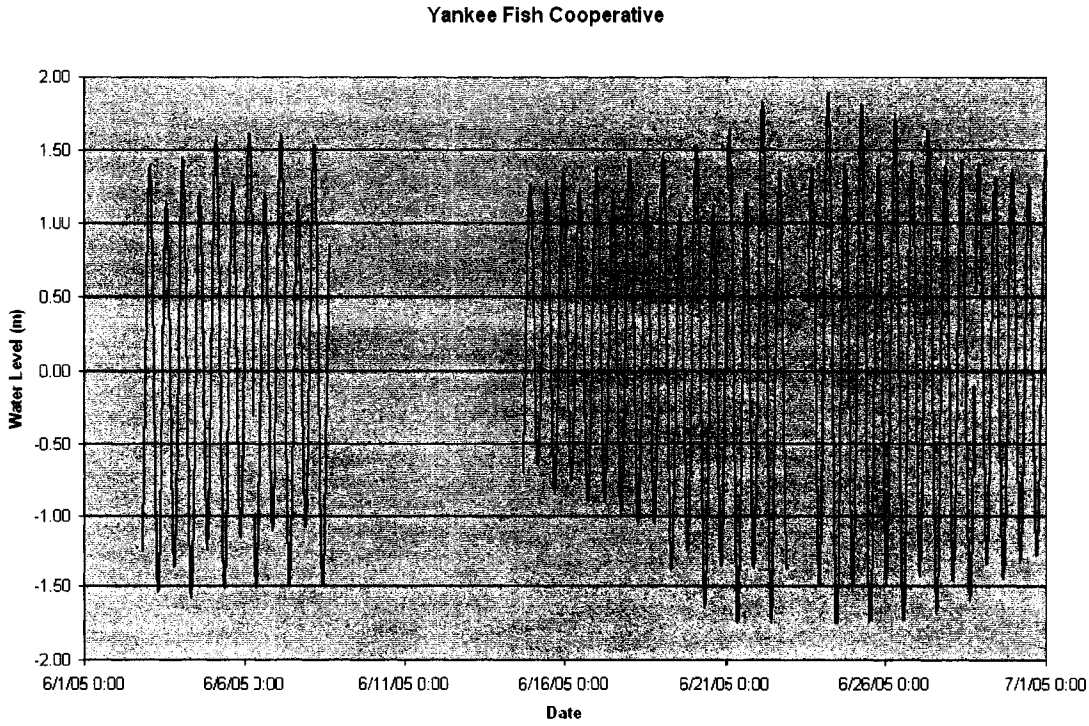

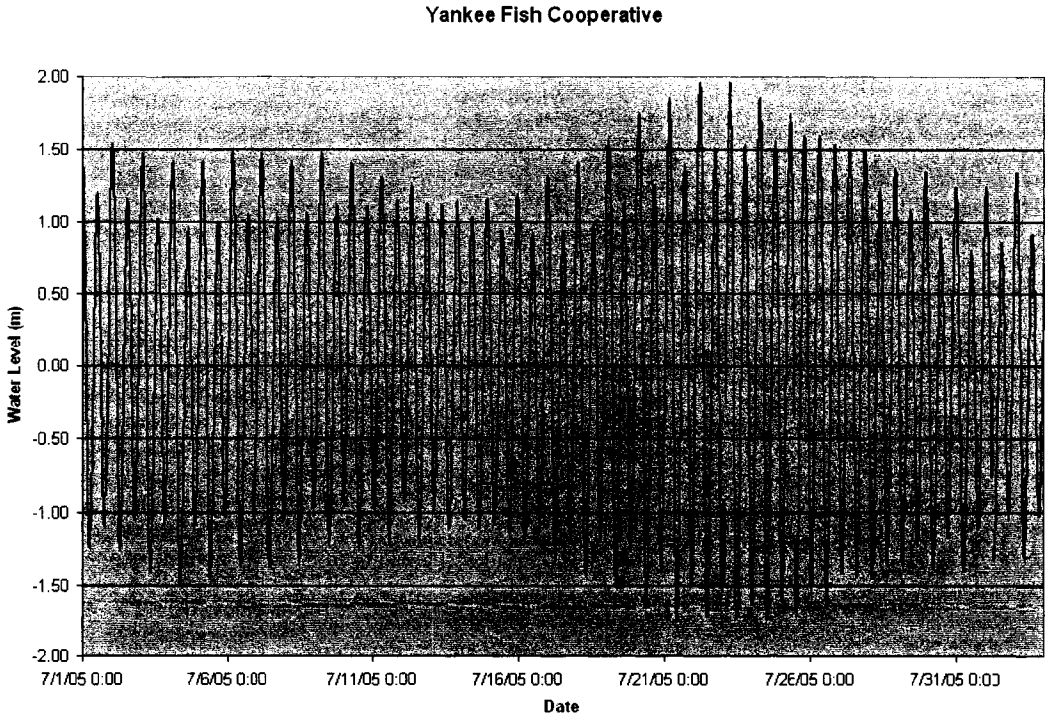

Reproduced with permission of the copyright owner. Further reproduction prohibited without permission.

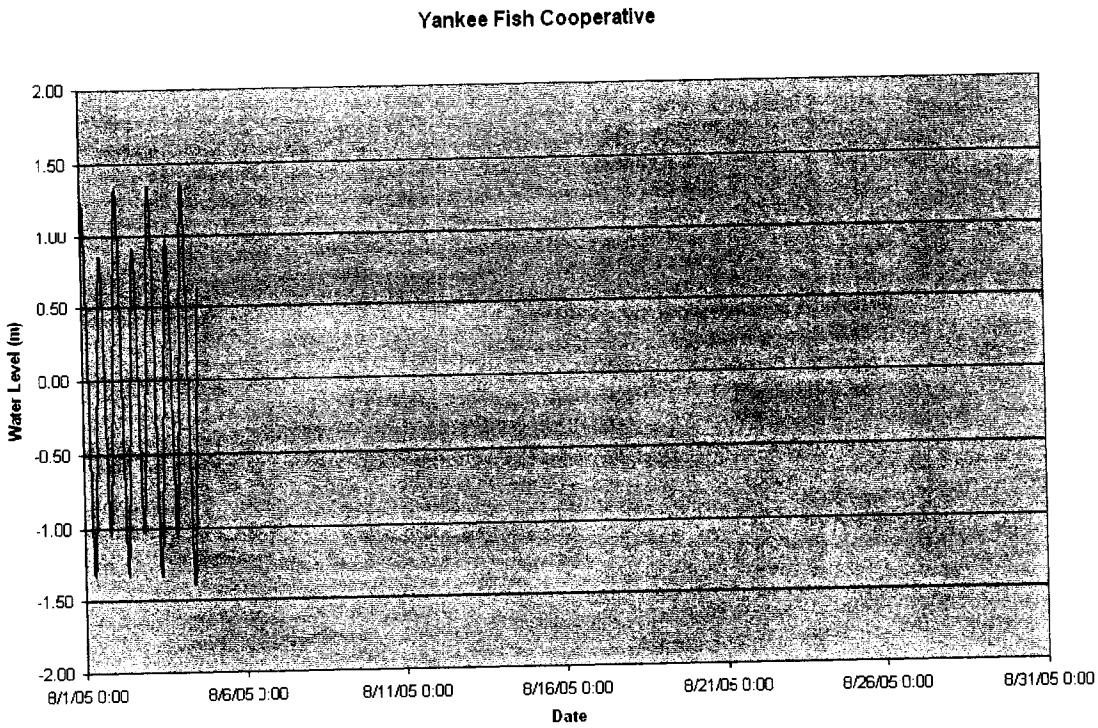

Reproduced with permission of the copyright owner. Further reproduction prohibited without permission.

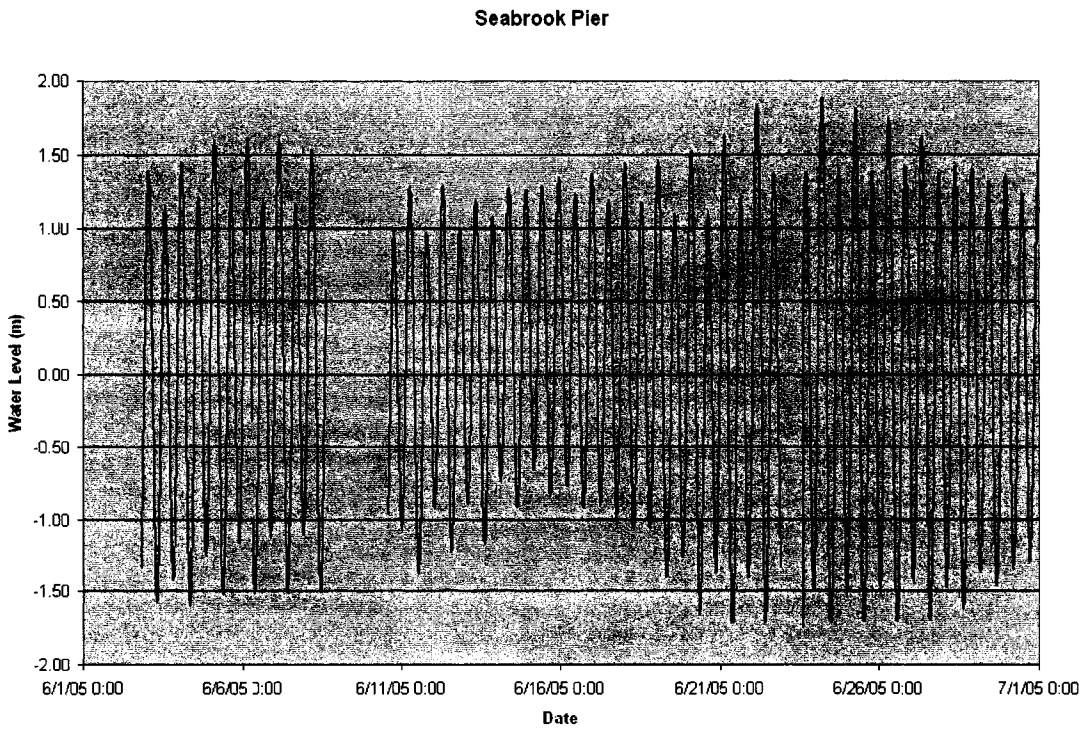

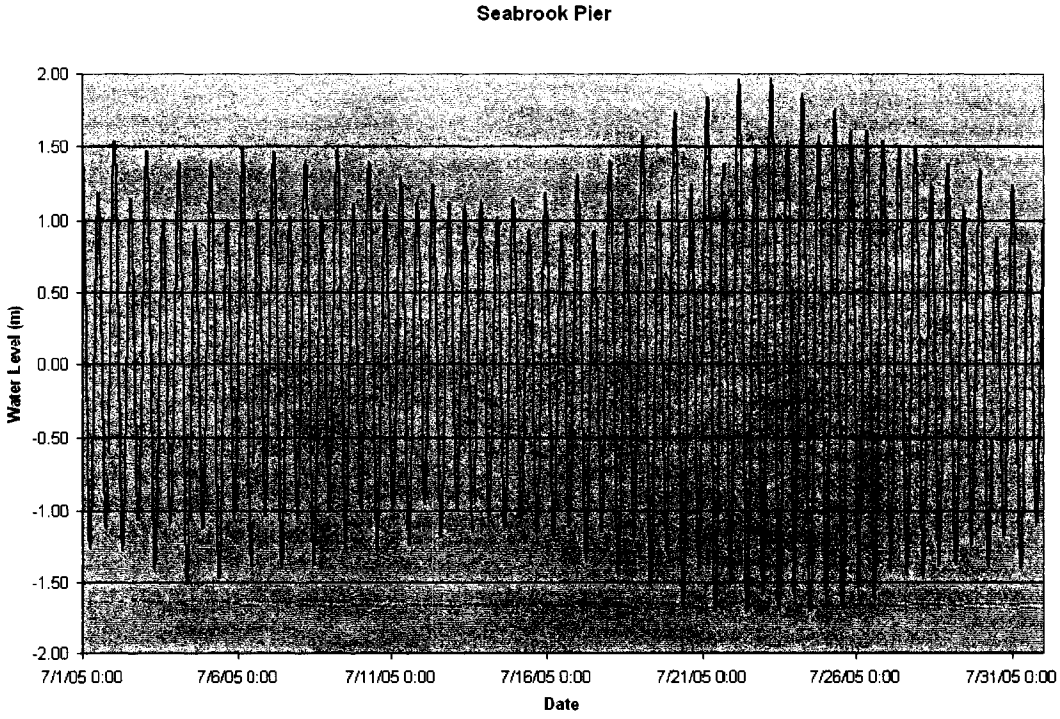

Reproduced with permission of the copyright owner. Further reproduction prohibited without permission.

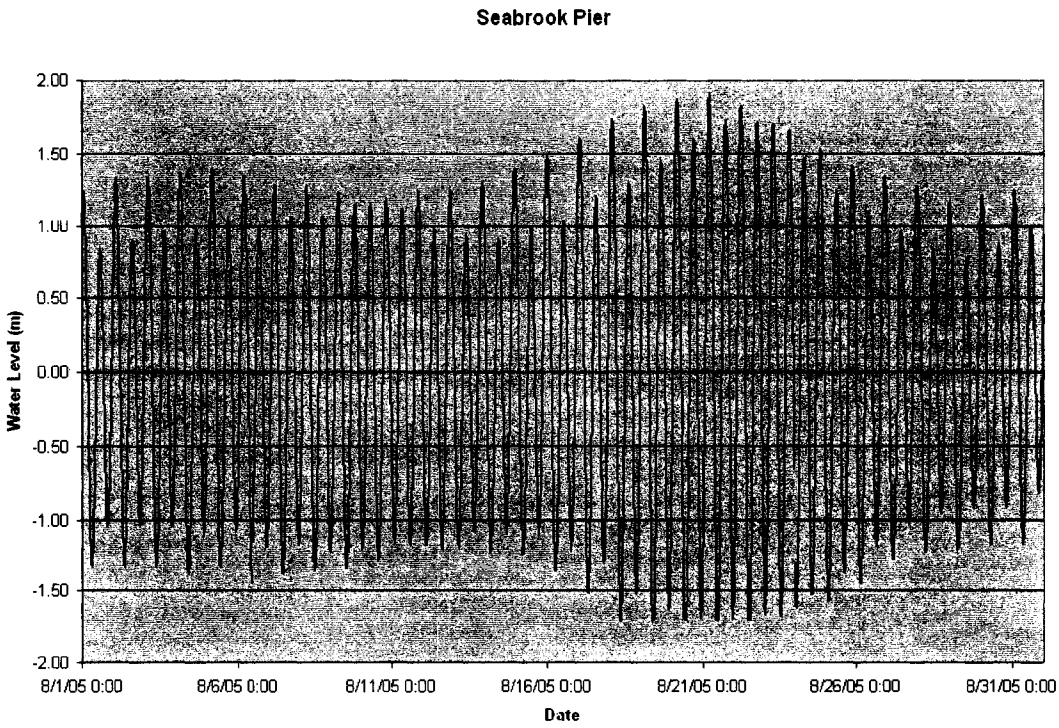

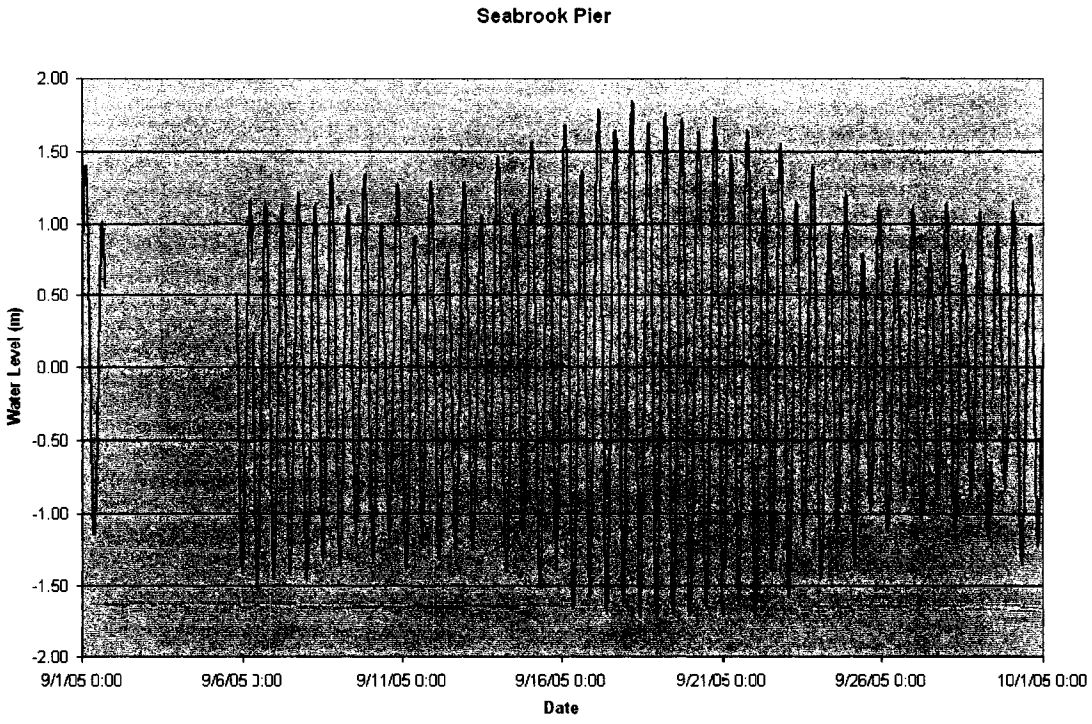

Reproduced with permission of the copyright owner. Further reproduction prohibited without permission.

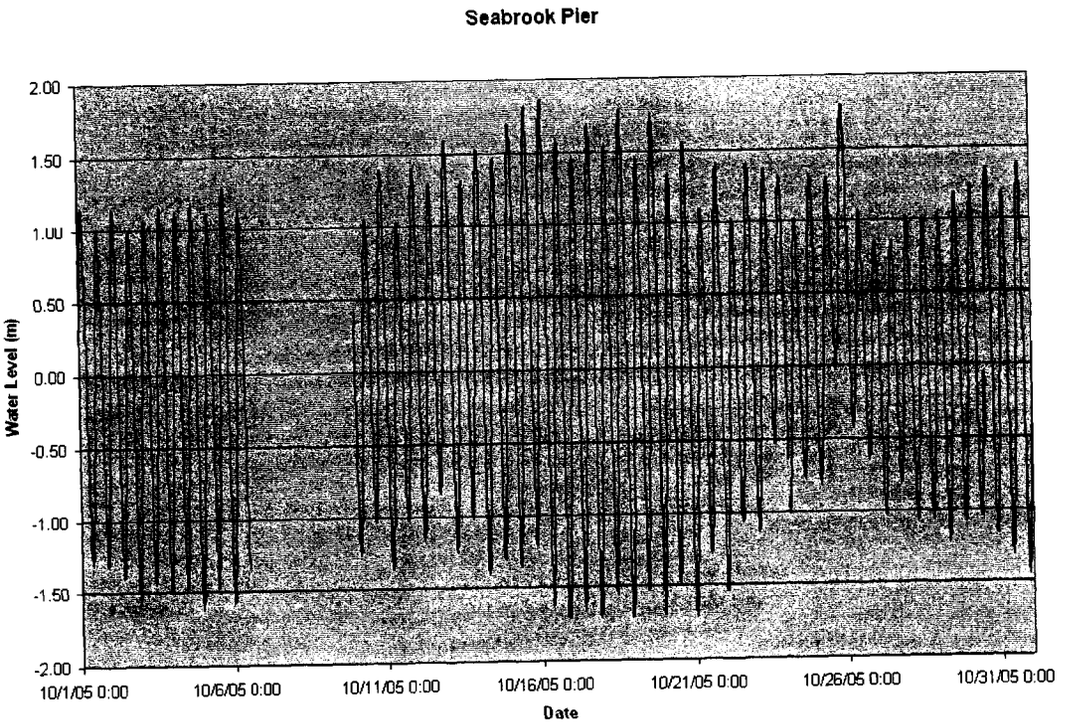

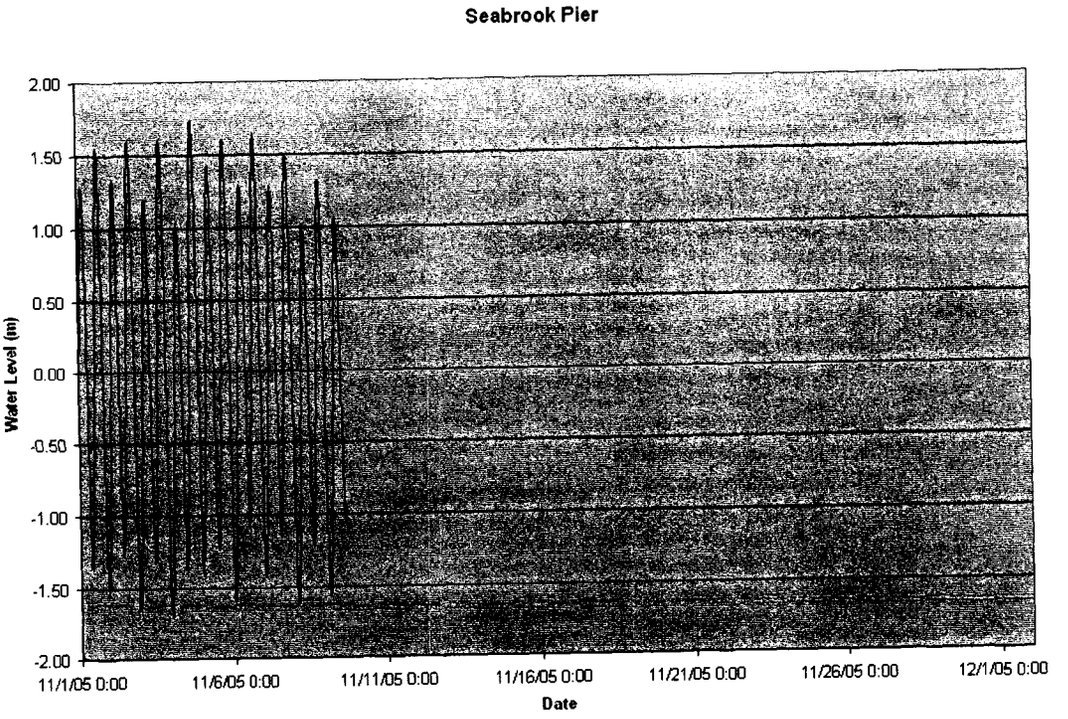

Reproduced with permission of the copyright owner. Further reproduction prohibited without permission.

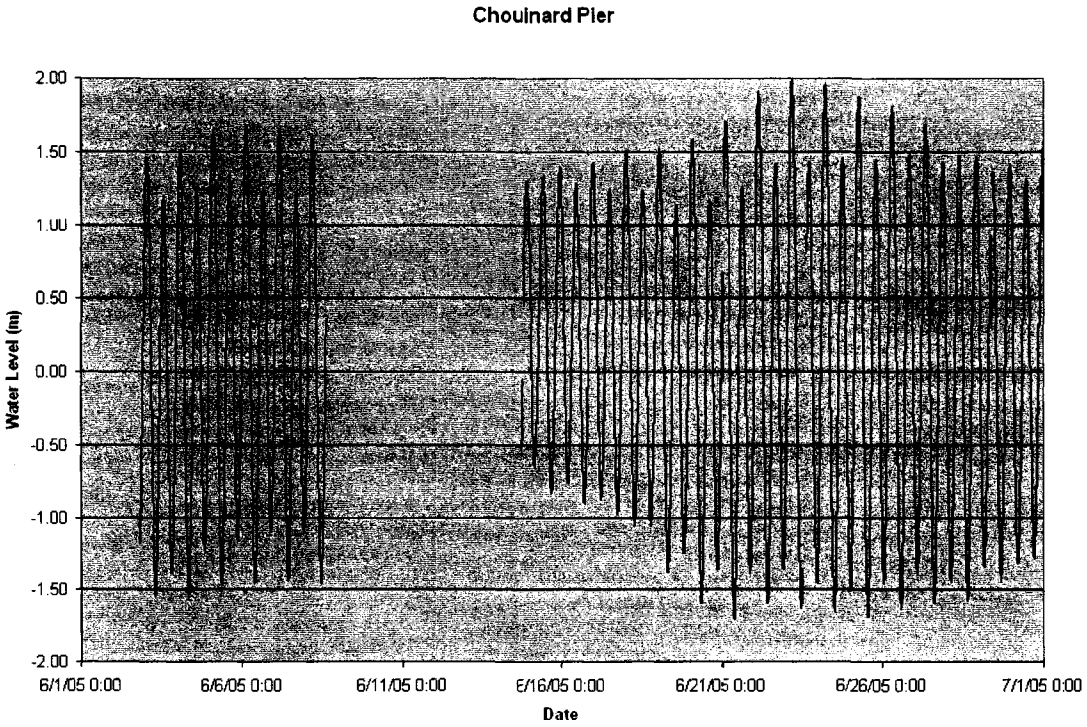

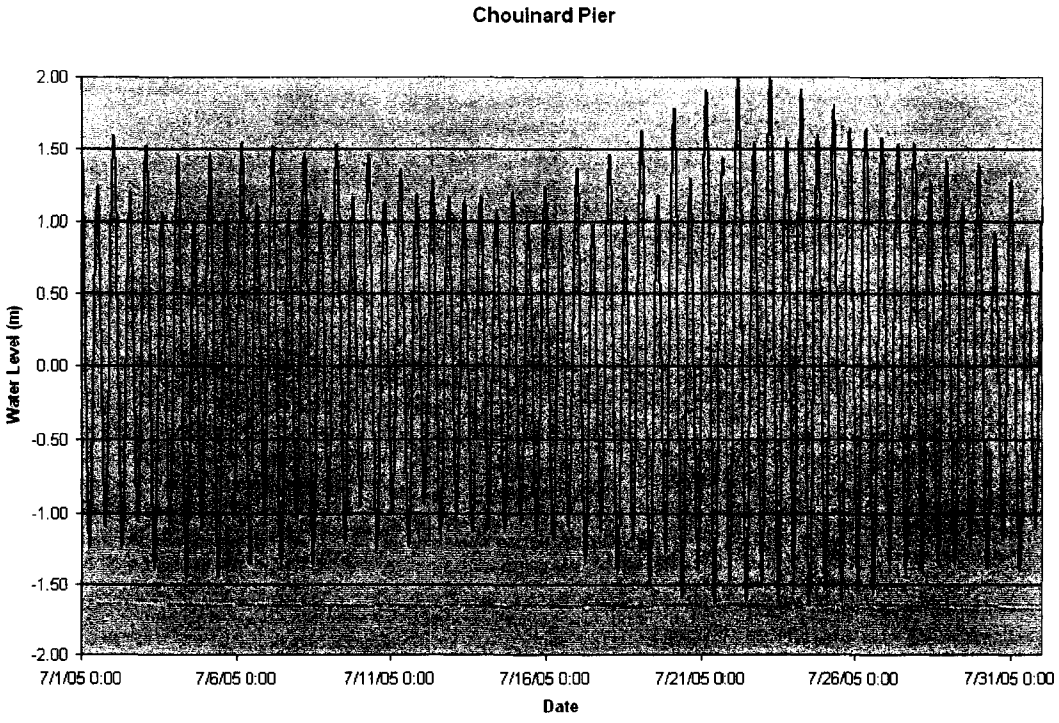

Reproduced with permission of the copyright owner. Further reproduction prohibited without permission.

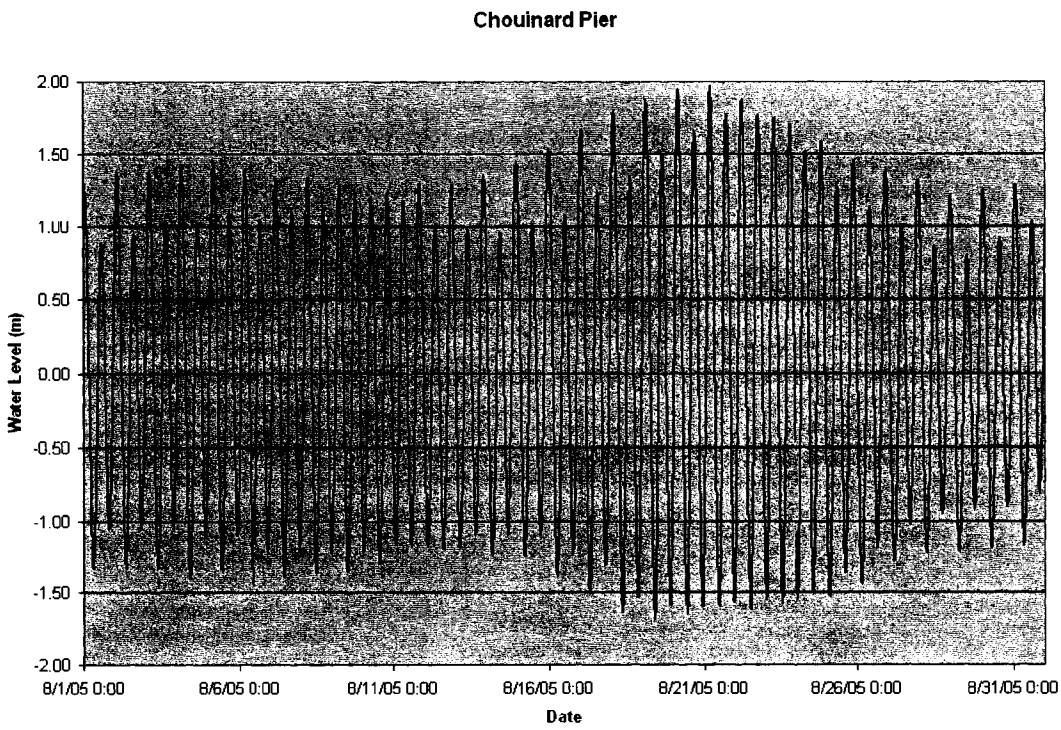

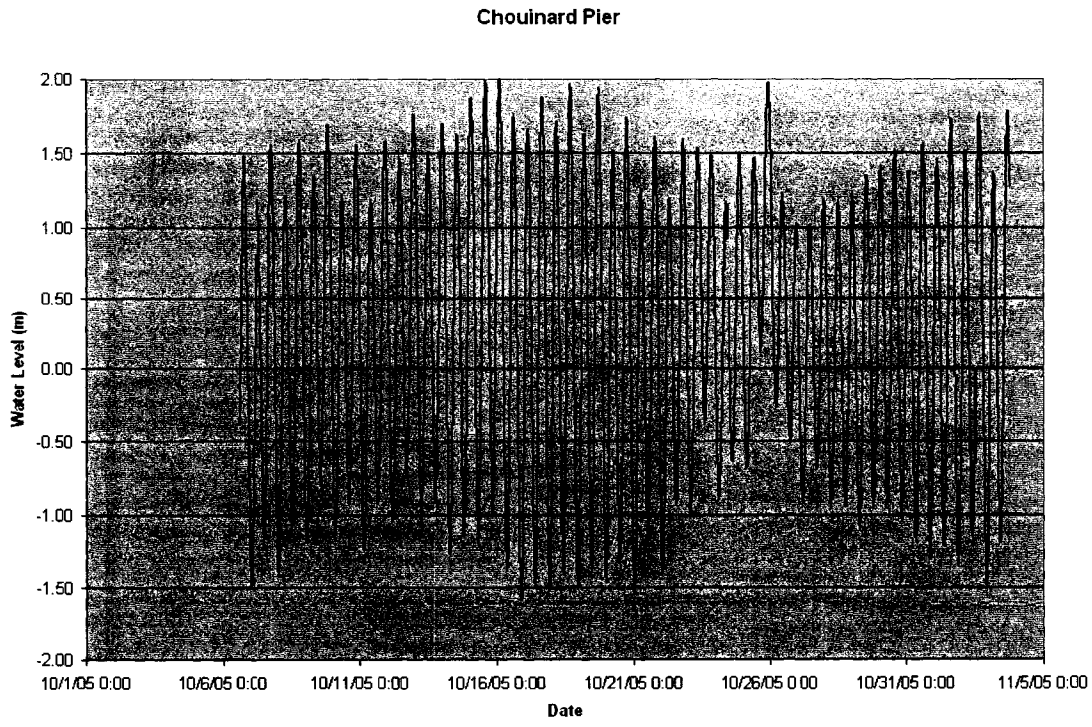

Reproduced with permission of the copyright owner. Further reproduction prohibited without permission.

APPENDIX C

Current Cross-section Plots: Transect Velocity Magnitudes

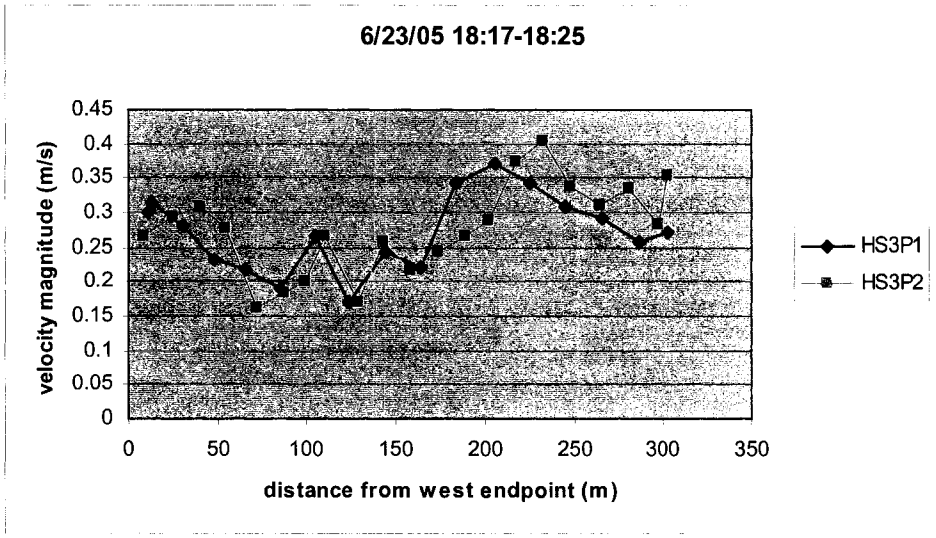

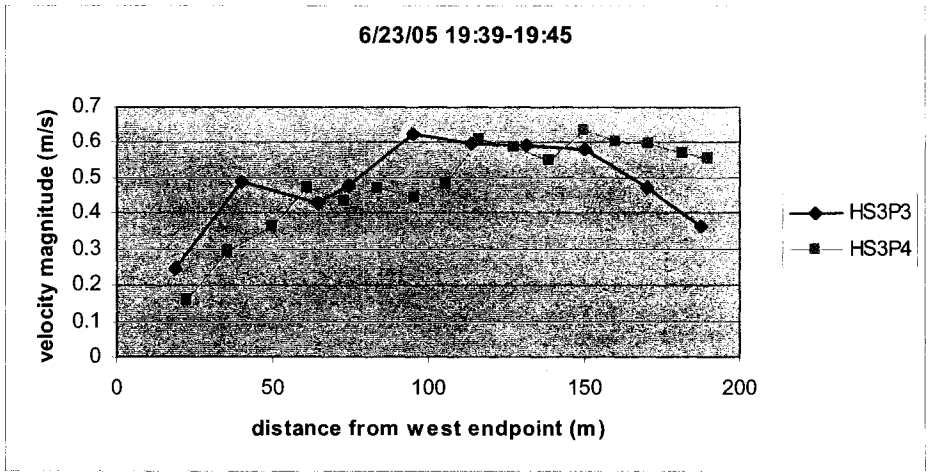

Reproduced with permission of the copyright owner. Further reproduction prohibited without permission.

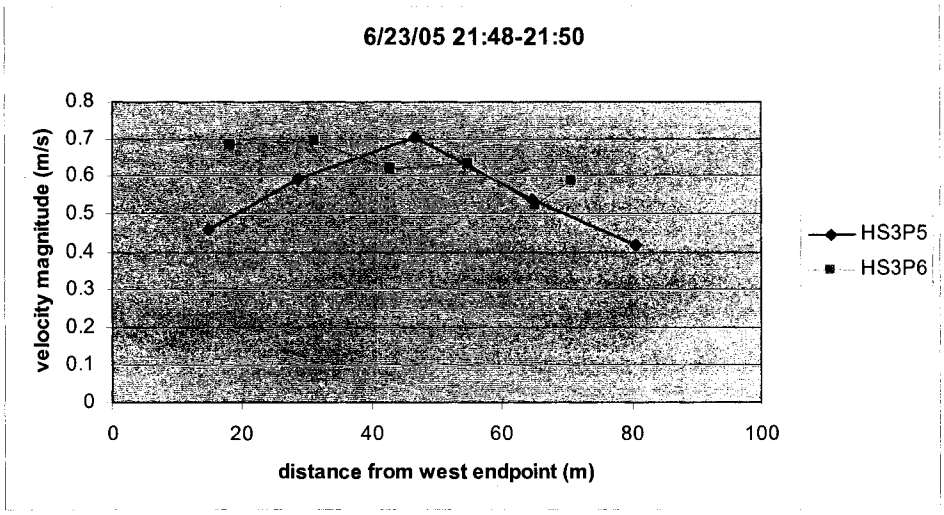

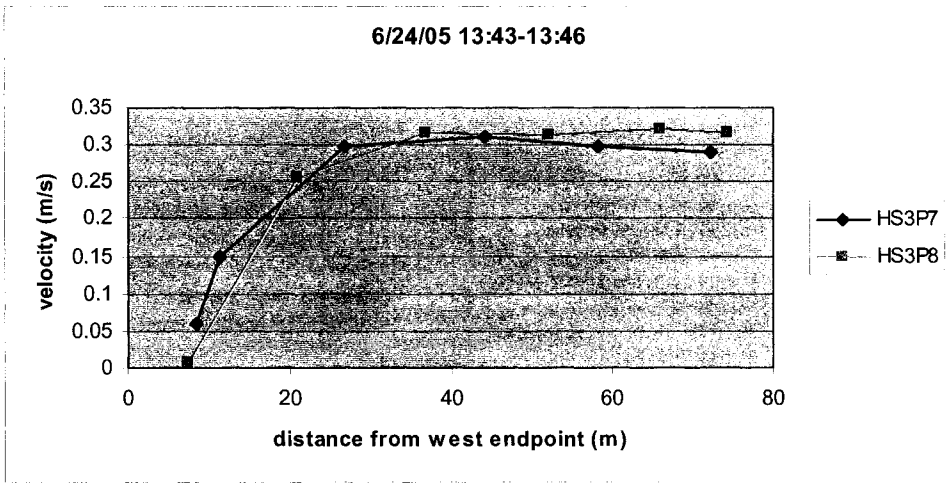

Reproduced with permission of the copyright owner. Further reproduction prohibited without permission.

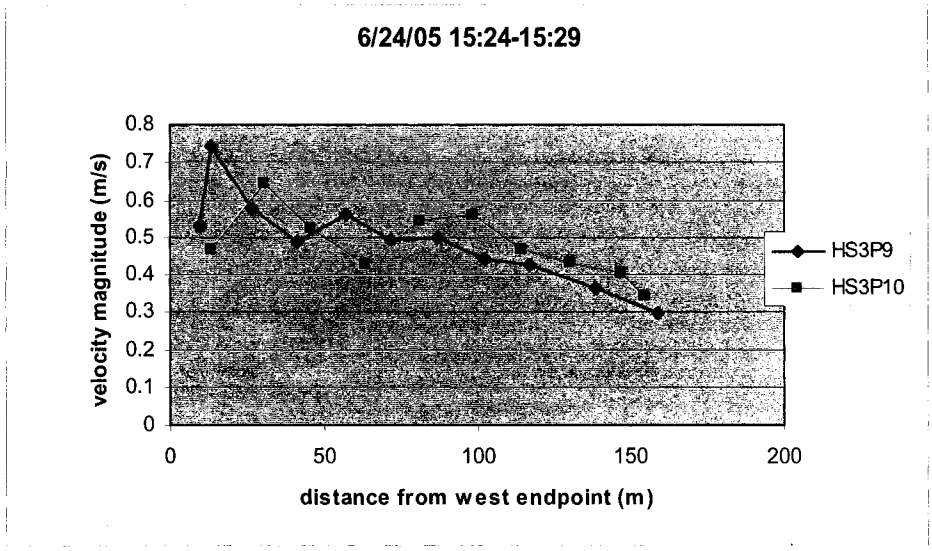

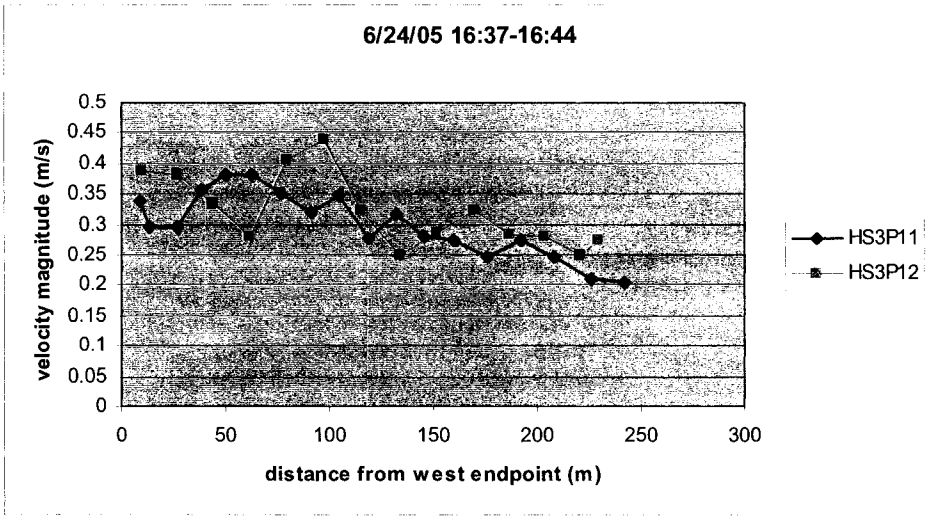

Reproduced with permission of the copyright owner. Further reproduction prohibited without permission.

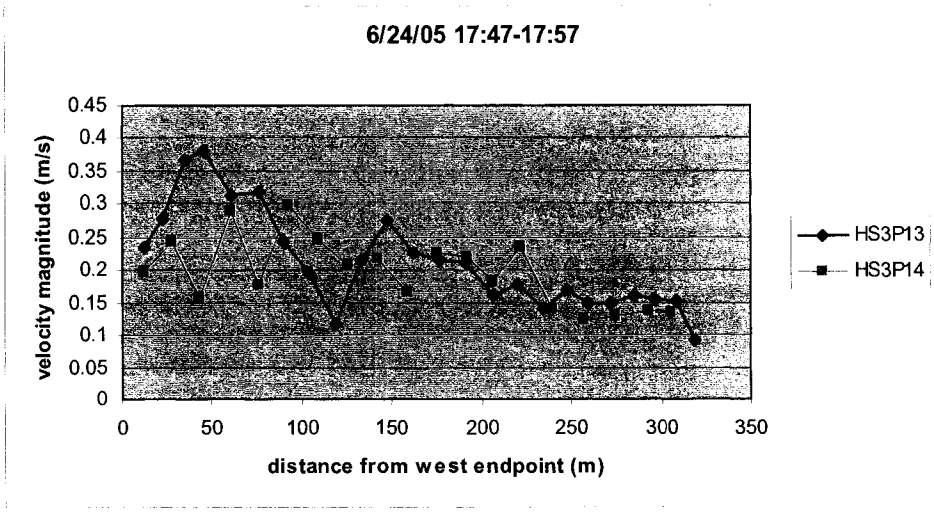

Reproduced with permission of the copyright owner. Further reproduction prohibited without permission.

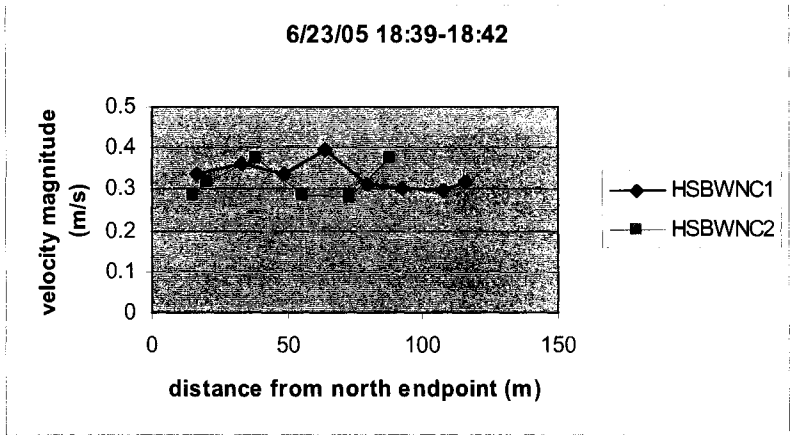

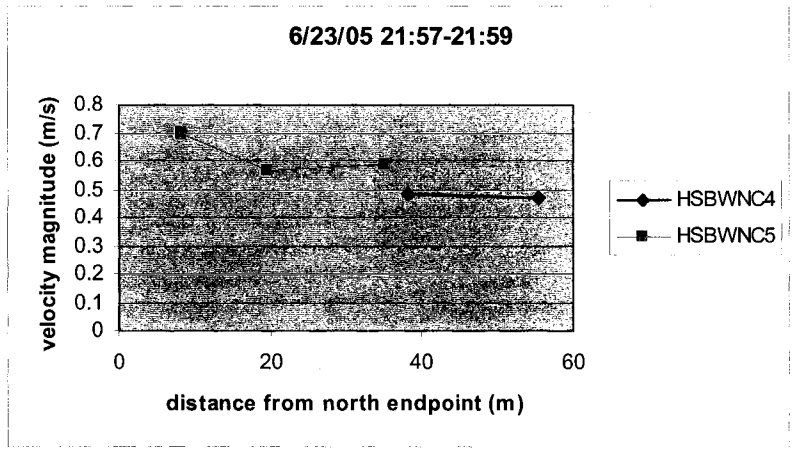

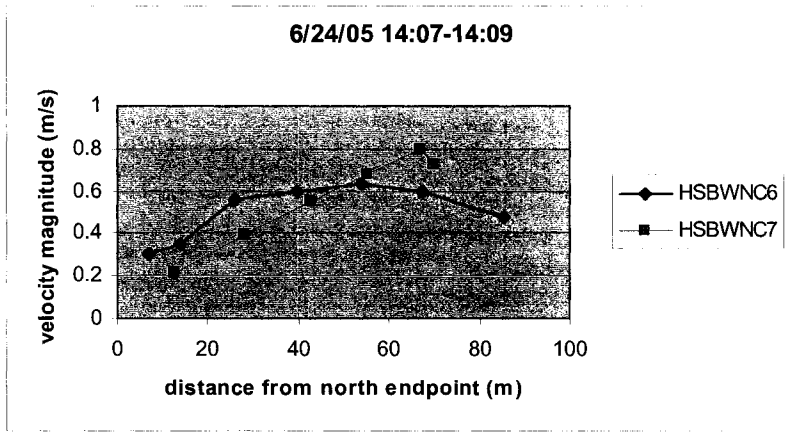

Reproduced with permission of the copyright owner. Further reproduction prohibited without permission.

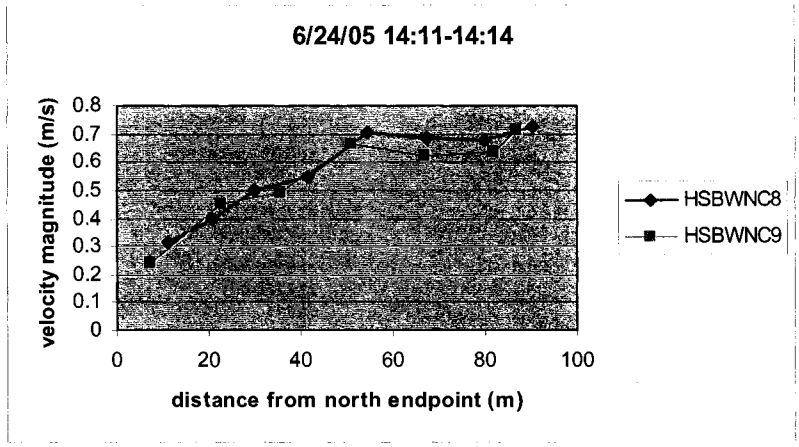

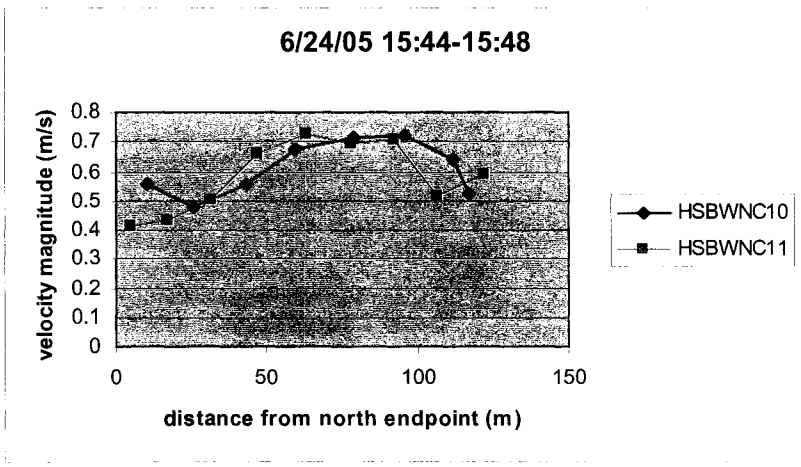

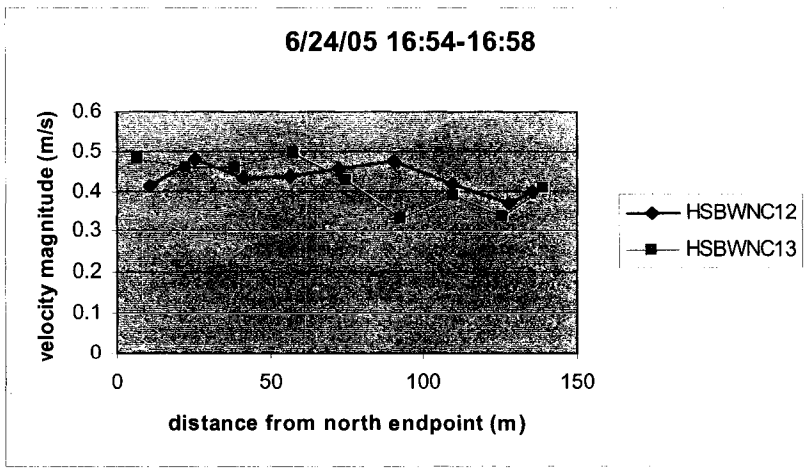

Reproduced with permission of the copyright owner. Further reproduction prohibited without permission.

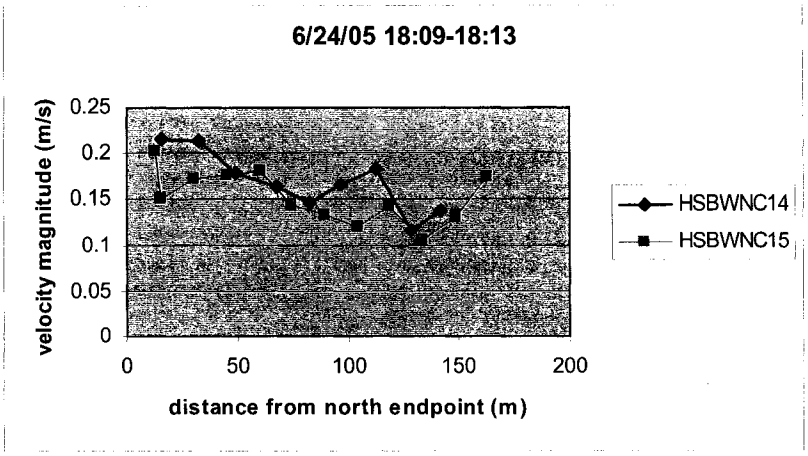

Reproduced with permission of the copyright owner. Further reproduction prohibited without permission.

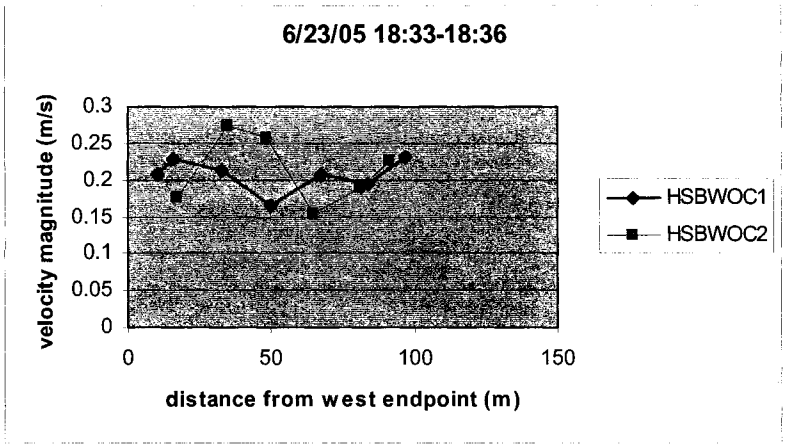

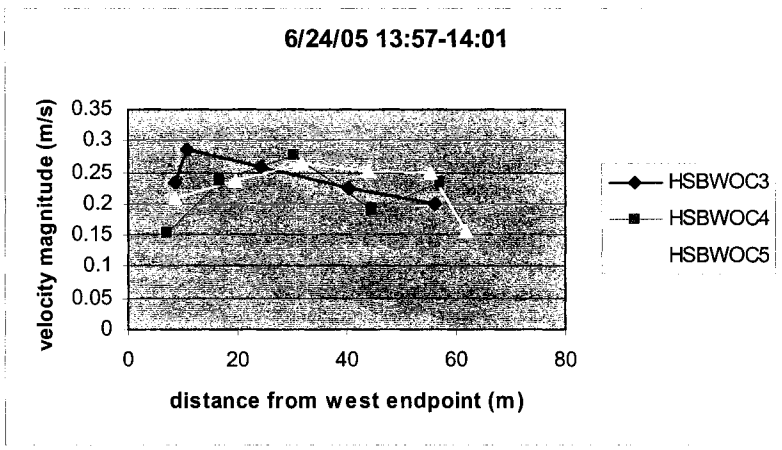

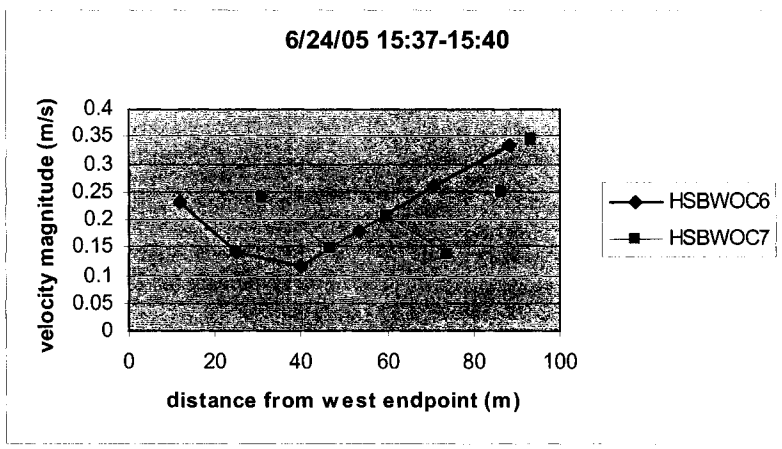

Reproduced with permission of the copyright owner. Further reproduction prohibited without permission.

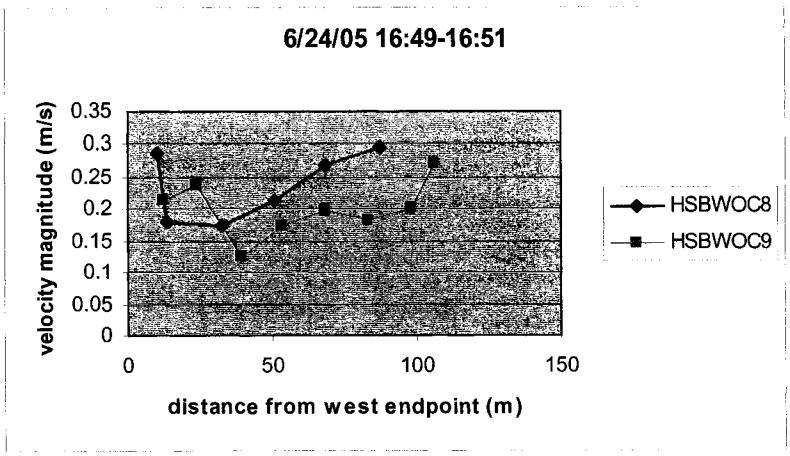

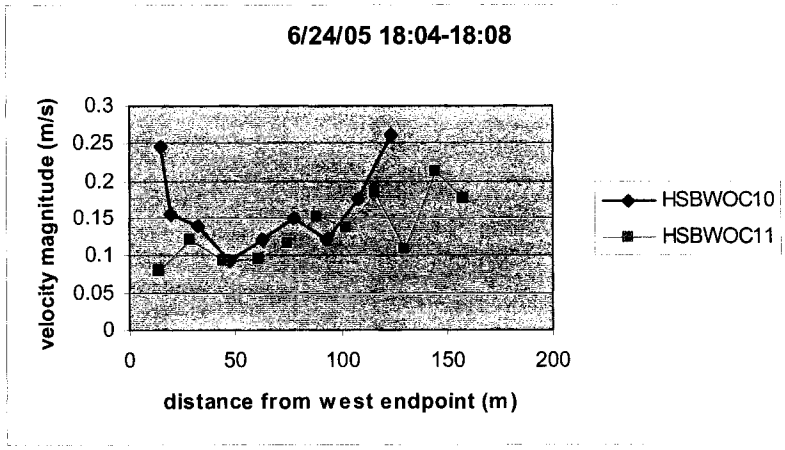

Reproduced with permission of the copyright owner. Further reproduction prohibited without permission.

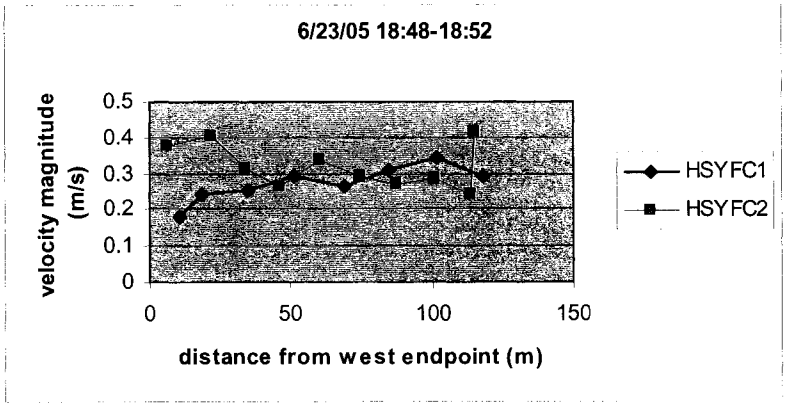

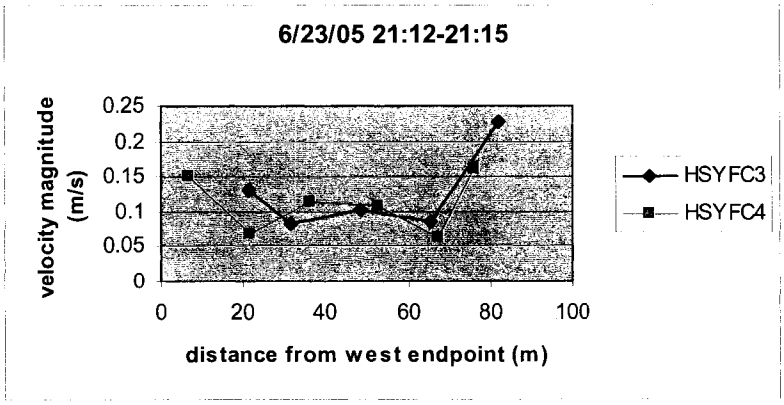

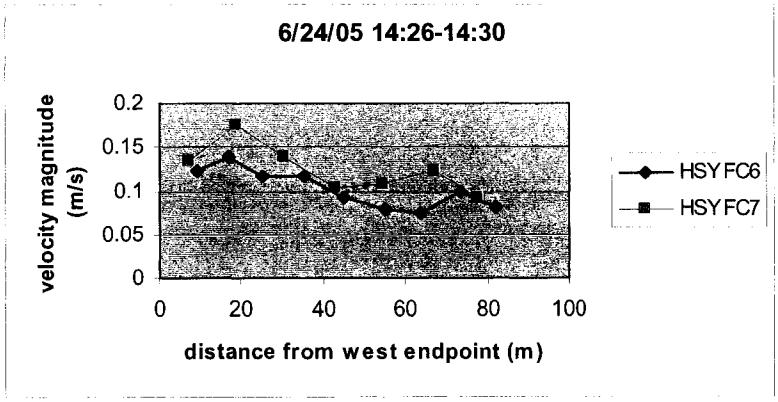

Reproduced with permission of the copyright owner. Further reproduction prohibited without permission.

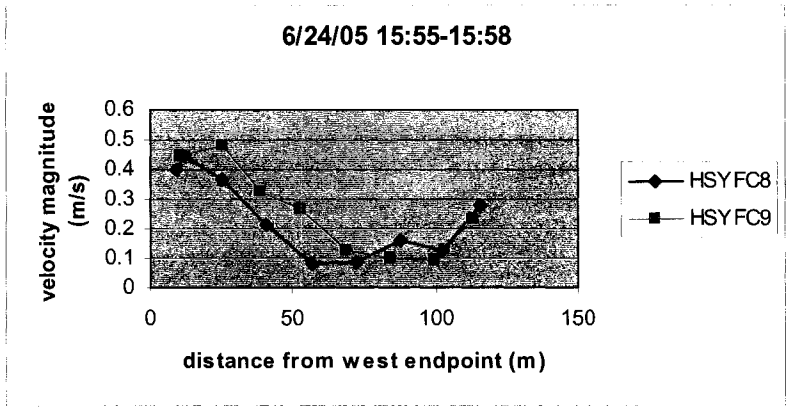

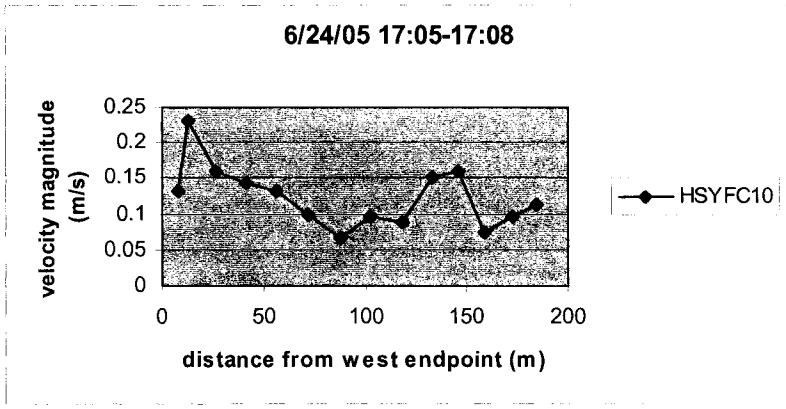

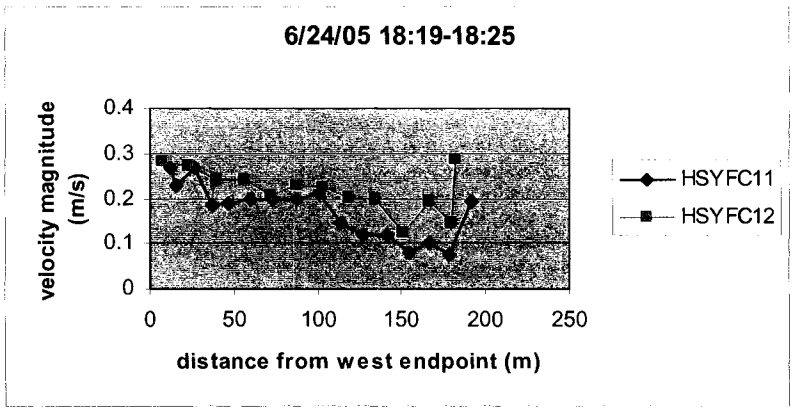

Reproduced with permission of the copyright owner. Further reproduction prohibited without permission.

APPRENDIX D

Matlab Code for Boundary Condition Generation

This section contains the code for bcgenM2N2S2K1O1.m, tcon_int.m, and t_predic.m

bcgenM2N2S2K1O1.m

```
%%%%%%%%%%%%%%%%%%%%%%%%%%%%%%%%%%%%%%%%%%%%%%%%%%%%%%%%%%%%%%%%%%%%%%%%%%
%
%     This program reads a 2dm file and a amp/phase file to make a bc
file.
%
%%%%%%%%%%%%%%%%%%%%%%%%%%%%%%%%%%%%%%%%%%%%%%%%%%%%%%%%%%%%%%%%%%%%%%%%%%

fni = input('What is the full path of the xyphase.station input filename:
', 's');
fno = input('What is the full path of the boundary condition output
filename: ', 's');
tt  = input('What is the total run time: ');
dt  = input('What is the time increment: ');
st  = input('What is the starting time: ');
ts  = input('What is the number of time steps: ');

fid =fopen(fni,'r');
fid2 =fopen(fno,'w');

M = fscanf(fid,'%g %g %g %g %g %g %g %g %g %g %g %g',[12 inf]);

%[m,n]=size(M);

xi = 369500:5:372000;
yi = 42300 :5:46800;
[XI,YI] = meshgrid(xi,yi);

fclose(fid);
clear xi yi fni fid

ZIM2 = griddata(M(1,:),M(2,:),M(3,:),XI,YI,'linear');
```


Reproduced with permission of the copyright owner. Further reproduction prohibited without permission.

```
ZIIM2 = griddata(M(1,:),M(2,:),M(4,:),XI,YI,'linear');
ZIN2 = griddata(M(1,:),M(2,:),M(5,:),XI,YI,'linear');
ZIIN2 = griddata(M(1,:),M(2,:),M(6,:),XI,YI,'linear');
ZIS2 = griddata(M(1,:),M(2,:),M(7,:),XI,YI,'linear');
ZIIS2 = griddata(M(1,:),M(2,:),M(8,:),XI,YI,'linear');
ZIK1 = griddata(M(1,:),M(2,:),M(9,:),XI,YI,'linear');
ZIIK1 = griddata(M(1,:),M(2,:),M(10,:),XI,YI,'linear');
ZIO1 = griddata(M(1,:),M(2,:),M(11,:),XI,YI,'linear');
ZIIO1 = griddata(M(1,:),M(2,:),M(12,:),XI,YI,'linear');


fni2 = input('What is the full path of the 2dm input filename: ', 's');
fid =fopen(fni2,'r');

i=1;

TM2=12.4206;    %tidal period
wM2=2*pi/TM2;   %tidal frequency
TN2=12.6583;    %tidal period
wN2=2*pi/TN2;   %tidal frequency
TS2=12.00;      %tidal period
wS2=2*pi/TS2;   %tidal frequency
TK1=23.9345;    %tidal period
wK1=2*pi/TK1;   %tidal frequency
TO1=25.8193;    %tidal period
wO1=2*pi/TO1;   %tidal frequency


while (~feof(fid) & i<156)
   line = fgetl(fid);
   card = sscanf(line,'%s',[1,1]);
   [m,n]=size(card);
   if  m==1 & n==2 & card =='ND'
      nn(i) = sscanf(line,'ND %d',[1,1]);
      x(i) = sscanf(line,'ND %*d%f',[1,1]);
      y(i) = sscanf(line,'ND %*d%*f%f',[1,1]);
      z(i) = sscanf(line,'ND %*d%*f%*f%f',[1,1]);
      amM2(i)=findz(x(i),y(i),XI,YI,ZIM2);
```


Reproduced with permission of the copyright owner. Further reproduction prohibited without permission.

```
      phM2(i)=findz(x(i),y(i),XI,YI,ZIIM2);
      amN2(i)=findz(x(i),y(i),XI,YI,ZIN2);
      phN2(i)=findz(x(i),y(i),XI,YI,ZIIN2);
      amS2(i)=findz(x(i),y(i),XI,YI,ZIS2);
      phS2(i)=findz(x(i),y(i),XI,YI,ZIIS2);
      amK1(i)=findz(x(i),y(i),XI,YI,ZIK1);
      phK1(i)=findz(x(i),y(i),XI,YI,ZIIK1);
      amO1(i)=findz(x(i),y(i),XI,YI,ZIO1);
      phO1(i)=findz(x(i),y(i),XI,YI,ZIIO1);
      i=i+1;
   end
end

%phase differences

fprintf(fid2,'T1\nT2 Created by BCGEN Author Serkan Mahmutoglu\nT3\n');
fprintf(fid2,'SI   1\n');
fprintf(fid2,'$L  0  62  60  64  0  3  59\n');
fprintf(fid2,'$M 1\n');
fprintf(fid2,'TR  1  1  1  0\n');
fprintf(fid2,'TZ  %10.5f  %10.5f  %7d  %7d\n',dt,tt,ts,st);
fprintf(fid2,'TI  4  4  0.0000  0.00010\n');
fprintf(fid2,'TR  1  1  1  0\n');
fprintf(fid2,'DM  1  8  4  0.02  0\n');
fprintf(fid2,'TRN  4269  9634  9410  11286  12187  19696  20723  20687
20981\n');
fprintf(fid2,'FT  15\n');
fprintf(fid2,'IC  1.66  0  0\n');
fprintf(fid2,'EV   1  2500  2500  2500  2500  0.02\n');
fprintf(fid2,'EV   2  2500  2500  2500  2500  0.03\n');
fprintf(fid2,'EV   3  2500  2500  2500  2500  0.02\n');
fprintf(fid2,'EV   4  2500  2500  2500  2500  0.02\n');
fprintf(fid2,'EV   5  2500  2500  2500  2500  0.03\n');
fprintf(fid2,'EV   6  3000  3000  3000  3000  0.02\n');
fprintf(fid2,'EV   7  3000  3000  3000  3000  0.02\n');
fprintf(fid2,'EV   8  2500  2500  2500  2500  0.02\n');
fprintf(fid2,'EV   9  7500  7500  7500  7500  0.02\n');
fprintf(fid2,'EV  10  2500  2500  2500  2500  0.02\n');
```


Reproduced with permission of the copyright owner. Further reproduction prohibited without permission.

```
fprintf(fid2,'EV  11  3500  3500  3500  3500  0.02\n');

for t=st:dt:tt
   for j=1:155
      fprintf(fid2,'BCN %7d  200  0.00  0.00
%10.5f\n',j,(amM2(j)*sin(wM2*t-phM2(j)*pi/180) + amN2(j)*sin(wN2*t-
phN2(j)*pi/180) + amS2(j)*sin(wS2*t-phS2(j)*pi/180) + amK1(j)*sin(wK1*t-
phK1(j)*pi/180) + amO1(j)*sin(wO1*t-phO1(j)*pi/180)));
   end
   fprintf(fid2,'END Simulation at time = %10.5f\n',t);
end

fprintf(fid2,'STOP\n');

fclose('all')
```

tcon_int.m

```
% This program takes 5 tidal constituents at 5 stations
%   and interpolates each constituent to a particular
%   point.

% Written by Kimberly Leung (2006)

% The order of stations in each array:
%   ps - Portsmouth
%   pl - Portland
%   cp - Cape Porpoise
%   bo - Boston
%   cl - Cashes Ledge


%   x = x-coordinate of station in NHSP (easting)
%   y = y-coordinate of station in NHSP (northing)
%

% need list of times called timelist.txt in format: [yyyy,m,d,h,mm,ss]

% boundaries of study area
xi = 369500:5:373000;
yi = 42300 :5:46800;
[XI,YI] = meshgrid(xi,yi);  % creating grid of points within study area


% coordinates of stations
x = [375999.671 414288.016 412398.143 350808.772 510017.760];
y = [65222.409 128729.440 80541.043 -16477.478 79149.930];
```


Reproduced with permission of the copyright owner. Further reproduction prohibited without permission.

```
% tidal constituents (phase and amplitude) for each station
zM2a = [1.303 1.330 1.272 1.345 1.200];
zM2p = [107 103 103 111 98];
zN2a = [.278 .296 .299 .301 .282];
zN2p = [76 73 71 82 66];
zS2a = [.203 .217 .203 .219 .195];
zS2p = [143 138 134 146 126];
zK1a = [.141 .139 .129 .140 .125];
zK1p = [204 202 204 207 198];
zO1a = [.112 .111 .106 .111 .101];
zO1p = [185 183 185 189 186];


% gridding data to mesh
ZIM2a = griddata(x,y,zM2a,XI,YI);
ZIM2p = griddata(x,y,zM2p,XI,YI);
ZIN2a = griddata(x,y,zN2a,XI,YI);
ZIN2p = griddata(x,y,zN2p,XI,YI);
ZIS2a = griddata(x,y,zS2a,XI,YI);
ZIS2p = griddata(x,y,zS2p,XI,YI);
ZIK1a = griddata(x,y,zK1a,XI,YI);
ZIK1p = griddata(x,y,zK1p,XI,YI);
ZIO1a = griddata(x,y,zO1a,XI,YI);
ZIO1p = griddata(x,y,zO1p,XI,YI);


% interpolating to node 81 - (372000,44050) are coordinates of node 81
%    in NHSP
M2a = interp2(xi,yi,ZIM2a,372000,44050);
M2p = interp2(xi,yi,ZIM2p,372000,44050);
N2a = interp2(xi,yi,ZIN2a,372000,44050);
N2p = interp2(xi,yi,ZIN2p,372000,44050);
S2a = interp2(xi,yi,ZIS2a,372000,44050);
S2p = interp2(xi,yi,ZIS2p,372000,44050);
K1a = interp2(xi,yi,ZIK1a,372000,44050);
K1p = interp2(xi,yi,ZIK1p,372000,44050);
O1a = interp2(xi,yi,ZIO1a,372000,44050);
O1p = interp2(xi,yi,ZIO1p,372000,44050);


% setting up tidecon for t_predic.m
fmaj = [M2a;N2a;S2a;K1a;O1a];
emaj = [.6;.6;.5;.7;.6];
ph = [M2p;N2p;S2p;K1p;O1p];
eph = [1;3;2;4;4];

tidecon = [fmaj emaj ph eph];

names = ['M2';'N2';'S2';'K1';'O1'];

load timelist.txt

format long

% conversion to serial date number
time = datenum(timelist);
```


Reproduced with permission of the copyright owner. Further reproduction prohibited without permission.

```
% frequencies of each constituent
freq = [1/12.42;1/12.66;1/12.00;1/23.93;1/25.82];

% computing water surface elevation time series
y_out = t_predic(time,names,freq,tidecon,'latitude',42+53.6/60);

% converting back to calendar days
timed = datestr(time,0);


% saving to .mat file
save bc_tseries timed y_out
```

t_predic.m

```
function yout=t_predic(tim,varargin);
% T_PREDIC Tidal prediction
% YOUT=T_PREDIC(TIM,NAMES,FREQ,TIDECON) makes a tidal prediction
% using the output of T_TIDE at the specified times TIM in decimal
% days (from DATENUM). Optional arguments can be specified using
% property/value pairs:
%
%       YOUT=T_PREDIC(...,TIDECON,property,value,...)
%
% Available properties are:
%
%    In the simplest case, the tidal analysis was done without nodal
%    corrections, and thus neither will the prediction. If nodal
%    corrections were used in the analysis, then it is likely we will
%    want to use them in the prediction too and these are computed
%    using the latitude.
%
%     'latitude'        decimal degrees (+north) (default: none)
%
%    The tidal prediction may be restricted to only some of the
%    available constituents:
%
%     'synthesis'    0 - Use all selected constituents.  (default)
%                   scalar>0 - Use only those constituents with a SNR
%                              greater than that given (1 or 2 are
%                              good choices).
%
%
%  It is possible to call t_predic without using property names, in
%  which case the assumed calling sequence is
%
%    YOUT=T_PREDIC(TIM,NAMES,FREQ,TIDECON,LATITUDE,SYNTHESIS);
%
%  T_PREDIC can be called using the tidal structure available as an
%  optional output from T_TIDE
%
%    YOUT=T_PREDIC(TIM,TIDESTRUC,...)
%
% R. Pawlowicz 11/8/99
```


Reproduced with permission of the copyright owner. Further reproduction prohibited without permission.

```
% Version 1.0

if nargin<2,  % Not enough
  error('Not enough input arguments');
end;

if isstruct(varargin{1}),
  names=varargin{1}.name;
  freq=varargin{1}.freq;
  tidecon=varargin{1}.tidecon;
  varargin(1)=[];
else
  if length(varargin)<3,
    error('Not enough input arguments');
  end;
  names=varargin{1};
  freq=varargin{2};
  tidecon=varargin{3};
  varargin(1:3)=[];
end;

lat=[];
synth=0;

k=1;
while length(varargin)>0,
  if ischar(varargin{1}),
    switch lower(varargin{1}(1:3)),
      case 'lat',
         lat=varargin{2};
      case 'syn',
         synth=varargin{2};
      otherwise,
         error(['Can''t understand property:' varargin{1}]);
    end;
    varargin([1 2])=[];
  else
    switch k,
      case 1,
        lat=varargin{1};
      case 2,
        synth=varargin{1};
      otherwise
        error('Too many input parameters');
     end;
     varargin(1)=[];
  end;
  k=k+1;
end;

% Do the synthesis.

snr=(tidecon(:,1)./tidecon(:,2)).^2;  % signal to noise ratio
if synth>0,
   I=snr>synth;
   if ~any(I),
     warning('No predictions with this SNR');
```


Reproduced with permission of the copyright owner. Further reproduction prohibited without permission.

```
      yout=NaN+zeros(size(tim));
      return;
    end;
    tidecon=tidecon(I,:);
    names=names(I,:);
    freq=freq(I);
end;


if size(tidecon,2)==4,   % Real time series
  ap=tidecon(:,1)/2.*exp(-i*tidecon(:,3)*pi/180);
  am=conj(ap);
else
  ap=(tidecon(:,1)+tidecon(:,3))/2.*exp( i*pi/180*(tidecon(:,5)-
tidecon(:,7)));
  am=(tidecon(:,1)-tidecon(:,3))/2.*exp(
i*pi/180*(tidecon(:,5)+tidecon(:,7)));
end;

% Mean at central point (get rid of one point at end to take mean of
% odd number of points if necessary).
jdmid=mean(tim(1:2*fix((length(tim)-1)/2)+1));

const=t_getconsts;
ju=zeros(size(freq));

% Check to make sure names and frequencies match expected values.

for k=1:size(names,1),
  ju(k)=strmatch(names(k,:),const.name);
end;
%if any(freq~=const.freq(ju)),
%  error('Frequencies do not match names in input');
%end;

% Get the astronical argument with or without nodal corrections.
if ~isempty(lat) & abs(jdmid)>1,
  [v,u,f]=t_vuf(jdmid,ju,lat);
elseif abs(jdmid)>1, % a real date
  [v,u,f]=t_vuf(jdmid,ju);
else
   v=zeros(length(ju),1);
   u=v;
   f=ones(length(ju),1);
end;

ap=ap.*f.*exp(+i*2*pi*(u+v));
am=am.*f.*exp(-i*2*pi*(u+v));


tim=tim-jdmid;

[n,m]=size(tim);
tim=tim(:)';

yout=sum(exp( i*2*pi*freq*tim*24).*ap(:,ones(size(tim))),1)+ ...
     sum(exp(-i*2*pi*freq*tim*24).*am(:,ones(size(tim))),1);
```


Reproduced with permission of the copyright owner. Further reproduction prohibited without permission.

```
yout=reshape(yout,n,m);
```


Reproduced with permission of the copyright owner. Further reproduction prohibited without permission.